Summer 8-17-2018

Arid1b and Macf1 in Murine Brain Development and Behavior

Jeffrey Jay Moffat
University of Nebraska Medical Center

ARID1B AND MACF1 IN MURINE BRAIN DEVELOPMENT AND BEHAVIOR

BY

Jeffrey Jay Moffat

A DISSERTATION

Presented to the Faculty of
the University of Nebraska Graduate College
in Partial Fulfillment of the Requirements
for the Degree of Doctor of Philosophy

Pharmacology & Experimental Neuroscience
Graduate Program

Under the Supervision of Professor Woo-Yang Kim

University of Nebraska Medical Center

Omaha, Nebraska

July 2018

Supervisory Committee:

Anna Dunaevsky, Ph.D.

Sung-Ho Huh, Ph.D.

Daniel Monaghan, Ph.D.

Huangui Xiong, M.D., Ph.D.

ACKNOWLEDGMENTS

I would first like to thank my advisor, Dr. Woo-Yang Kim for his patience and support throughout my graduate career. You have given me enough independence to stretch myself and develop and thoughtful advice when I needed it most. Thank you for always encouraging me to be diligent and dedicated and showing me how to think like a scientist.

I would also like to thank my committee members, Dr. Anna Dunaevsky, Dr. Sung-Ho Huh, Dr. Dan Monaghan, and Dr. Huangui Xiong. Thank you for devoting your time to my academic development and for your thoughtful feedback and guidance. Each of you helped me to view my research from a different perspective, thus strengthening my project and my augmenting my scientific training.

I owe special thanks to both of my grandfathers, Bruce N. Smith and Arlo J. Moffat. They were two scientists who challenged me to open my mind and view the world in new ways. I am also deeply indebted to my parents, Rebecca B. Moffat and Jeffrey L. Moffat. You both have always believed in me and encouraged me to reach higher and always maintain my integrity.

I am grateful for my daughter, Alice K. Moffat, as well. Thank you for the sleepless nights and the big smiles when I came home at the end of the day. Coming home to you and your mom at the end of each day made all of the hard work and planning worth it.

I would finally like to thank my wife, Kelsey M. Moffat. You have been an unwavering pillar of support to me during this adventure. Thank you for coming to Omaha with me. Thank you for picking up the slack when I needed to work late and on the weekends. Thank you for encouraging me and challenging me and keeping me on the right path. I never could have done this without you. You are the best thing that’s ever happened to me. I love you!

ARID1B AND MACF1 IN MURINE BRAIN DEVELOPMENTA AND BEHAVIOR

Jeffrey J. Moffat, Ph.D.

University of Nebraska, 2018

Supervisor: Woo-Yang Kim, Ph.D.

Intellectual disability (ID) and autism spectrum disorder (ASD) affect between one and three percent of the global population. These disorders represent a significant emotional and financial burden for affected individuals and their families. Treatment for these conditions remains limited because many of the key molecular factors and associated pathogenic mechanisms are still poorly understood.

In this report we examine two genes related to ASD and ID, AT-rich interactive domain-containing protein 1B (*ARID1B*) and Microtubule-actin crosslinking factor 1 (MACF1). ARID1B is a subunit of the mammalian BRG1/BRM associated factor (BAF) chromatin-remodeling complex, which broadly regulates gene expression. ARID1B also interacts with the transcription factor β-catenin, which regulates neurogenesis. Haploinsufficiency of *ARID1B* causes ID and ASD and mouse models of *Arid1b* haploinsufficiency exhibit abnormal cognitive and social behaviors and have fewer GABAergic interneurons. MACF1 is a member of the spektraplakin family of proteins and is responsible for regulating microtubule and actin interaction and dynamics. As such, MACF1 plays a role in many cellular processes, such as migration and proliferation. *MACF1* is a candidate gene for 1p34.2-p34.3 deletion syndrome, a chromosomal deletion disorder characterized by a greatly increased risk for autism and neurodevelopmental delay. We developed conditional knockout mice for both *Arid1b* and *Macf1* in order to better delineate their respective roles in brain development and mouse behavior.

We detect a decrease in excitatory and inhibitory neural progenitor proliferation and survival as well aberrant cell cycle progression in *Arid1b* mutants. We also report decreased nuclear β-catenin localization and ID- and ASD-like behavioral phenotypes in both excitatory and inhibitory neural progenitor-specific *Arid1b* knockout mice. Conditional deletion of *Macf1* in radial progenitors leads to cortical malformations and agenesis of the corpus callosum. It also causes increased neural progenitor proliferation accompanied by aberrant neuronal positioning. *Macf1* conditional knockout mice also display ASD- and ID-like behavioral dysfunctions.

Altogether, these results demonstrate a critical role for *Arid1b* and *Macf1* in neural development and behavior and provide insight into the pathogenesis of ASD and ID.

TABLE OF CONTENTS

LIST OF FIGURES AND TABLES

Tables

Figures

LIST OF ABBREVIATIONS

Abbreviation	Description
+TIP	Plus-end tracking protein
ABD	Actin-binding domain
ACF7	Actin crosslinking factor 7
ADHD	Attention deficit hyperactivity disorder
ALDH2	Aldehyde dehydrogenase 2
ANOVA	Analysis of variance
A-P	Anteroposterior
APC	Adenomatous polyposis coli
ARID1B	AT-rich interactive domain containing protein 1B
ARL13B	ADP-ribosylation factor-like protein 13B
ASD	Autism spectrum disorder
BAF	BRG1/BRM associated factor
BLBP	Brain lipid-binding protein
BPAG1	Bullous pemphigoid antigen1
BrdU	Bromodeoxyuridine
BRG1	Brahma-related gene 1
BRM	Brahma
CBP	CREB-binding protein
CDH8	Cadherin-8
CH	Calponin homology domain

cKO	Conditional knockout
cl. Cas 3	Cleaved Caspase 3
CLASP2	Cytoplasmic linker-associated protein 2
CNS	Central nervous system
CNTNAP2	Contactin-associated protein like 2
CP	Cortical plate
CREB	cAMP response element binding protein
CRISPR	Clustered Regularly Interspaced Short Palindromic Repeats
CSS	Coffin-Siris syndrome
Ctnnb1	Gene encoding β-catenin
CUX1	Cut-like homeobox 1
DA	Dopamine(rgic)
DAPI	4’,6-diamidino-2-phenylindole
Dcx	Gene encoding doublecortin
DG	Dentate gyrus
DISC1	Disrupted in schizophrenia 1
DOCK 180	Dedicator of cytokines 180
DTNBP1	Dysbindin
E/I	Excitatory/Inhibitory
EB1	Microtubule-associated protein RP/EB family member 1
EGR2	Early growth response protein 2
ELMO	Engulfment and cell motility protein

EPHA6	Ephrin type-A receptor 6
ESC	Embryonic stem cell
FAK	Focal adhesion kinase
FMR1	Fragile X mental retardation 1
FXS	Fragile-X syndrome
GABA	Gamma-aminobutyric acid
GAD1	Glutamic acid decarboxylase 1
GAD2	Glutamic acid decarboxylase 2
GAR	Gas2-related protein
GFAP	Glial fibrillary acidic protein
GFP	Green fluorescent protein
GH	Growth hormone
GHRH	Growth hormone-releasing hormone
GRIN2B	Glutamate (NMDA) receptor subunit epsilon-2
GSK3-β	Glycogen synthase kinase 3β
HAT	Histone acetyl-transferase
HDAC	Histone deacetylase
HOMER1	Homer protein homolog 1
ID	Intellectual disability
IGF	Insulin-like growth factor
INM	Interkinetic nuclear migration
ITGA4	Integrin alpha 4

IZ	Intermediate zone
IZ	Intermediate zone
KIF5A	Kinesin heavy chain isoform 5A
KO	Knockout
LAMA1	Laminin subunit alpha-1
Lef1	Gene encoding Lymphoid enhancer-binding factor 1
LGE	Lateral ganglionic eminence
LHX2	LIM/homeobox protein Lhx2
LMNA	Lamin A/C
LRP5/6	Genes encoding Low-density lipoprotein receptor-related protein 5 and 6
MACF1	Microtubule-actin crosslinking factor 1
MAP2	Microtubule-associated protein 2
mATG9	Autophagy-related protein 9A
MECP2	Methyl-CpG-binding protein 2
MGE	Medial ganglionic eminence
MGE	Medial ganglionic eminence
mIPSC	Miniature inhibitory postsynaptic current
MKL2	MKL/myocardin-like protein 2
MTOC	Microtubule-organizing center
MTOR	Mammalian target of rapamycin
MZ	Marginal zone
NBEA	Neurobeachin

nNOS	Nitric oxide synthase
NTNG1	Netrin G1
Ntrk2	Gene encoding Tropomyosin receptor kinase B
PCAF	P300/CBP-associated factor
PD	Parkinson's disease
PH3	Phosphorylated Histone H3
PNS	Peripheral nervous system
PRICKLE1	Prickle planar cell polarity protein 1
PRICKLE2	Prickle planar cell polarity protein 2
PSD	Post-synaptic density
PV	Parvalbumin
Pvalb	Gene encoding Parvalbumin
RBFOX1	Fox-1 homolog A
RGC	Retinal ganglion cell
RGC	Radial glial cell
RGP	Radial glial progenitor
RhoA	Ras homolog gene family, member A
RMS	Rostral migratory stream
ROBO1	Roundabout homolog 1
SBH	Subcortical band heterotopia
SEM	Standard error of the mean
SFARI	Simons Foundation Autism Research Initiative

SGZ	Subgranular Zone
SHANK3	SH3 and multiple ankyrin repeat domains protein 3
shRNA	Short hairpin RNA
siRNA	Short interfering RNA
SR0	Spectrin repeat 0
SSPO	SCO-spondin
Str	Striatum
SVZ	Subventricular zone
SVZ	Subventricular zone
TBR1/2	T-box, brain, 1/2
VAMP	Vesicle-associated membrane protein
VGAT	Vesicular inhibitory amino acid transporter
VIAAT	Vesicular inhibitory amino acid transporter-positive
VZ	Ventricular zone
VZ	Ventricular zone
WT	Wild type
ZBTB20	Zinc finger and BTB domain-containing protein 20
β-cat	β-catenin

CHAPTER 1: INTRODUCTION

1.1 Genetic regulation of brain development

1.1.1 Neuronal progenitor proliferation

Brain development is a complex and tightly-regulated process. A precise interplay between genetic factors and environmental influences is required for the proper differentiation and organization of brain structures (Stiles and Jernigan, 2010) and a breakdown in one of these developmental processes can lead to severe cognitive and behavioral deficiencies (Machado-Salas, 1984; Takashima et al., 1991; Shinozaki et al., 2002; Segarra et al., 2006; Dranovsky and Hen, 2007; Duan et al., 2007; Paul et al., 2007; Lee et al., 2012; Riviere et al., 2012; Beguin et al., 2013; Callicott et al., 2013; Sharaf et al., 2013; Chinn et al., 2015).

Neurons are the primary component of the brain, and they work, in concert with other brain glial cells, to carry out neural functions. Neurons arise from neural stem cells, primarily during embryonic development, in a process called neurogenesis (Stiles and Jernigan, 2010). In the developing cerebral cortex, neural progenitors can undergo self-renewal or give rise to neurons within the ventricular/subventricular zone (Rakic, 2009; Franco and Muller, 2013; Greig et al., 2013). Reduced numbers of neural progenitors caused by depletion of progenitor pools or protracted proliferation may result in microcephaly with otherwise normal brain structures (Tang, 2006; Wu and Wang, 2012). Dysregulated neural progenitor proliferation has also been linked to genetic mutations and environmental insults related to many neurodevelopmental and psychiatric disorders, including ASD and schizophrenia (Kioussi et al., 2002; Sheen et al., 2004; Gotz and Huttner, 2005; Guerrini and Filippi, 2005; Hatton et al., 2006; Dranovsky and Hen, 2007; Duan et al., 2007; Moulding et al., 2007; Gulacsi and Anderson, 2008;

Yingling et al., 2008; Kim et al., 2009; Ming and Song, 2009; Ishizuka et al., 2011; Wu et al., 2013; Ka et al., 2014b; Hu et al., 2015; Koludrovic et al., 2015; Mariani et al., 2015; Pucilowska et al., 2015; Ka et al., 2017). The disruptive functions of neural progenitor renewal and neurogenesis may also interfere with later developmental aspects, such as neuronal migration and positioning in the developing brain.

1.1.2 Neuronal migration and positioning

Neuronal positioning is an integral part of the coordinated steps comprising neural circuit formation in embryonic and neonatal development (Martini et al., 2009). This process takes place throughout the nervous system at different time points depending on the type of neuron. Although neuronal positioning and migration occur throughout the central nervous system, I will primarily focus on neuronal positioning in the neocortex of the developing brain.

Correct positioning of neurons by normal migration plays a critical role in establishing cognitive functions and emotion. Human cognitive activity depends on appropriate brain circuit formation. Disrupted brain wiring due to abnormal neuronal development, such as improper neuronal positioning, can result in brain malformations, cognitive dysfunction, and seizures (Gleeson and Walsh, 2000; Kaufmann and Moser, 2000; Wegiel et al., 2010). The causes of brain malformations associated with positioning and migration defects are varied and include genetic mutations and environmental toxins (Martini et al., 2009; Guerrini and Parrini, 2010; Liu, 2011). Studies of neuronal migration disorders have progressed due to advances in molecular genetics and brain magnetic resonance imaging. The commonly identified disorders of neuronal positioning include lissencephaly and heterotopia (Barkovich et al., 2012).

After neurons are born, they migrate from their birthplaces to their final destinations (Figure 1.1). There are two types of embryonic neuronal migration: radial and tangential. The migration of excitatory pyramidal neurons from the cortical ventricular zone (where they are born) is an example of radial migration (Figure 1.1A). These neurons migrate into the cortical plate alongside radial glial processes (Rakic, 1972; Chanas-Sacre et al., 2000; Hartfuss et al., 2001; Noctor et al., 2001). The layers of the cortex form in an "inside-out" manner with later-born pyramidal neurons migrating past earlier-born predecessors in the cortical plate so that they are more superficial in their final position than earlier born neurons (Tan et al., 1998; Liu, 2011; Evsyukova et al., 2013; Sultan et al., 2013). In humans, neuronal migration takes place predominantly between 12 and 20 weeks in gestation. The migration of inhibitory interneurons (GABAergic neurons) from the medial ganglionic eminence of the ventral telencephalon (where they are born) is an example of tangential migration (Figure 1.1B). Interneurons migrate tangentially to the dorsal telencephalon and then change direction to enter the cortical plate radially (Rakic, 1978; Anderson et al., 2001; Molyneaux et al., 2007; Sultan et al., 2013). Subsets of these cells display ventricle-directed migration followed by radial movement to the cortical plate. Thus, neuronal migration determines the positioning of developing neurons into cortical layers and thereby is important in generating lamina-specific neural circuits. Normal development and function of the neocortex critically depends on the coordinated production and positioning of excitatory and inhibitory neurons (Powell et al., 2003; Bedogni et al., 2010; Lodato et al., 2011; Bartolini et al., 2013). Abnormal neuronal migration can arrest different types of neurons at the wrong positions along the migratory path resulting in brain malformations and neurological disorders.

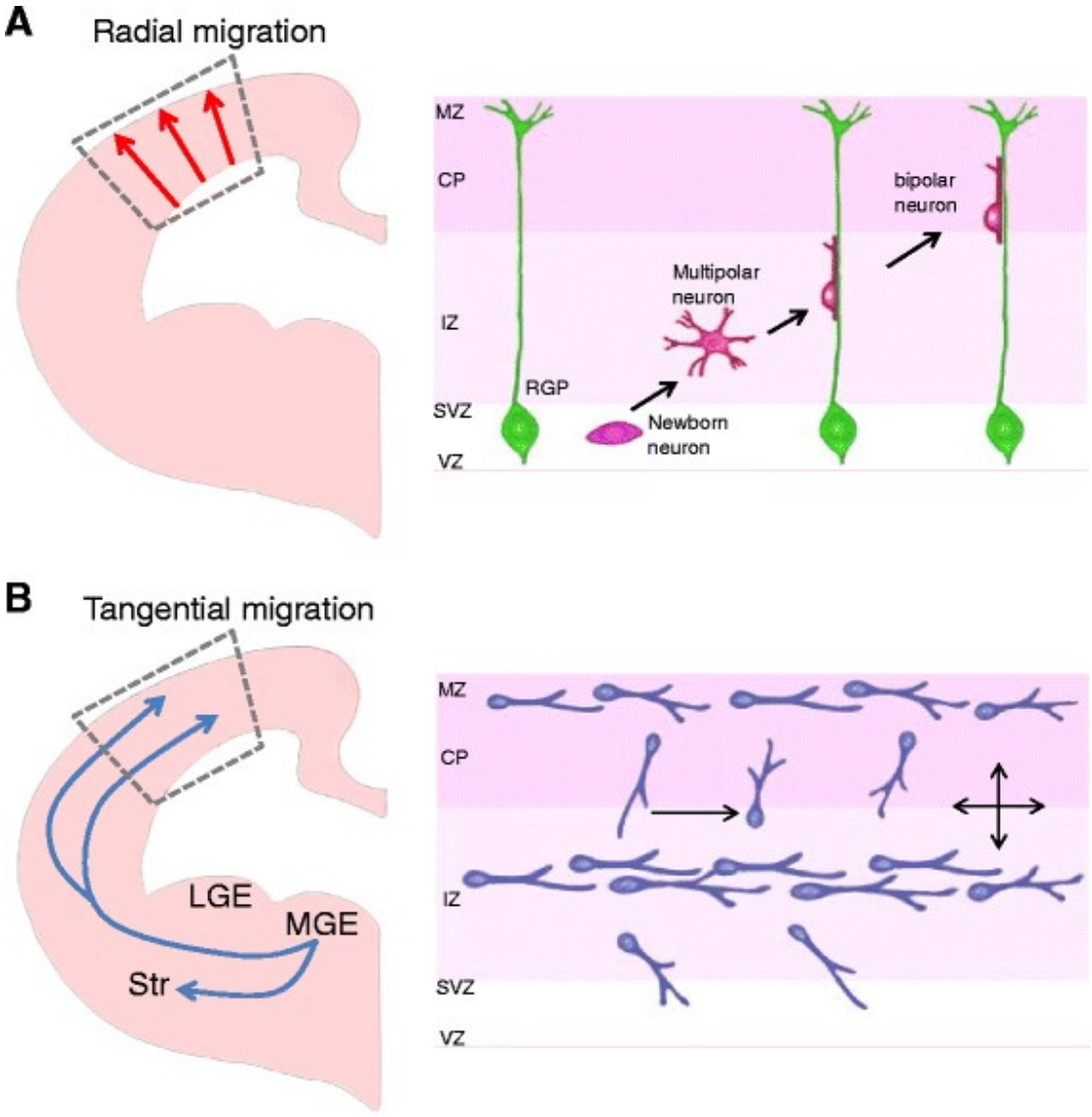

Figure 1.1 Two modes of neuronal migration in the developing brain

(A**)**. Radial migration. Excitatory pyramidal projection neurons migrate from the ventricular zone to the cortical plate in the developing brain. The right panel shows what happens in the rectangular box in the left panel. Newly-born neurons from radial glial progenitors (RGP) at the ventricular zone (VZ) migrate along the radial processes of RGPs. MZ: marginal zone. CP: cortical plate. IZ: intermediate zone. SVZ: subventricular zone. (B**)**. Tangential migration. Inhibitory interneurons originate from distinct proliferative zones in the developing brain. Interneurons are born in the medial ganglionic eminence (MGE) of ventral brain and migrate in multiple streams into the cerebral wall. Once interneurons reach appropriate spots in the cerebral cortex, they establish their final positions by local adjustment of radial and tangential movement. Unlike pyramidal neurons, these neurons extend multiple leading branches during migration. LGE: lateral ganglionic eminence. LGE: lateral ganglionic eminence. Str: striatum

In addition to these well-defined modes of embryonic neuronal migration, a limited number of neurons and neuronal precursors have been shown to migrate and differentiate in the early postnatal rodent and human cerebellum and hypothalamus (Taupin and Gage, 2002; Ghashghaei et al., 2007). Another, more extensive mode of neuronal migration has been observed in adult rodents and non-human primates, in which neuronal precursors migrate along glial projections from the subventricular zone into the olfactory bulbs. This particular passage is referred to as the rostral migratory stream (RMS) (Luskin, 1993; Taupin and Gage, 2002; Ghashghaei et al., 2007), which continues well into adulthood, but has not been observed in humans (Sanai et al., 2004; Ghashghaei et al., 2007). In the RMS, neuronal precursors migrate via a “tunnel” made up of astrocytes into the olfactory bulb, where they then radially migrate in a glial-independent manner toward the glomeruli and differentiate. The majority of these cells eventually become inhibitory neurons, mainly GABAergic granule neurons (Ghashghaei et al., 2007; Malagelada et al., 2011). Because the application of research tools is currently limited in humans, there is still ongoing debate about whether the RMS exists in humans (Sanai et al., 2004; Ghashghaei et al., 2007; Malagelada et al., 2011).

It is important that further research also be done to understand the mechanisms of neuronal migration and the maintenance of neuronal precursor pools in adults, because of the potential to promote regeneration and repair in individuals with neuronal positioning disorders, neurodegenerative disorders, and severe brain injuries.

1.2 The role of chromatin-remodeler ARID1B in neural development

ARID1B encodes AT-rich-interactive-domain-containing protein 1B (ARID1B), a chromatin remodeler. Haploinsufficiency of this gene has recently been linked to autism spectrum disorder (ASD) and intellectual disability (ID) (Hoyer et al., 2012; Santen et al., 2012; Tsurusaki et al., 2012; Sim et al., 2015). New studies from our group and others have now examined the effects of heterozygous deletion of *Arid1b* in mice, which provides multiple novel insights into the mechanisms and roles of *Arid1b* in the developing brain and in behavior (Celen et al., 2017; Jung et al., 2017; Shibutani et al., 2017). There have also been recent breakthroughs in potential pharmacologic treatments for *ARID1B*-related neurodevelopmental disorders. In this review we summarize and analyze these recent findings and provide potential plans for future research. Further understanding of ARID1B and its functions in the developing brain are now much more feasible with the availability and description of knockout animals and may play an important role in the future of neurodevelopmental and psychiatric disorder research.

1.2.1 ARID1B mutations in human patients

ARID1B mutations are prevalent in multiple neurodevelopmental disorders, including ASD, ID, and Coffin-Siris syndrome (CSS). ID is a developmental disorder characterized by significant limitations in both intellectual function and adaptive behavior, with an overall incidence estimated to be 2-3% (Sim et al., 2015). As ID is a severely incapacitating condition that imposes a significant burden on affected individuals and their families, much work has been done to identify its underlying causes. ID has a genetic origin in the majority of cases, and studies of X-linked, autosomal-recessive, syndromic and sporadic cases have resulted in the identification of several hundred ID-associated genes. Mutational analysis in 887 patients with unexplained ID reveals nine

different *de novo* nonsense or frameshift mutations predicted to cause *ARID1B* haploinsufficiency, indicating haploinsufficiency of ARID1B as a common cause of ID (Hoyer et al., 2012).

CSS is a rare autosomal-dominant anomaly syndrome and most affected individuals present with mild to severe ID. Additional features of CSS include growth deficiencies, microcephaly, coarse facial features, and a hypoplastic nail on the fifth finger and/or toe (Tsurusaki et al., 2012). To identify the genetic basis of CSS, Santen et al. utilize whole-exome sequencing on three diagnosed individuals, revealing *de novo* truncating mutations in one copy of *ARID1B* in all cases. Array-based copy-number variation analysis in 2,000 individuals diagnosed with ID reveals 3 subjects with deletions in the *ARID1B* gene who also have phenotypes partially overlapping with that of CSS (Santen et al., 2012). Using exome sequencing in 23 individuals with CSS, another group show 6 patients with *de novo* heterozygous mutations in the *ARID1B* gene, providing further evidence of *ARID1B* haploinsufficiency as a cause of CSS (Tsurusaki et al., 2012).

ASD is characterized by significant communication and social interaction deficits as well as restricted interests and stereotyped behaviors (Walsh et al., 2011). ID is also a highly prevalent phenotype in individuals with ASD, seen in approximately 75% of those affected. Next generation sequencing and microarray analysis of samples from eight patients, all presenting with ID, shows *de novo* translocations or deletions resulting in a truncated copy of *ARID1B* in all cases (Halgren et al., 2012). Of these patients, 5 are diagnosed with ASD or have autistic traits. In addition, 4 of these 5 patients show corpus callosum abnormalities demonstrated by brain imaging. This finding suggests that structural defects may be associated with the cognitive and behavioral phenotypes

stemming from *ARID1B* haploinsufficiency. A separate study shows that the transcript level of the ARID1B gene is reduced in individuals with ASD (Nord et al., 2011).

Taken together, these studies all emphasize the role ARID1B plays in proper brain development and behavior. Various *de novo* mutations resulting in haploinsufficiency cause ID, CSS, ASD, and corpus callosum abnormalities to varying degrees. These findings add to the growing evidence that mutations in chromatin-remodeling genes are important contributors to neurodevelopmental disorders (Ronan et al., 2013; Sokpor et al., 2017; Gabriele et al., 2018), and that several of these disorders with overlapping phenotypes have converging genetic causes.

1.2.2 Arid1b knockdown and neuronal development

Proper neurite outgrowth and maintenance, which involve coordinated changes between the actin cytoskeleton and the microtubule network, are critical for normal neural development and brain function (Tsaneva-Atanasova et al., 2009). This process is regulated by the SWI/BAF complex (Weinberg et al., 2013; Choi et al., 2015; Bachmann et al., 2016). ARID1B is a component of the BAF chromatin remodeling complex (Ho and Crabtree, 2010; Ronan et al., 2013) and plays an essential role in neurite outgrowth and maintenance. Using in utero shRNA delivery, Ka et al. show that ARID1B is required for dendrite outgrowth and arborization in cortical and hippocampal pyramidal neurons during brain development (Ka et al., 2016b). In addition to decreased dendritic branching, ARID1B-deficient neurons exhibit markedly decreased dendritic innervation into cortical layer I and fewer attachments of dendritic terminals at the pial surface (Ka et al., 2016b). It is noteworthy that layer I of the cerebral cortex receives inputs primarily from neurons in higher-order thalamic and cortical areas, and neurons in this layer preferentially increase their activity during attention-demanding processes (Baluch and

Itti, 2011; van Gaal and Lamme, 2012; Larkum, 2013). Thus, the decreased dendritic innervation into cortical layer I caused by ARID1B deficiency may disrupt balanced excitatory and inhibitory inputs and thereby give rise to pathologic conditions of ID and ASD.

Dendritic spines are the major sites of excitatory synaptic input in the brain and, therefore, form the basis of synaptic circuitry (Harris and Kater, 1994; Bourne and Harris, 2008). Ka et al. show that ARID1B contributes to spine formation, maturation and maintenance (Ka et al., 2016b). ARID1B-deficient neurons exhibit a decreased number of dendritic spines and a prevalence of filopodia-like immature spines (Ka et al., 2016b). The aberrant dendrites and spines in ARID1B-deficient pyramidal neurons greatly resemble the unbranched dendritic and filopodia-like spine morphology observed in mouse models of ID and ASD, as well as in RETT, Down, and fragile-X syndrome (FXS) models (Irwin et al., 2002; McKinney et al., 2005; Jentarra et al., 2010). Thus, ARID1B abnormalities may contribute to clinical outcomes by creating inappropriate synaptic connectivity. Incorrect growth and differentiation of dendrites is linked to the pathology of many neurodevelopmental and psychiatric diseases including ID, ASD and schizophrenia (Machado-Salas, 1984; Kaufmann and Moser, 2000; Fiala et al., 2002; Chapleau et al., 2009; Penzes et al., 2011). Abnormalities in the dendritic differentiation of cortical pyramidal neurons are seen in postmortem brain samples from individuals with ID (Huttenlocher, 1974). A reduction in spine size along dendrites is also reported in Down syndrome (Marin-Padilla, 1976; Roberts et al., 1996) and altered dendrite arborization in cortical pyramidal neurons is found in the brains of Rett syndrome patients (Belichenko et al., 1994; Armstrong, 2005).

1.2.3 Neural phenotypes of Arid1b knockout mice

Three recent independent studies, including our own, describe significant differences in brain anatomy and cellular composition in *Arid1b* heterozygous mice (Celen et al., 2017; Jung et al., 2017; Shibutani et al., 2017). Jung et al. observe normal density and distribution of pyramidal neurons, oligodendrocytes and astrocytes in *Arid1b* heterozygous mice, but find that GABAergic interneuron numbers are significantly reduced in *Arid1b* mutant mice, due to increased apoptosis and decreased proliferation of progenitors in the ganglionic eminence (Jung et al., 2017). The ventral ganglionic eminence is essential for the generation of GABAergic interneurons (Pleasure et al., 2000; Brandao and Romcy-Pereira, 2015). GABAergic interneurons containing parvalbumin (PV), calretinin, somatostatin or calbindin-D_{28k} are the primary source of GABA in the nervous system and play an important role in neural circuitry and activity (Kelsom and Lu, 2013; Butt et al., 2017). Specifically, the number of PV-positive interneurons is reduced in several brain regions including the cortex, amygdala, thalamus, and hippocampus in *Arid1b* heterozygous mice, but *Arid1b* haploinsufficiency does not lead to significant changes in the somatostatin-, calbindin- or calretinin-positive interneuron number in *Arid1b* heterozygous cortices (Jung et al., 2017). Decreases in GABAergic interneuron numbers in the cortex and hippocampus have previously been linked to autism and schizophrenia (Benes and Berretta, 2001; Pizzarelli and Cherubini, 2011) and, more specifically, the number of PV-positive interneurons has been shown to be significantly reduced in autism and schizophrenia in both mouse models and postmortem brain tissue (Gogolla et al., 2009; Lawrence et al., 2010). Consistently, ASD-like behavioral profiles, such as social interaction and communication deficits with repetitive and stereotyped behavior, can be observed in PV knockout mice (Wohr et al., 2015). Neuronal excitatory/inhibitory balance is regulated at the synaptic level, and a reduction in inhibitory synapse number or strength results in a shift of that balance (Gao and Penzes, 2015; Nelson and Valakh, 2015). As a result, excitatory/inhibitory

imbalance leads to broken synaptic homeostasis and facilitates the risk of the neurological disorders such as autism and schizophrenia. *Arid1b* heterozygous mice exhibit fewer inhibitory synaptic puncta, namely vesicular inhibitory amino acid transporter- (VGAT) and glutamic acid decarboxylase 2- (GAD2) positive puncta, in the cerebral cortex (Jung et al., 2017). In addition, glutamic acid decarboxylase 1 (*Gad1*) and *Gad2* expression levels are markedly decreased in *Arid1b* haploinsufficient mouse brains. Heterozygous deletion of *Arid1b* also leads to abnormal miniature inhibitory postsynaptic currents (mIPSC) frequencies, characterized by increased inter-event intervals and increased inhibitory synaptic cleft width (Jung et al., 2017). Furthermore, GABAergic interneuron neurite number and length are decreased in *Arid1b* heterozygous mice (Jung et al., 2017). Thus, *Arid1b* haploinsufficiency results in excitatory/inhibitory imbalance via decreased GABAergic interneuron numbers and impaired synaptic transmission of inhibitory signals.

Two other reports indicate that a small subset of *Arid1b* heterozygous mice are born with hydrocephalus (Celen et al., 2017; Shibutani et al., 2017), which corresponds well with some individuals with ASD (Turner et al., 2016) and a portion of patients with CSS who present with Dandy-Walker malformations (Schrier Vergano et al., 1993; Imai et al., 2001). Celen et al. also report reductions in the size of the cerebral cortex, corpus callosum and dentate gyrus, as well as decreased adult hippocampal neurogenesis, in *Arid1b* mutant mice (Celen et al., 2017).

1.2.4 Gene expression changes in Arid1b knockout mice

The ATP-dependent BAF chromatin remodeling complex regulates gene expression via nucleosome remodeling (Singhal et al., 2010; Alver et al., 2017). Considering ARID1B's role as a member of the BAF chromatin remodeling complex, it is unsurprising that

heterozygous deletion of *Arid1b* leads to broad changes in gene expression in the brain. Shibutani et al. report that many of the genes shown to be up- and down-regulated in *Arid1b* heterozygous brains are similarly altered in human patients with ASD and in another animal model of autism (*Cdh8* heterozygous mice) (Shibutani et al., 2017). Celen et al. also report multiple changes in gene expression in *Arid1b* heterozygous mice, when compared to wild-type controls. In the adult hippocampus they find that genes associated with nervous system development and psychological, behavioral and developmental disorders appear to be distinctly affected. More specifically, they describe marked expression changes in Ephrin, nNOS, axonal guidance and glutamate receptor signaling pathway-related genes (Celen et al., 2017). Of the 140 differentially-expressed genes they identify, 91 are thought to be directly targeted by the BAF chromatin remodeling complex (Attanasio et al., 2014; Celen et al., 2017) and 14 are included amongst the highest ranking autism risk genes in the SFARI database (Basu et al., 2009; Celen et al., 2017). A list of these genes can be found in Table 1.1.

Histone modifications such as acetylation and deacetylation are important for the regulation of gene expression (Eberharter and Becker, 2002; Kurdistani and Grunstein, 2003; Shahbazian and Grunstein, 2007; Bannister and Kouzarides, 2011; Lawrence et al., 2016). Jung et al. report that *Arid1b* haploinsufficiency leads to an overall decrease in the acetylation of histone H3 at lysine 9 (H3K9ac) and tri-methylation of histone H3 at lysine 4 (H3K4me3), both markers of transcriptional activation, and an increase in tri-methylation of histone H3 at lysine 27, a marker for transcriptional repression (Figure 1.2) (Jung et al., 2017). They do not, however, report any global changes in histone acetyl-transferase (HAT) or histone deacetylase (HDAC) activity in *Arid1b* heterozygous brains, but do observe decreases in the level of acetyl-CREB-binding protein (CBP), which has been shown to enhance HAT function (Vecsey et al., 2007; Jung et al., 2017).

In a similar vein, a previous study shows that HAT and HDAC activities are regulated by the interaction of ARID1B with HATs or HDACs in mouse osteoblast cells (Nagl et al., 2007). Jung et al. also report decreased protein levels for PCAF, a HAT, in *Arid1b* homozygous embryonic brains, but not in *Arid1b* heterozygous brains, and decreased binding of several HATs to H3K9 acetylated sites in *Arid1b* heterozygous brains (Jung et al., 2017).

Table 1.1 Selected genes with altered expression in *Arid1b* heterozygous mice

GENE	FUNCTION/DESCRIPTION	ASD ASSOCIATION*
ARID1B	Chromatin Remodeler	High confidence (syndromic)
GRIN2B	NMDA receptor subunit	High confidence
ZBTB20	Transcription factor	Suggestive evidence (syndromic)
PRICKLE1	Nuclear receptor	Suggestive evidence
PRICKLE2	Nuclear receptor	Suggestive evidence
RBFOX1	Alternative splicing regulator	Suggestive evidence
HOMER1	Postsynaptic density scaffolding	Minimal evidence
LAMA1	Lamanin alpha 1 subunit	Minimal evidence
MKL2	Transcriptional coactivator	Minimal evidence
NBEA	A-kinase anchor protein	Minimal evidence
NTNG1	Neurite outgrowth-promoting protein	Minimal evidence
SOX5	Transcription factor	Minimal evidence
SSPO	Neuronal aggregation modulator	Minimal evidence
EGR2	Transcription factor	Hypothesized
EPHA6	Receptor tyrosine kinase	Hypothesized
ITGA4	Integrin subunit	Hypothesized
ROBO1	Membrane protein involved in axon guidance and cell migration	Hypothesized

* Based on Simons Foundation Autism Research Initiative (SFARI) numerical gene scoring: 1 = High confidence; 2 = Strong candidate; 3 = Suggestive evidence; 4 = Minimal evidence; 5 = Hypothesized; 6 = Not supported.

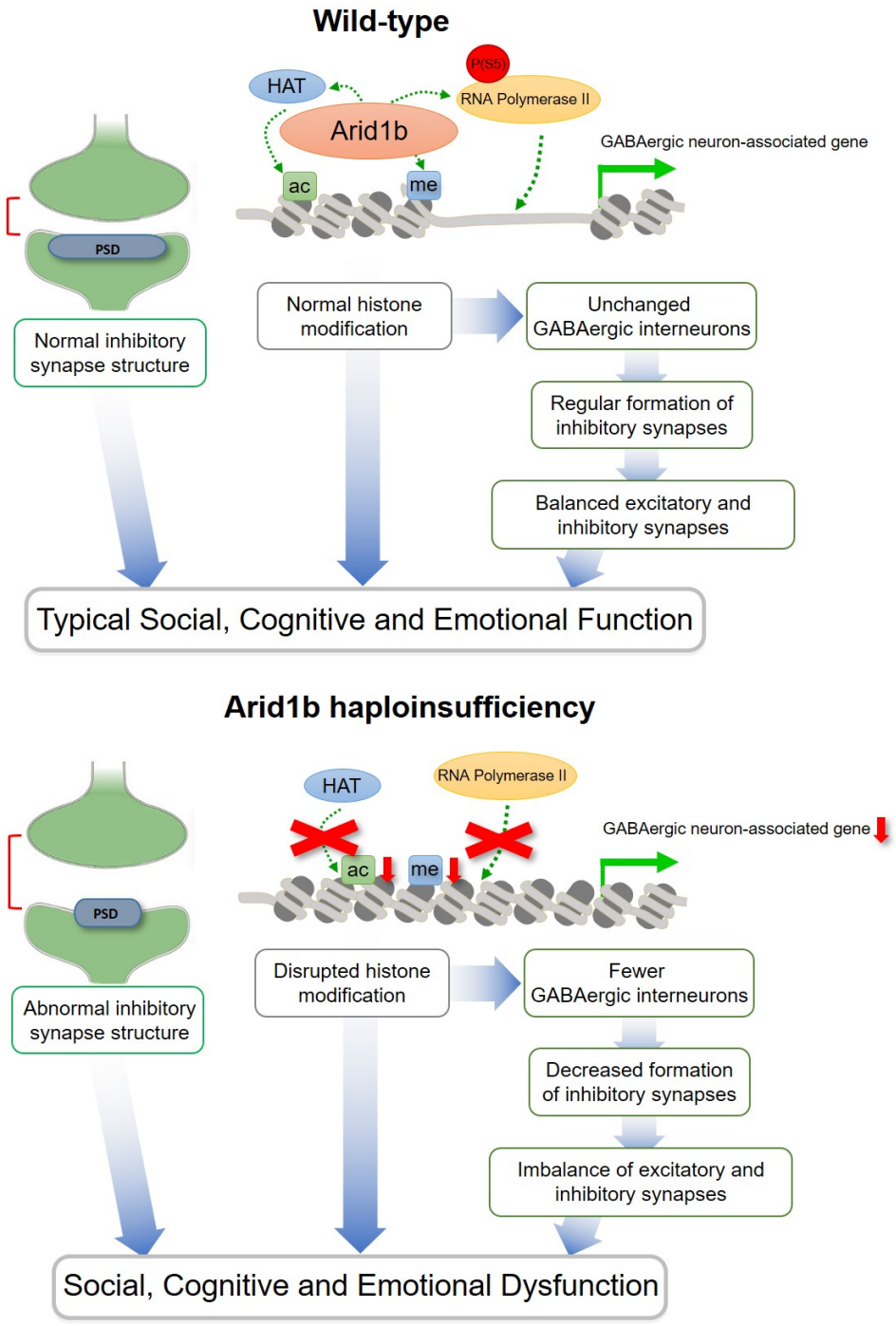

Figure 1.2 Graphical model of the neuronal effects of *Arid1b* haploinsufficiency

Arid1b heterozygous mice exhibit wider inhibitory synaptic clefts and lower levels of transcription-activating histone post-translational modifications at specific GABAergic neuron-associated promoters. The latter leads to decreased phosphorylation of Ser 5 within the CTD of RNA polymerase II at these DNA loci, which is necessary for gene transcription. These changes in gene expression contribute to the functional, anatomical and behavioral abnormalities observed in *Arid1b* mutant mice.

Corresponding with the overall reduction in PV-positive interneurons in *Arid1b* heterozygous cortices, Jung et al. observe a decrease in *Pvalb* and *Ntrk2* transcripts in mutant brains. They also report that ARID1B binds to the *Pvalb* promoter in wild-type brains and that this localized binding is decreased in *Arid1b* heterozygous brains along with decreased H3K9ac in this region. One presumed effect of these changes is the decrease in transcriptional initiation for the *Pvalb* gene, shown by lower levels of the phosphorylated (ser5)-carboxy-terminal-domain of RNA polymerase II at the *Pvalb* promoter (Figure 1.2) (Jung et al., 2017). Therefore, ARID1B is an essential factor in regulating GABA neuron-associated genes through recruiting histone modification molecules to specific promoters and promoting chromatin remodeling for RNA polymerases to initiate gene transcription. These findings, in particular, provide insight into novel mechanisms for ARID1B-mediated gene regulation, as it appears that ARID1B-histone modifier interactions may act to facilitate gene transcription. It remains to be seen whether this is the case at the promoters of other genes altered in the *Arid1b* heterozygous mouse brain. Particularly, ARID1B may regulate histone modification at the Wnt signaling genes because *Arid1b* haploinsufficiency reduces the expression of Wnt-β-catenin signaling-related genes including *Cyclin D1*, *c-Myc*, *n-Myc*, *Creb*, *Lef1*, *Ctnnb1*, and others. (Jung et al., 2017). A number of studies show that histone modifications can regulate cell proliferation and differentiation as well as cell death (Mehnert and Kelly, 2007; Roidl and Hacker, 2014; Li et al., 2018). Wnt signaling plays important roles in ventral progenitor proliferation during brain development (Liebner et al., 2008; Brandao and Romcy-Pereira, 2015). Furthermore, expression of c-Myc, a key target of Wnt signaling and a cell cycle regulator, is decreased in ARID1B-deficient cells (Nagl et al., 2007). ARID1B deficiency also prevents the self-renewal capacity of ES cells (Yan et al., 2008). Thus, future studies should consider whether ARID1B can control Wnt-β-catenin signaling in ventral progenitor proliferation and development.

1.3 Genetic influences on mouse behavior

1.3.1 The utility of mice in behavioral studies

Due to the broad array of genetic tools available for mouse studies and the complexity of mouse behavior, mice have become an ideal model organism for behavioral genetics. In the early days of rodent studies, most behavioral abnormalities arose spontaneously in colonies and were only later shown to be heritable (Keeler et al., 1928; Bucan and Abel, 2002; Greenspan, 2008). With the rise of genetics and genomics, as well as improved strategies for targeted genetic manipulation, researchers are now able to dissect the behavioral influences of genetic mutations in mice (Bucan and Abel, 2002; Heidenreich and Zhang, 2016). This is especially useful in studies of neurodevelopmental and psychiatric disorders, in which novel mutations are detected in human patients and can then be examined in mouse models with relative ease.

1.3.2 Mouse models of autism spectrum disorder

ASD is associated with a variety of mutated genes or copy-number variants. Because experimental mouse models are important for discovering the causes and pathogeneses of human disorders, there have been many attempts to develop genetic animal models of ASD based on human ASD-linked genetic mutations (Kazdoba et al., 2014). Typical hallmarks of ASD include impaired social behavior and communication, and repetitive and/or stereotyped behaviors. Additionally, ASD often presents with other co-occurring conditions, including depression, epilepsy, anxiety (Wing and Gould, 1979), attention deficit hyperactivity disorder (ADHD), ID, and motor coordination problems (Purpura et al., 2016). Similar behaviors are seen in animal models of ASD using specific tests developed to measure these behavioral abnormalities. One of the most commonly inherited genetic causes of ASD is FXS, which is caused by an expanded CGG repeat in the 5' untranslated portion of the fragile X mental retardation 1 gene (*FMR1*), leading to

deficiency or absence of the FMR1 protein (Harris et al., 2008; Kogan et al., 2009). Mouse models of FXS (*Fmr1* knockout mice) exhibit several ASD- and ID-like behaviors such as anxiety, social behavior deficits, and cognitive deficiencies (Harris and Kater, 1994; Peier et al., 2000; Yabe et al., 2004; McNaughton et al., 2008; Pietropaolo et al., 2011; Kazdoba et al., 2014).

Another protein closely associated with ASD is Contactin-Associated Protein Like 2, which is encoded by the gene *CNTNAP2*. Homozygous deletion of *CNTNAP2* leads to core ASD-like behavioral symptoms, including social interaction deficits, stereotyped behaviors and impaired vocalization, as well as hyperactivity and seizures (Penagarikano et al., 2011). These mice also exhibit fewer GABAergic interneurons in the cortex and other brain regions, indicative of excitatory/inhibitory imbalance, and treatment with risperidone rescues some, but not all behavioral abnormalities (Penagarikano et al., 2011).

Mutations within the gene that encodes methyl-CpG binding protein 2 (MECP2) cause Rett syndrome, symptoms of which include ASD-like behaviors (Chahrour and Zoghbi, 2007). Mouse models of Rett syndrome demonstrate multiple ASD-like phenotypes (Chen et al., 2001; Guy et al., 2001; Shahbazian et al., 2002; Calfa et al., 2011) and, interestingly, conditional deletion of *Mecp2* in Vesicular inhibitory amino acid transporter-positive (*Viaat*$^{+}$) inhibitory neurons is sufficient to cause ASD-like behaviors and seizures (Chao et al., 2010).

Another set of commonly used mouse models of ASD are *Shank3* mutant mice. SHANK3 is a scaffolding protein enriched in postsynaptic densities (Kreienkamp, 2008) and mutations to *SHANK3* have been observed in patients with ASD (Gauthier et al., 2009). Three *Shank3* mouse models have been developed to date, each affecting a different isoform or protein functional domain, and all exhibit ASD-like behavioral phenotypes to varying degrees (Bangash et al., 2011; Peca et al., 2011). *Shank3B* mice,

in which both the *Shank3α* and *Shank3β* forms are eliminated, exhibit the strongest ASD-like behaviors, including social deficits and stereotyped behavior (Peca et al., 2011).

There are many other genetic mutations that have been associated with ASD, some of which have been extensively studied while others have not (Provenzano et al., 2012). Comparing and contrasting the molecular, anatomical and behavioral abnormalities caused by each of these mutations provide insight into the pathogenesis of ASD and related disorders. Further detailed examinations of the roles of these genes in brain development and function will be necessary in order to develop effective interventions for individuals with sever ASD.

1.4 The role of ARID1B in behavior

Recently, three independent groups, including our own, developed mouse models of ARID1B haploinsufficiency. Two of the groups delete exon 5 of the *Arid1b* gene (Celen et al., 2017; Jung et al., 2017) while the other removes exon 3 (Shibutani et al., 2017), but both strategies appear to result in haploinsufficiency due to frameshift mutations. Celen et al. and Shibutani et al. generate the mutant mice using CRISPR/Cas9 gene editing while Jung et al. use a more traditional knockout strategy. The genetic background of the three mouse models is C57BL/6. Each group performed a different array of behavioral assays, many overlapping, and the results are generally concurrent, with a few exceptions. A summary of each group's results is described in Table 1.2. All three groups performed the elevated plus maze test for anxiety-like behavior. *Arid1b* heterozygous mice spend less time in the open arms of the maze and exhibit a lower percentage of entries into open arms, which indicates heightened anxiety (Celen et al., 2017; Jung et al., 2017; Shibutani et al., 2017). In the open field test, *Arid1b* heterozygous mice spend less time in the center area and enter the center area less

frequently than controls, although their total travel distance is not different, which may also indicate anxiety-like behavior (Celen et al., 2017; Jung et al., 2017). In addition, *Arid1b* heterozygous mice avoid exploring the brightly-lit section in the light-dark box test, another common anxiety assay (Celen et al., 2017). *Arid1b* heterozygous mice also spend more time immobile in the forced swim and tail suspension tests, used to assess depression-like behavioral phenotypes (Jung et al., 2017), although Shibutani et al. report opposite results in the forced swim test (Shibutani et al., 2017).

Table 1.2 Summary of behavioral findings from three studies utilizing *Arid1b* heterozygous mice

HUMAN BEHAVIORAL CORRELATE	BEHAVIORAL ASSAY	CELEN ET AL. 2017	JUNG ET AL. 2017	SHIBUTANI ET AL. 2017
ANXIETY	Elevated Plus Maze	Heightened Anxiety	Heightened Anxiety	Heightened Anxiety
ANXIETY	Open Field	Heightened Anxiety	Heightened Anxiety	Unclear
ANXIETY	Light-Dark Box	Heightened Anxiety	n/a	No Change
DEPRESSION	Forced Swim	n/a	Increased Depression	Increased Activity
DEPRESSION	Tail Suspension	n/a	Increased Depression	n/a
SOCIAL INTERACTION	Three-Chamber Test for Sociability	n/a	Decreased Social Interaction	No Change
SOCIAL INTERACTION	Three-Chamber Test for Social Novelty Preference	n/a	Decreased Social Interaction	No Change
SOCIAL INTERACTION	Home-Cage Social Interaction	n/a	n/a	Decreased Social Interaction
SOCIAL INTERACTION	Open Field Social Interaction	Decreased Social Interaction	Decreased Social Interaction	No Change
COMMUNICATION	Ultrasonic Vocalizations	Altered Communication	n/a	n/a
REPETITIVE BEHAVIOR	Grooming	Increased Repetitive Behavior	Increased Repetitive Behavior	No Change
BEHAVIORAL INFLEXIBILITY	Barnes Maze	n/a	n/a	Decreased Behavioral Flexibility
INTELLECTUAL DISABILITY	Morris Water Maze	No Change	Impaired Spatial Memory	n/a
INTELLECTUAL DISABILITY	Novel Object Recognition	n/a	Impaired Recognition Memory	n/a
INTELLECTUAL DISABILITY	T-Maze	n/a	Impaired Learning	No Change
INTELLECTUAL DISABILITY	Barnes Maze	n/a	n/a	No Change
INTELLECTUAL DISABILITY/FEAR LEARNING	Fear Conditioning	No Change	n/a	Increased Long-Term Fear Memory and Fear Generalization
PAIN RESPONSE	Response to Foot Shock	No Change	n/a	Heightened Response to Stimulus

As discussed above, one of the key characteristics of ASD is deficits in social behavior (Cohen et al., 1988). Jung et al. use the three-chamber social assay to assess social interaction and social novelty preference. *Arid1b* heterozygous mice spend less time in the chamber containing an unfamiliar mouse than in the empty chamber, indicative of impaired social interaction, and also spend less time with a novel stranger mouse than they do with a more-familiar stranger (Jung et al., 2017). Celen et al. report that *Arid1b* heterozygous mice spend less time interacting with unfamiliar juvenile mice compared to WT littermates, when placed together in a fresh cage (Celen et al., 2017). Jung et al. report that *Arid1b* heterozygous mice also spend less time interacting with one another when two unfamiliar mice of the same genotype are placed in the open field, compared with WT controls (Jung et al., 2017). Shibutani et al. evaluate social behavior between mice of the same genotype in a home-cage environment and observe decreased interaction between *Arid1b* heterozygous mice, compared with WT controls. In open field social interaction and three-chamber sociability and social novelty tests, however, Shibutani et al. do not report any differences between *Arid1b* heterozygous and control mice (Shibutani et al., 2017). This discrepancy could be due to a multitude of factors including animal stress, differences in protocols or environmental stimuli. Taken together, however, all three groups report significant impairments in social behavior in *Arid1b* heterozygous mice (Celen et al., 2017; Jung et al., 2017; Shibutani et al., 2017). These results agree with those seen in other mouse models of ASD, including haploinsufficiency of *Chd8* (Katayama et al., 2016).

Intellectual disability is a common comorbid disorder with ASD and is present in patients with haploinsufficient mutations of ARID1B (Yu et al., 2015a), as well as in FXS (Harris

et al., 2008). *Arid1b* heterozygous mice present with learning and memory deficits (Jung et al., 2017), which have also been observed in previous animal models of ASD (Kim et al., 2014). Jung et al. perform the Morris water maze test to assess cognitive function in *Arid1b* heterozygous mice. These mutant mice exhibit increased escape latencies during training trials and spend less time in the target quadrant during probe trials, with no changes in the distance or speed of swimming, compared with controls (Jung et al., 2017). However, another group reports that *Arid1b* heterozygous mice do not exhibit cognitive deficits as measured by the Morris water maze test (Celen et al., 2017). Celen and colleague's results are unexpected and somewhat surprising given the strong neurogenetic evidence of *Arid1b* haploinsufficiency causing intellectual disability (Halgren et al., 2012; Hoyer et al., 2012; Santen et al., 2012). Jung et al. also perform the novel-object recognition test to assess recognition memory. They find that *Arid1b* heterozygous mice demonstrate no preference for a novel object over a familiar one, whereas control mice spend considerably more time interacting with the novel object (Jung et al., 2017). *Arid1b* heterozygous mice are also less successful in the T-maze test, compared to controls (Jung et al., 2017). However, Shibutani et al. report that their *Arid1b* heterozygous mice do not demonstrate any deficiencies in the T-maze test, although they did not publish any of this data or report the method or protocol used (Shibutani et al., 2017). In addition, Celen et al. report that *Arid1b* heterozygous mice respond normally to foot shocks and perform similarly to controls in fear conditioning tests, while Shibutani et al. report that *Arid1b* heterozygous mice display a heightened response to foot shocks and enhanced performance in fear conditioning tests (Shibutani et al., 2017). Reports on FXS mouse models are also inconsistent in contextual and cued fear conditioning tests (Paradee et al., 1999; Dobkin et al., 2000; Van Dam et al., 2000; Auerbach et al., 2011; Ding et al., 2014; Kazdoba et al., 2014), which implies that

these fear conditioning paradigms may be unreliable methods for testing cognitive deficits in genetic mouse models of ID

In summary, *Arid1b* heterozygous mice demonstrate anxiety-like behavior, social behavior deficits and learning/memory impairments. Although there exists some contradiction regarding the results of a subset of individual behavioral assays, *Arid1b* heterozygous mice conveniently recapitulate many ASD-like and ID-like behavioral profiles, similar to those seen in other mouse models (Bilousova et al., 2009; Kazdoba et al., 2014; Katayama et al., 2016). Therefore, *Arid1b* heterozygous mouse models present a useful opportunity for advancing our understanding of the pathogenesis and underlying mechanisms of neurodevelopmental disorders and related behavioral defects.

1.5 GABA modulation as a therapeutic intervention for Arid1b haploinsufficiency-induced neurodevelopmental conditions

As stark decreases in PV-positive interneurons are seen in *Arid1b* heterozygous cortices, Jung et al. attempt to rescue some of the behavioral deficits in these mice using a positive allosteric modulator for the $GABA_A$ receptor, clonazepam (Jung et al., 2017). Clonazepam is shown to be effective in treating seizures and anxiety in humans (Dahlin et al., 2003) and also effectively ameliorates some of the behavioral deficits in the BTBR mouse ASD model (Han et al., 2014). Accordingly, Jung et al. observe that intraperitoneal injection of clonazepam at a concentration of 0.0625 mg/kg 30 minutes prior to behavioral assays is sufficient to rescue impaired recognition memory, social memory and heightened anxiety-like behavior in *Arid1b* heterozygous mice but has no measurable effect on depression-like behaviors. Clonazepam treatment also rescues the decreased mIPSC frequency in *Arid1b* heterozygous mice (Jung et al., 2017). While it is

encouraging to see that treatment with a GABA allosteric modulator is sufficient to rescue several of the hallmark behavioral abnormalities in this mouse model of ASD and ID, attempted restoration of the excitatory/inhibitory imbalance in *Arid1b* heterozygous mice does not lead to improvements in all behavioral tests. Thus, there appears to be more at play in this mouse model than a gross reduction in the interneuron population. Clonazepam, or related drugs, may still prove to alleviate some of the symptoms caused by excitatory/inhibitory imbalance, be it due to *ARID1B* haploinsufficiency or other causes. It is especially promising that this treatment leads to improved behavior in adult mice, which may indicate that treatment during a critical developmental window may not be entirely necessary to treat all consequences of *ARID1B* haploinsufficiency. A deeper understanding of the cell-types and circuits regulating the behaviors related to ASD and ID will be required to develop more targeted therapies.

1.6 Arid1b haploinsufficiency and body growth

All three groups find reduced body weight at multiple ages in *Arid1b* heterozygous mice, compared with controls (Celen et al., 2017; Jung et al., 2017; Shibutani et al., 2017). Jung et al. report that females show less obvious weight differences than males (Jung et al., 2017). Mice lacking one copy of *Arid1b* also develop disproportionately small kidneys and hearts (Celen et al., 2017). Celen et al. hypothesize that the growth hormone-releasing hormone–growth hormone–Insulin-like growth factor (GHRH-GH-IGF) axis deficiencies could be responsible for the smaller body size observed in *Arid1b* heterozygous mice and the short stature reported in *ARID1B* human patients (Santen et al., 2012; Celen et al., 2017). They report reduced IGF1 protein levels in the plasma and lower *Igf1* mRNA levels in the liver but no changes in GH in the pituitary gland or fasting plasma of *Arid1b* heterozygous mice. The pituitary gland also appears to respond normally to GHRH stimulation and they detect no change in *Ghrh* mRNA levels in the

hypothalamus.

To ascertain whether this reduction in IGF1 in *Arid1b* heterozygous mice is indeed due to a problem with CNS control of the GHRH-GH-IGF axis, Celen et al. conditionally delete one copy of *Arid1b* in the CNS and PNS or in the liver by crossing *Arid1b*$^{Fl/+}$ mice with *Nestin-Cre* mice or *Albumin-Cre* mice, respectively. The *Nestin-Cre; Arid1b*$^{Fl/+}$ mice present with a similar growth impairment and a reduction in plasma IGF1 levels with no accompanying increase in GH. *Albumin-Cre; Arid1b*$^{Fl/+}$ mice do not demonstrate any significant differences in body size or in plasma IGF levels, when compared to controls. Neuron-specific haploinsufficiency of *Arid1b* is, therefore, the cause of the growth retardation and GHRH-GH-IGF deficiencies observed in *Arid1b* heterozygous mice (Celen et al., 2017). It should be noted, however, that the *Nestin-Cre* mouse driver line has been reported to have hypopituitarism, decreased anxiety-like behavior and lower body weight (Galichet et al., 2010; Harno et al., 2013; Giusti et al., 2014; Declercq et al., 2015). As Celen et al. do not include the Cre-driver lines as controls in their conditional knockout experiments (Celen et al., 2017), these results should be cautiously interpreted until they can be independently confirmed. Celen et al. also attempt to treat the smaller body size and weight by correcting the apparent GHRH-GH-IGF deficiencies. They first treat *Arid1b* heterozygous mice with recombinant human IGF1, but this does not have any measurable effects on body weight or anxiety-like behavior. Treatment with recombinant mouse GH for 40 consecutive days, however, is sufficient to rescue the growth deficits and grip weakness in *Arid1b* haploinsufficient mice but has no measurable effect on anxiety-like behavior (Celen et al., 2017).

1.7 MACF1 in nervous system development and maintenance

Microtubule-actin crosslinking factor 1 (MACF1), also widely known as actin crosslinking factor 7 (ACF7), is a member of the spectraplakin family of cytoskeletal crosslinking proteins. Spectraplakins are large proteins distinguished by their ability to bind to different cytoskeletal networks. There are only two known mammalian spectraplakins, MACF1/ACF7 and bullous pemphigoid antigen 1 (BPAG1)/dystonin, but this family of proteins is evolutionarily conserved in most multicellular organisms (Suozzi et al., 2012). MACF1 was originally identified as an actin-crosslinking protein in 1995 (Byers et al., 1995) and it belongs to a subset of microtubule plus-end tracking proteins (+TIPs), functioning at the microtubule plus-end to coordinate microtubule and F-actin interactions at the plasma membrane (Gupta et al., 2010). The most widely researched function of MACF1 is in regulation of cytoskeletal proteins, specifically F-actin and microtubules (Leung et al., 1999). Microtubules, the actin cytoskeleton and their interacting components are involved in many polarized cellular processes including cell shape, cell division, intracellular transport, adhesion, and cell migration (Goode et al., 2000; Yarm et al., 2001; Palazzo and Gundersen, 2002; Rodriguez et al., 2003). MACF1 interacts with microtubules and F-actin via distinct microtubule and actin-binding domains to regulate the polarization of cells and coordination of cellular movements (Leung et al., 1999; Sun et al., 2001; Suozzi et al., 2012). MACF1 stabilizes the downstream cytoskeleton structure by either directly binding to microtubules or forming links between microtubules and F-actin (Kodama et al., 2003), and plays an important role in cell migration via its regulation of Golgi polarization (Etienne-Manneville, 2004; Siegrist and Doe, 2007). This large and complex protein, however, is involved in a wide range of cellular signaling networks and processes, including Wnt/β-catenin signaling, cell migration, proliferation, survival and autophagy (Chen et al., 2006; Goryunov et al., 2010; Munemasa et al., 2012; Jorgensen et al., 2014; Sohda et al., 2015; Ka et al., 2016a). MACF1 has recently received increased attention due to its broad expression in

the nervous system, more specifically, in the brain (Bernier et al., 2000; Goryunov et al., 2010; Ka et al., 2014a). *MACF1* mutations have been linked to neurological diseases including Parkinson's disease (PD), autism spectrum disorder (ASD), and schizophrenia (Levinson et al., 2011; Kenny et al., 2014; Wang et al., 2016). On a related note, several contemporary studies from our group and others have found that MACF1 is essential for proper neural progenitor proliferation, neuronal migration and neurite development (Sanchez-Soriano et al., 2009; Goryunov et al., 2010; Ka et al., 2014a; Ka and Kim, 2016; Ka et al., 2016a).

Here, we provide a brief overview of the MACF1 protein and its known functions and interactions, followed by an in-depth analysis of the roles of MACF1 in nervous system development and function. We also seek to highlight current research questions and potential explanations relating to MACF1 and its neuronal activities and related disorders.

1.7.1 Isotype structure and expression

MACF1 is expressed in multiple tissues throughout the body and has various isoforms with distinctive structures. MACF1 is a large protein of ~600 kD (Byers et al., 1995) and its primary function is cross-linking microtubules and F-actin microfilaments. MACF1 is encoded by the *MACF1* gene, which is located on the human chromosome 1p32 and on chromosome 4 in mice (Byers et al., 1995; Bernier et al., 1996; Gong et al., 2001), and is a unique hybrid of dystrophin/spectrin and plakin genetic domains (Leung et al., 1999; Gong et al., 2001). The MACF1 actin-binding domain (ABD) is located at the N-terminus and is composed of either one or two calponin homology domains, CH1 and CH2, respectively (Way et al., 1992; Winder et al., 1995; Leung et al., 1999; Karakesisoglou et

al., 2000; Bandi et al., 2015). Furthermore, the MACF1 ABD is conserved within the spectrin superfamily (Winder et al., 1995; Leung et al., 1999). Adjacent to the ABD in the N-terminus, all MACF1 isoforms possess a plakin domain stemming from spectrin repeats (Leung et al., 1999; Karakesisoglou et al., 2000; Sun et al., 2001; Jefferson et al., 2007), which can be observed throughout the plakin superfamily (Roper et al., 2002). Separating the functionally distinct N- and C-terminal domains, each MACF1 protein exhibits 23 flexible, α-helical spectrin repeats in one domain (Yan et al., 1993; Pascual et al., 1997; Leung et al., 1999; Roper et al., 2002; Suozzi et al., 2012). At the C-terminus of MACF1, two calcium-binding EF-hand motifs can be found (Sun et al., 2001), followed by a spectraplakin-specific Gas2-related protein (GAR) domain responsible for microtubule binding and stabilization (Figure 1.3A) (Leung et al., 1999; Sun et al., 2001; Roper et al., 2002).

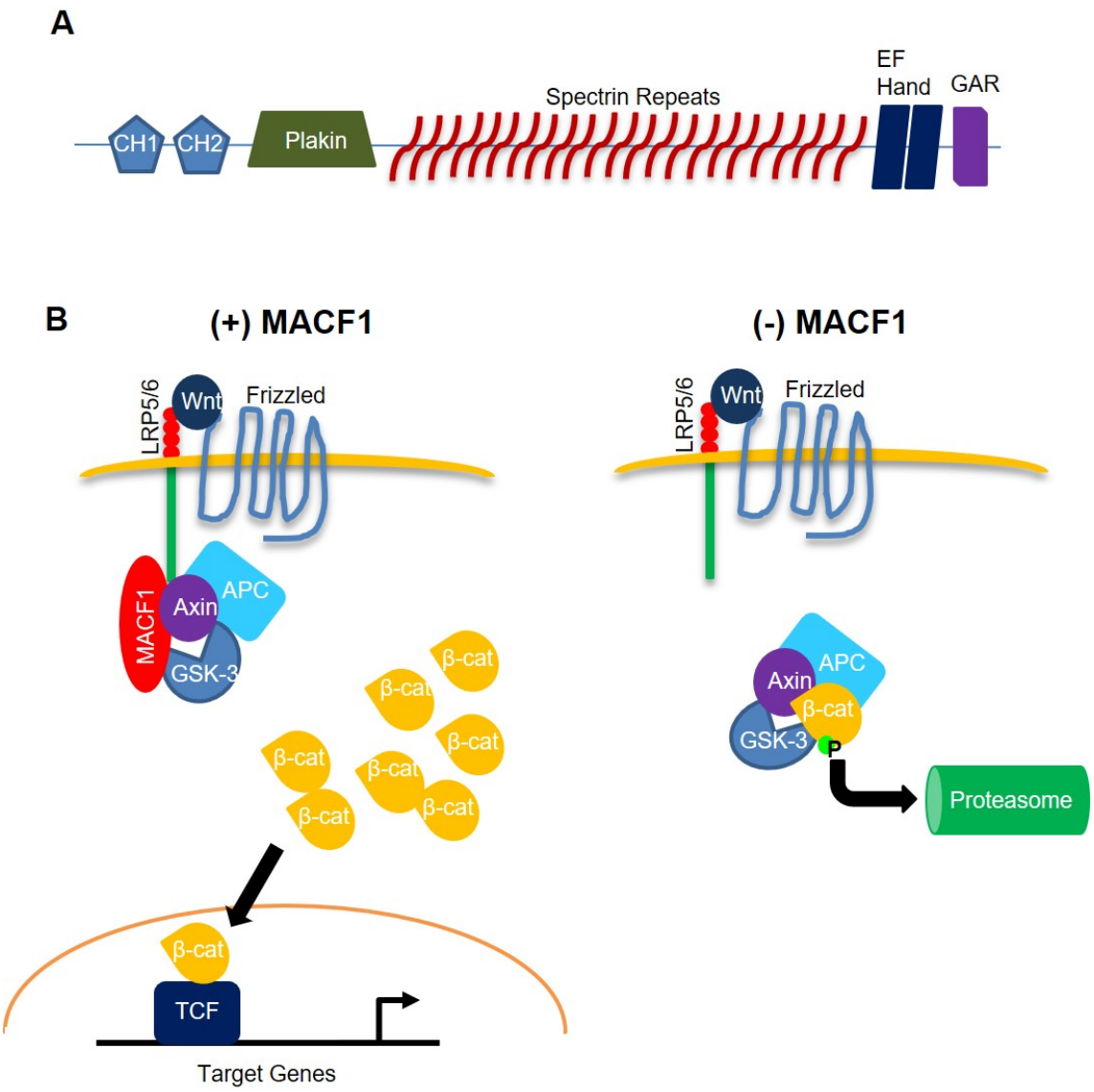

Figure 1.3 MACF1 structure and role in the Wnt/β-catenin signaling

(A) General protein structure of MACF1. The five functional domains found in most MACF1 isotypes are shown: the actin-binding domain (ABD) comprised of CH1 and CH2 fragments, a plakin domain, 23 α-helical spectrin repeats, two EF hand motifs, and a GAR domain at the C-terminus. CH1: calponin homology domain 1. CH2: calponin homology domain 2. GAR: Gas2-related domain. (B) MACF1 knockdown inhibits Wnt/β-catenin signaling. In the absence of MACF1, Axin is unable to translocate to the cell membrane and facilitate the release of β-catenin from its destruction complex. LRP5/6: low-density lipoprotein receptor-related protein 5/6. GSK-3: glycogen synthase kinase-3. APC: adenomatous polyposis coli.

There are six identified murine MACF1 isoforms (Hu et al., 2016). The first three isoforms to be discovered are currently known as MACF1a1, MACF1a2 and MACF1a3 (Bernier et al., 1996; Lin et al., 2005). They possess identical 3' RNA sequences, but display significant variation in the 5' region leading to distinct protein N-termini (Bernier et al., 1996). MACF1a1 and MACF1a2 are both broadly expressed, although MACF1a1 is more predominantly found in the kidney, stomach and skin (Bernier et al., 1996; Bernier et al., 2000; Lin et al., 2005). MACF1a2 is detected at higher levels in the lung and central nervous system (Bernier et al., 1996; Okuda et al., 1999; Bernier et al., 2000; Lin et al., 2005). MACF1a3 expression is mainly restricted to the brain and spinal cord (Bernier et al., 1996; Bernier et al., 2000). In 2001, a fourth MACF1 isoform, MACF1-4, was discovered, with heightened expression levels in the placenta, pituitary gland, heart and lung. MACF1-4 is unique in that it lacks an ABD and instead expresses a series of plectin repeats at its N terminus (Gong et al., 2001). Successively, a further, exceptionally-large MACF1 isoform, MACF1b, was found to be expressed throughout the body. It contains additional plakin repeats between its N-terminal plakin domain and its spectrin repeat domain (Lin et al., 2005). The most recent MACF1 isoform to be isolated, MACF1c, is thought to only be expressed in the nervous system. It is structurally similar to the MACF1a isoforms but lacks an ABD at its N-terminus (Goryunov et al., 2010). A recent, brief review from Hu et al. provides a summary of all MACF1 isotypes and their functions (Hu et al., 2016).

In mice, MACF1 is broadly expressed throughout the developing brain. MACF1 protein can be detected in somas and neurites of cortical neurons (Ka et al., 2014a). During early brain development, MACF1 levels are highest in the ventricular zone and upper cortical areas near the marginal zone of the developing cerebral cortex (Ka et al.,

2014a). As neurodevelopment progresses, MACF1 expression in the ventricular zone gradually decreases while MACF1 levels in the cortical plate steadily increase, following the established pattern of radial neuronal migration (Ka et al., 2014a). Additionally, MACF1 expression in postmitotic neurons is mainly restricted to the marginal zone at early stages of brain development, but transitions into the cortical plate by embryonic day 15.5 (E15.5) (Ka et al., 2014a), indicating that MACF1 may participate in neuronal migration and differentiation.

1.7.2 Cellular signaling associated with MACF1

Beyond its role crosslinking cytoskeletal proteins, MACF1 is actively involved in multiple signaling cascades. In 2006, Chen and colleagues published that *Macf1* knockout (*Macf1*$^{-/-}$) mice do not survive beyond gastrulation, as evidenced by a failure to develop a primitive streak, node or axial mesoderm. Interestingly, they also found that knockout of *BPAG1*, a closely related plakin protein, had strikingly different effects (mice survived until weaning), indicating a unique role for MACF1 in regulation of embryonic development (Chen et al., 2006). They further noted that the developmental defects present in *Macf1*$^{-/-}$ embryos mirror those seen in *Wnt3*$^{-/-}$ and *LRP5/6* double-knockout mice (Liu et al., 1999; Kelly et al., 2004; Chen et al., 2006), indicating a potential role for MACF1 in the Wnt/β-catenin signaling pathway. Consequently, they demonstrated that MACF1 interacts with the β-catenin destruction complex in the cell, binding directly to Axin using the MACF1-spectrin repeat 0 (SR0) domain. The SR0 domain is defined as the region between the MACF1 plakin domain and the first Spectrin repeat (Chen et al., 2006; Ortega et al., 2016). They also illustrated that MACF1 knockdown successfully inhibits Wnt/β-catenin signaling, acting upstream of GSK-3β. It was further shown that MACF1 interacts directly with Wnt co-receptors LRP5/6 at the cell membrane via its SR0

domain and that MACF1 knockdown or overexpression of a mutant MACF1 SR0 dominant-negative protein fragment prevents Axin translocation to the cell membrane (Figure 1.3B) (Chen et al., 2006).

Interestingly, it was later shown that MACF1 is directly phosphorylated by GSK-3 at its C-terminal microtubule-binding domain in skin stem cells, effectively preventing MACF1-microtubule interactions and nullifying microtubule polarization along actin focal-adhesion networks (Wu et al., 2011). We have demonstrated that MACF1 and GSK-3 physically bind to one another and that MACF1 is phosphorylated in a GSK-3-dependent manner in the developing brain (Ka et al., 2014a), similar to what was seen in skin stem cells (Wu et al., 2011). It is unclear, however, whether the GSK-3 and MACF1 interaction is part of the Wnt destruction complex or downstream of growth factor signaling. While Wnt signaling utilizes a protein-protein interaction mechanism to control GSK-3, growth factors regulate a different pool of GSK-3 in the cell by phosphorylation at serine 21 (α) and 9 (β). Both signaling pathways are thought to be insulated. Wu and colleagues have shown that phosphorylation-refractile constructs of GSK-3 modulate MACF1 phosphorylation and activity in skin cells (Wu et al., 2008; Wu et al., 2011). Thus, at least a part of MACF1 regulation by GSK-3 appears to be induced by growth factor signaling. In a breast carcinoma model, it was found that MACF1 is involved in microtubule stabilization via an ErbB2 receptor tyrosine kinase signaling pathway. Heregulin β activates ErbB2, which leads to the phosphorylation and inhibition of GSK-3 through the Memo-RhoA-mDial pathway. Inhibition of GSK-3 kinase activity blocks the phosphorylation of two other cytoskeletal regulators, adenomatous polyposis coli (APC) and cytoplasmic linker-associated protein 2 (CLASP2), and their subsequent

translocation to the cell membrane. MACF1 is recruited to the membrane by APC, but not CLASP2, where it regulates microtubule dynamics (Zaoui et al., 2010).

Additionally, MACF1 plays a role in DOCK 180-ELMO-Rac signaling in cell protrusion/lamellipodium extension during cell migration. In this system, ELMO recruits MACF1 to sites of emerging protrusions, where MACF1 orchestrates microtubule capture and stabilization (Margaron et al., 2013). Following stimulation by integrin, Elmo and MACF1 colocalize at the cell membrane (Margaron et al., 2013; Hu et al., 2016). MACF1 then organizes the cytoskeleton to extend stable membrane protrusions (Margaron et al., 2013).

MACF1 is also integrally involved in some forms of vesicular trafficking, specifically relating to axonal vesicle transport (Burgo et al., 2012) and autophagy (Sohda et al., 2015). MACF1 can act as a Rab21 effector. The complex of Rab21, Kif5A, GolginA4, and MACF1 acts together to transport TI-VAMP from the Golgi to neurite tips along microtubule (Burgo et al., 2012). In autophagy, MACF1 and its binding partner, the *trans*-Golgi protein p230, are responsible for trafficking of mAtg9 from the *trans*-Golgi network to the cell surface, a necessary step in phagophore formation. MACF1 knockdown impairs mAtg9 transport and blocks early steps in autophagy in a state of amino acid starvation (Sohda et al., 2015).

1.7.3 MACF1 in cell proliferation

Cell proliferation is the process that results in an increased number of cells. During cell division, microtubule and actin interactions regulate spindle positioning and cytokinesis.

Abnormal microtubules and actin cytoskeleton dynamics cause cytokinesis defects, thus altering cell proliferation (Hossain et al., 2003; Zhu et al., 2005; Moulding et al., 2007). In osteoblast cells, MACF1 knockdown inhibits cell proliferation and induces S phase cell cycle arrest (Hu et al., 2015). Additionally, the microtubule organizing center (MTOC) fails to form in proximity to the condensed α-tubulin fibers surrounding the nucleus in osteoblasts(Hu et al., 2015). These observations indicate dysregulated cytokinesis following MACF1 knockdown (Hossain et al., 2003; Zhu et al., 2005; Moulding et al., 2007; D'Avino et al., 2015). Wu and colleagues, however, have observed no significant deficit in cell proliferation in epidermal or endodermal cells in the absence of MACF1 expression (Wu et al., 2008; Wu et al., 2011). This cell type-specific function of MACF1 could be explained by unknown unique MACF1 protein-protein interactions in osteoblast cells or by additional proteins fulfilling the same functional role as MACF1 in epidermal and endodermal cells during cytokinesis (D'Avino et al., 2015; Hu et al., 2015). Taken together, these findings may provide insight into the role of MACF1 in the proliferation of neural progenitor cells.

In dividing neural progenitor cells, proper positioning of the centrosome, the main MTOC, is necessary for cell proliferation (Higginbotham and Gleeson, 2007). Neurons originate from a limited number of neural progenitor cells during embryonic development (Homem et al., 2015). Neural progenitors can either self-renew (symmetric division) or undergo the process of neurogenesis, in which one daughter remains a neural progenitor cell and the other undergoes sequential differentiations toward becoming a neuron (asymmetric division) (Gotz and Huttner, 2005; Huttner and Kosodo, 2005; Rakic, 2009; Franco and Muller, 2013; Greig et al., 2013; Homem et al., 2015). This process takes place in the ventricular zone (VZ) or subventricular zone (SVZ) of the

developing cerebral cortex for most excitatory pyramidal neural progenitors and in the VZ or SVZ of the medial ganglionic eminence (MGE) for most inhibitory interneuron progenitors (Gotz and Huttner, 2005; Huttner and Kosodo, 2005; Franco and Muller, 2013; Greig et al., 2013; Homem et al., 2015). Throughout the process of neurogenesis, a significant reorganization of cellular components is required before mitosis can take place. Following the completion of S phase, the nucleus must migrate before apical mitosis can be undergone in a process known as interkinetic nuclear migration, which requires the interplay of the actin and microtubule cytoskeletons (Taverna and Huttner, 2010; Miyata et al., 2014; Mora-Bermudez and Huttner, 2015). Initially, neural progenitors and/or stem cells divide symmetrically along a vertical axis before asymmetrical division along a horizontal axis can begin (Gotz and Huttner, 2005; Taverna et al., 2014; Mora-Bermudez and Huttner, 2015). The plane of neural progenitor division is highly regulated by the cytoskeleton, specifically the orientation of mitotic spindles (Konno et al., 2008; Mora-Bermudez et al., 2014; Mora-Bermudez and Huttner, 2015), thus microtubules and their regulatory proteins are crucial to proper proliferation and cell division throughout neural progenitor proliferation (Mora-Bermudez et al., 2014; Zigman et al., 2014; Homem et al., 2015; Mora-Bermudez and Huttner, 2015). During mitosis, microtubule assembly and disassembly at the plus- and minus-ends is required for proper separation of chromosomes and cytokinesis (Tanenbaum et al., 2006; Howard and Hyman, 2007; Mayr et al., 2007; Ferreira et al., 2014). +TIPs crucially regulate microtubule dynamics during cell division and must be maintained at proper levels (Wade, 2009; Ferreira et al., 2014), as abnormal microtubule stabilization can suppress microtubule dynamics, preventing cell division and resulting in apoptosis (Wood et al., 2001; Wade, 2009). Like other +TIPs, MACF1 is localized to microtubule plus-ends and physically interacts with several other +TIPs, including EB1, APC and CLASP (Chen et al., 2006; Scheffler and Tran, 2012), and regulates centrosome movement (Ka et al.,

2014a). All of this circumstantial evidence suggests the importance of MACF1 in neural cell proliferation. However, its function in this process is still unclear.

Examining a *Macf1* conditional knockout mouse model (*Macf1* cko), in which *Macf1* expression is eliminated in the developing nervous system, Goryunov and colleagues observed extensive heterotopia, or distinct disorganization of neural layers, in the cortex and hippocampus of *Macf1* cko mice (Goryunov et al., 2010). The majority of early-born cortical neurons were found in their proper, deep layers, whereas neurons with a late-born phenotype appeared to be mixed in with the deep-layer neurons and not in their typical outer cortical layers (Goryunov et al., 2010). Heterotopia is often attributed to neuronal migration impediments but can also be caused by defective neuronal proliferation. It is unclear whether the layer positioning defects in *Macf1* cko mice are due to a reduced neuronal migration rate, aberrant migratory guidance, or defective neuronal proliferation (Goryunov et al., 2010).

1.7.4 MACF1 in neuronal and non-neuronal cell migration

Cell migration is a fundamental cellular process and is essential for embryonic development, tissue repair and regeneration, and tumor metastasis (Watanabe et al., 2005). Cell migration begins with various extracellular cues such as chemokines and signals from the extracellular matrix that lead to the polarization and the extension of protrusions in the direction of movement (Horwitz and Webb, 2003). Migrating cells must acquire a polarized, asymmetric morphology and develop a single leading edge with one filopodia (Lauffenburger and Horwitz, 1996). During the migration process, cells actively reorganize the actin cytoskeleton and microtubules (Watanabe et al., 2005). MACF1 directly interacts with other +TIPs, such as the EB1 protein, to recruit cell polarity and

signaling molecules to microtubule tips (Slep et al., 2005). MACF1 also interacts with CLASP2, another +TIP protein, and regulates CLASP localization. CLASP2 is involved in microtubule stabilization and is required for efficient, persistent motility (Drabek et al., 2006). It was recently discovered that MACF1 also directly interacts with the ELMO protein (engulfment and cell motility protein), as mentioned above. ELMO1 recruits MACF1 to the cell membrane, where MACF1 regulates microtubule capture and stabilization of cellular protrusions (Margaron et al., 2013).

In *MACF1* null cells, many microtubules exhibit irregular trajectories and are more sensitive to depolymerizing agents. Moreover, loss of MACF1 causes defective polarization of stable microtubules in epidermal cells, and a lack of coordinated migration in response to wounding (Kodama et al., 2003). . In migrating skin stem cells, GSK-3β phosphorylates the microtubule-binding domain of MACF1, resulting in the dissociation of MACF1 from microtubules. Thus, phosphorylation of MACF1 is necessary for microtubule growth and for skin stem cell migration (Wu et al., 2011). Moreover, it was recently suggested that the FAK/Src kinase phosphorylation of MACF1 is essential for its binding to F-actin and coordination of cytoskeletal dynamics at focal adhesions. The effects of MACF1 phosphorylation in focal adhesion dynamics and cell motility have been clearly observed in epithelial cells (Yue et al., 2016). In motile fibroblasts, MACF1 regulates cortical CLASP localization, allowing microtubule stabilization and promoting directionally persistent motility (Drabek et al., 2006). In breast carcinoma cells, the ErbB2 receptor controls microtubule capture by recruiting MACF1 to the plasma membrane, where MACF1 contributes to microtubule guidance and capture in migrating cells (Zaoui et al., 2010). miR-34a regulates cytoskeletal proteins such as MACF1, LMNA, GFAP, ALDH2 and LOC100129335, and transfection of miR-34a into carcinoma

cells causes inhibition of cell migration and invasion (Cheng et al., 2010).

Neuronal migration and positioning are critical steps for establishing functional neural circuitry in the developing brain. Therefore, abnormal neuronal migration during development causes brain malformations, which have been linked to a variety of neurodevelopmental and neuropsychiatric diseases such as ASD, attention deficit hyperactivity disorder (ADHD), intellectual disability, and schizophrenia (Gleeson and Walsh, 2000; Kaufmann and Moser, 2000; Jan and Jan, 2010; Wegiel et al., 2010). Neuronal migration is also a dynamic process, which requires persistent reconstruction of the cytoskeleton. In this context microtubules and microtubule-related proteins, including MACF1, play important roles in the regulation of neuronal migration during brain development (Feng and Walsh, 2001; Bielas and Gleeson, 2004; Xie et al., 2006). We and others have reported that MACF1 is highly expressed in the nervous system and developing brain (Leung et al., 1999; Ka et al., 2014a). *Macf1* conditional knockout brains using a nestin-cre driver display partially-mixed upper- and deeper-layer neurons in the cerebral cortex (Goryunov et al., 2010). The expression pattern of MACF1 and the heterotopic cortical phenotype in *Macf1/nestin-cre* conditional knockout mice strongly suggest a role for MACF1 in neuronal migration. Indeed, our study shows that neuron-specific *Macf1* deletion using a Nex-cre driver or *in utero* electroporation of the Dcx-cre-iGFP construct suppresses the radial migration of cortical pyramidal neurons, resulting in aberrant positioning of excitatory pyramidal neurons in the cortical layers (Ka et al., 2014a). During radial neuron migration, MACF1 regulates leading process morphogenesis and dynamics. *Macf1*-deleted neurons develop short and unstable leading processes resulting in unidirectional and slow radial neuron migration. Also, *Macf1*-deleted pyramidal neurons exhibit microtubule destabilization and static

centrosomes (Ka et al., 2014a). Centrosomes show dynamic back-and-forth movements along the leading process to pull the soma during normal neuron migration. However, centrosomes in *Macf1*-deleted neurons have little movement and remain close to the cell body, resulting in the creation of insufficient tension for somal translocation. Thus, MACF1-mediated regulation of microtubule stability and centrosome movement contributes to radial neuron migration in the developing brain. Consistent with migrating skin stem cells, GSK-3-mediated phosphorylation is an important mechanism for the MACF1 function in neuronal migration (Wu et al., 2011; Ka et al., 2014a). In addition to the role of MACF1 in radial migration, we have recently shown that MACF1 is also a key molecule in tangential neuron migration (Ka et al., 2016a). MACF1 is highly expressed in the tangential migratory stream (Ka et al., 2016a). *Macf1* deletion in interneuron progenitors and progeny using Nkx2.1-cre or Dlx5/6-cre lines results in abnormal migration and defective positioning of GABAergic inhibitory interneurons in the mouse cerebral cortex and hippocampus (Ka et al., 2016a). *Macf1*-deleted GABAergic interneurons show slower speed and aberrant orientation of movement during migration. Importantly, MACF1 regulates the transition of migration direction from a tangential to a radial route during cortical development (Ka et al., 2016a). *Macf1*-deleted interneurons develop abnormal leading processes and disrupted microtubule stability and severing (Ka et al., 2016a). Overall, MACF1 is an essential regulator of cell migration via its management of microtubule and actin cytoskeleton dynamics.

1.7.5 MACF1 in neurite development

Neurite outgrowth is an essential event in neural development, which involves coordinated changes between the actin cytoskeleton and the microtubule network (da Silva and Dotti, 2002; Tsaneva-Atanasova et al., 2009). This process is regulated by

various proteins that manipulate the cytoskeletal network by various means (Belliveau et al., 2006; Tian et al., 2015). Recent studies indicate that MACF1 plays a vital role in neurite outgrowth. MACF1 controls the extension and differentiation of neurites in *Drosophila* neurons (Sanchez-Soriano et al., 2009). Knockdown of *MACF1* decreases axon outgrowth, a process dependent on its F-actin- and microtubule-binding domains in *Drosophila* neuronal cultures (Sanchez-Soriano et al., 2009). We have recently provided evidence that supports the MACF1 function in mouse neurite growth in vivo (Ka and Kim, 2016). Using an *in utero* electroporation method and conditional knockout mouse lines to generate temporal and spatial *Macf1* deletion, we have knocked out or down *Macf1* in developing cortical and hippocampal pyramidal neurons. We have found that MACF1 deletion decreases dendrite growth and branching in mouse pyramidal neurons. Accordingly, *Macf1*-deleted neurons show reduced density and abnormal morphology of dendritic spines. *Macf1*-deleted spines appear long and thin with short spine heads and necks (Ka and Kim, 2016). The cellular cytoskeletal network is critical in dendritic spine morphogenesis, a process which is regulated by a complex network of signaling molecules (Korobova and Svitkina, 2010; Penzes and Rafalovich, 2012; Shirao and Gonzalez-Billault, 2013). Dendritic spine morphology is dependent on the amount and structure of F-actin within neurons (Okamoto et al., 2004; Koleske, 2013). MACF1 interacts with F-actin to regulate cell polarization (Leung et al., 1999; Sun et al., 2001). Loss of MACF1 also impairs the elongation of callosal axons in the brain. MACF1 is thought to regulate neurite development via GSK-3 signaling in the brain (Figure 3). As described above, knockdown of the MACF1 protein inhibits Wnt signaling, which is mediated by GSK-3 (Chen et al., 2006). GSK-3 is a master-regulator of the cellular cytoskeletal network (Zhou and Snider, 2005), neural progenitor regulation (Kim et al., 2009) and neurite growth (Zhou et al., 2004; Kim et al., 2006). Over-expression of a constitutively-active GSK-3β (ca-GSK-3β) construct reduces the number and length of

dendrites. However, co-expression of MACF1 S:A (phosphorylation-refractile form) rescues the inhibitory effects of ca-GSK-3β (Ka and Kim, 2016), suggesting that GSK-3-mediated phosphorylation is an important mechanism for the MACF1 function in neurite development. Future studies will be needed to expand our understanding of MACF1 as to regulatory mechanisms and cellular signaling pathways in neurite development.

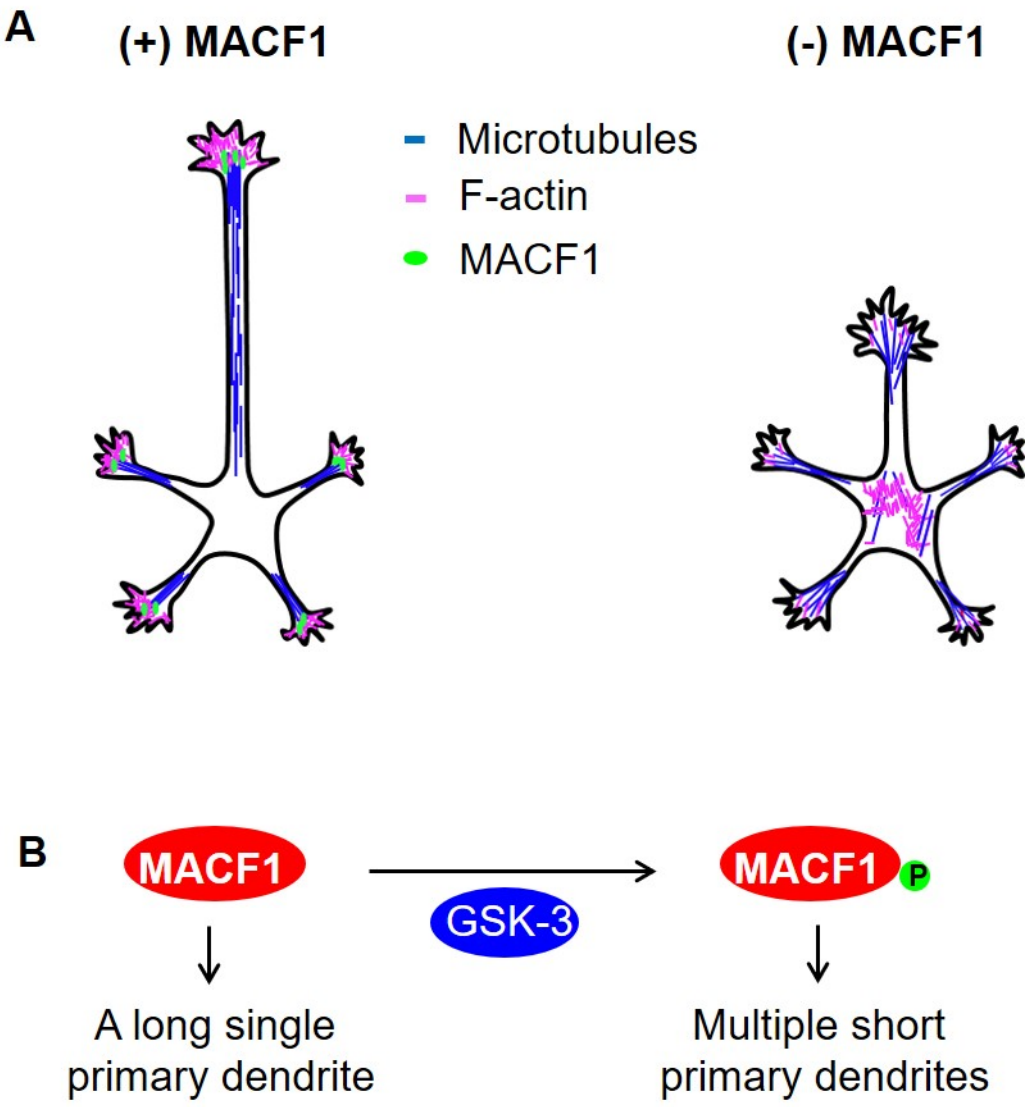

Figure 1.4 MACF1 in neurite outgrowth

(A) MACF1 regulation of neurite outgrowth. MACF1 localizes near the distal ends of growing axons and dendrites, where it stabilizes microtubule bundles and leads to the assembly of polymerized actin. In the absence of MACF1, microtubules and actin are

disorganized and unstable at the neurite tip and scattered in the cytosol. (B) GSK-3 regulates the activity of MACF1 in dendrite outgrowth and arborization. When MACF1 is phosphorylated by GSK-3, it results in multiple short primary dendrites. When MACF1 remains unphosphorylated, neurons extend a single long primary dendrite.

1.7.6 Neural diseases and MACF1

MACF1 gene mutations have been associated with neuromuscular diseases. Mutations in cytoskeletal genes, such as *dystonin*, *dystrophin*, and *plectin* result in myopathic consequences, thus suggesting MACF1 may have similar muscular phenotypes (Jorgensen et al., 2014). In a family with novel neuromuscular conditions including diminished motor skills, lax muscles, and occasional hypotonia, the *Macf1* gene product is found at a low level due to a chromosome modification in a gene locus. This novel myopathy is termed “spectraplakinopathy type I,” based on MACF1 belonging to the spectraplakin protein family (Jorgensen et al., 2014). Ultrastructural changes and altered motility are accompanied in muscle tissues of affected individuals (Jorgensen et al., 2014).

MACF1 mutations have been shown to contribute to psychological disorders. Two schizophrenia risk genes, *disrupted in schizophrenia 1* (*DISC1*) and *dysbindin* (*DTNBP1*), are associated with cognitive deficits in schizophrenics (Tamminga and Holcomb, 2005). DISC1 and DTNBP1 are important molecules in many aspects of neural development including neural progenitor proliferation and neurogenesis, neurite outgrowth, neuronal migration, and synaptic differentiation (Kamiya et al., 2005; Duan et al., 2007; Hayashi-Takagi et al., 2010; Ishizuka et al., 2011; Kang et al., 2011; Steinecke et al., 2012). Several instances of synaptic pathology have been reported in individuals diagnosed with schizophrenia (Harrison and Weinberger, 2005). Both proteins form a similar network of protein-protein interactions, and the profiles of proteins that they

interact with suggest similar functions in cytoskeletal stability and organization, intracellular transport, and cell cycle progression (Camargo et al., 2007). Camargo and colleagues have shown that MACF1 is one of the proteins involved in critical interactions with both DISC1 and DTNBP1. They suggest that DISC1 and DTNBP1 may play a converging role in affecting synapse structure and function by disrupting intracellular transport and cytoskeletal stability via interactions with MACF1, contributing to cognitive deficits in schizophrenics (Camargo et al., 2007). Furthermore, schizophrenia and ASD may share underlying pathology, as suggested by shared risk genes (Levinson et al., 2011). For example, rare mutations in genes that are functional in the synapse have been identified in ASD and schizophrenia cases (Kenny et al., 2014). Several novel loss-of-function variants overlap in both cases, including those coding for proteins involved in protein-protein interactions with DISC1, such as MACF1 (Kenny et al., 2014). These results suggest that mutations in multiple genes involved in synapse formation, including *Macf1*, are a risk factor for both ASD and schizophrenia.

Several neurodegenerative disorders show evidence of cytoskeletal collapse. In particular, a hallmark of Parkinson's Disease (PD) is degeneration of dopaminergic (DA) neurons in the substantia nigra pars compacta (Wang et al., 2016). It has been observed that both genetic and neurotoxic causes of PD may target the cytoskeleton, and resulting cytoskeletal disorganization and dysregulation may be a mechanistic cause of PD (Feng, 2006). Two lines of evidence suggest that MACF1 is involved in the pathogenesis of PD. First, *Macf1* knockout inhibits Wnt signaling, which is important in the development of dopamine neurons. Second, *MACF1* mRNA levels in DA neurons of PD patients are significantly lower than in controls (Simunovic et al., 2009). Thus, reduced MACF1 levels leading to dysregulation of the cytoskeleton may cause vulnerability of DA neurons to

neurodegeneration. More directly, *MACF1* has been shown to be a risk gene for PD (Wang et al., 2016). MACF1 is a downstream target of PD biochemical pathways and has been found to be significantly associated with PD in 713 families studied. In addition, knockdown of the *Macf1* orthologue *Vab-10* in *C. elegans* results in selective loss of DA neurons (Wang et al., 2016). These results suggest that MACF1 may contribute to genetic etiology of PD and may be a mechanistic cause.

Optic nerve injury is another neurological condition in which MACF1 has been implicated. Retinal ganglion cells (RGCs) are the final neuronal output of the retina, receiving visual signals from amacrine and bipolar cells and transmitting them to the brain via the optic nerve (Munemasa et al., 2012). Degeneration of RGCs and their axons in the optic nerve leads to vision loss in multiple optic neuropathies, including glaucoma most commonly. The work of Munemasa and colleagues shows strong Nell2 and MACF1 expression in RGCs (Munemasa et al., 2012). Nell2 has a strong neuroprotective function, increasing survival of neurons in the hippocampus and cerebral cortex. After an optic nerve injury, Nell2 interacts with MACF1 to promote survival of RGCs (Munemasa et al., 2012).

CHAPTER 2: ARID1B DELETION REGULATES CORTICAL NEURAL PROGENITORS AND INTERNEURON PROGENITORS IN MICE

Jeffrey J. Moffat[1], Eui-Man Jung[1], Minhan Ka[1,2], Amanda L. Smith[1] and Woo-Yang Kim[1]*

[1]Developmental Neuroscience, Munroe-Meyer Institute, University of Nebraska Medical Center, Omaha, NE 68198

[2]Research Center for Substance Abuse Pharmacology, Korea Institute of Toxicology, Daejeon 34114, Republic of Korea

2.1 Abstract

ARID1B gene encodes a critical DNA-binding subunit of the BAF chromatin-remodeling complex, which broadly regulates gene expression. ARID1B has been shown to interact with the transcription factor β-cat, which regulates neurogenesis, and genetic deletion of *Arid1b* in mice alters the expression of several β-cat-regulated genes involved in neurogenesis and cell cycle control. Genetic evidence indicates that haploinsufficiency of ARID1B causes ID and ASD, but the neural function of ARID1B is largely unknown. In this study we used both conditional and global *Arid1b* knockout mouse strains to exam the effects of *Arid1b* deletion on cortical and ventral neural progenitor populations. We detected an overall decrease in cortical and ventral neural progenitor proliferation following homozygous deletion of *Arid1b*, as well as altered cell cycle regulation and increased cell death. Each of these phenotypes was more pronounced in ventral neural progenitors. Furthermore, we observed decreased β-catenin protein nuclear localization in *Arid1b*-deficient neurons. Conditional homozygous deletion of *Arid1b* in ventral neural progenitors also led to pronounced ID- and ASD-like behaviors in mice, whereas cortical neural progenitor mutants only exhibited minor cognitive deficits. This study suggests an essential role for ARID1B in forebrain neurogenesis and clarifies its more pronounced role in inhibitory neural progenitors. Our findings also provide insights into the pathogenesis of ID and ASD.

2.2 Introduction

ID and ASD affect between one and three percent of the global population (Perou et al., 2013; Srivastava and Schwartz, 2014). These and other related neurodevelopmental disorders represent a significant emotional and financial burden for affected individuals and their families (Perou et al., 2013). Unfortunately, treatment for these conditions remains limited because many of the key molecular factors and their associated pathogenic mechanisms are still poorly understood. ARID1B is a sequence-specific, DNA-binding subunit in mammalian SWI/SNF or BAF chromatin-remodeling complexes (Collins et al., 1999; Wang et al., 2004), whose epigenetic modifications have been linked to ID and ASD (Son and Crabtree, 2014; Narayanan et al., 2015; Jung et al., 2017). As such, genetic *ARID1B* mutations can lead to widespread alterations in gene and protein expression. The vast majority of mutations affecting *ARID1B* observed in humans have been nonsense mutations, which result in the production of a truncated, non-functional ARID1B protein (Sim et al., 2015)**.** A few missense frameshift mutations have also been observed in patients with ID and/or ASD (Tsurusaki et al., 2012; Yu et al., 2015b). Because of the clear genetic correlation between *ARID1B* mutations and ASD and ID, defining the function of ARID1B in forebrain development is a crucial step toward understanding the neurological and developmental mechanisms responsible for these pathogenic phenotypes (Santen et al., 2012; Tsurusaki et al., 2012; Mariani et al., 2015).

As we and other groups have recently reported, deletion of one *Arid1b* allele in mice is sufficient to cause significant behavioral deficiencies, including ID- and ASD-like behaviors (Celen et al., 2017; Jung et al., 2017; Shibutani et al., 2017). These mouse models of *Arid1b* haploinsufficiency are useful because they mirror the gene dosage effects seen in human patients, but are less useful for deciphering the neurobiological function of the ARID1B protein, whose levels remain above fifty percent in *Arid1b* mutant heterozygotes, compared to their wild-type littermates (Celen et al., 2017; Jung et al., 2017; Shibutani et

al., 2017).

Despite their prevalence and severity, the underlying pathogeneses of ID and ASD remain unknown. One prevailing theory posits that an imbalance of neuronal excitation and inhibition in the developing brain underlies the neurological dysfunctions observed in patients with these neurodevelopmental disorders (Rubenstein and Merzenich, 2003; Gatto and Broadie, 2010; Cellot and Cherubini, 2014; Nelson and Valakh, 2015). This theory is supported by several studies demonstrating either decreased inhibitory GABAergic signaling and/or increased excitatory signaling in autistic brains (Cellot and Cherubini, 2014; Nelson and Valakh, 2015). The balanced and coordinated function of pyramidal neurons and interneurons regulates excitatory and inhibitory tones in the brain. Importantly, the numbers of these excitatory and inhibitory neurons are determined by the proliferation of cortical and ventral neural progenitors, respectively, in the developing brain (Nagl et al., 2007). We previously reported a significant decrease in the total number of GABAergic interneurons in the cerebral cortex of *Arid1B* mutant mice, suggesting that excitatory/inhibitory (E/I) imbalance may play a role in the pathology of *ARID1B*-related neurodevelopment disorders.

During mouse brain development, forebrain excitatory and inhibitory neurons are generated in distinct brain regions and migrate along separate pathways before converging in the cerebral cortex. Excitatory neurons are born in the ventricular zone (VZ) of the developing cerebral cortex and migrate radially into the cortical plate, usually along radial glial processes (Rakic, 1972; Chanas-Sacre et al., 2000; Hartfuss et al., 2001; Noctor et al., 2001; Stiles and Jernigan, 2010). Most inhibitory interneurons (GABAergic neurons) originate from a population of neural progenitors within the MGE of the ventral telencephalon and migrate tangentially into the dorsal telencephalon and then radially into the cortical plate (Anderson et al., 2001; Molyneaux et al., 2007; Sultan et al., 2013). Cortical and ventral neural progenitors both need to be tightly regulated to ensure proper

brain development as they have distinct and complimentary roles in the mature brain and each is each under the control of different pathways (Gatto and Broadie, 2010; Nelson and Valakh, 2015).

In order to separately identify the neurobiological function of ARID1B in excitatory and inhibitory neurons and their progenitors, we used conditional knockout mouse models to explicitly delete the *Arid1B* in either cortical or ventral neural progenitors. In this study, we utilize an *Emx1-Cre* driver line to conditionally delete *Arid1b* in cortical neural progenitors and both a *Dlx5/6-Cre* and *Nkx2.1-Cre* driver line to knockout *Arid1b* in ventral neural progenitors (Zerucha et al., 2000; Gorski et al., 2002; Monory et al., 2006; Xu et al., 2008; Taniguchi et al., 2011). We report impaired proliferation in the cortical neural progenitor population and, to a greater extent, in ventral neural progenitors. This may be due to altered cell cycle regulation, as we observe decreased cell cycle speed in ventral neural progenitors with homozygous *Arid1b* deletion and a decreased rate of cell cycle re-entry in both cortical and ventral neural progenitors. In both progenitor populations we also report an increased number of apoptotic cells.

Brahma-related gene-1 (BRG1), encoded by *SMARCA4*, is the core subunit of the mammalian BAF chromatin remodeling complex (Chiba et al., 1994; Hodges et al., 2016) and interacts directly with ARID1B in the nucleus (Hurlstone et al., 2002; Inoue et al., 2002). BRG1 has also been shown to physically interact with nuclear β-catenin at target gene promoters and facilitate transcriptional activation, most likely via chromatin remodeling (Barker et al., 2001). Intriguingly, two recent reports suggest that ARID1B represses β-catenin's transcription factor activity in concert with BRG1 in vitro and in blood lymphocytes from patients with *ARID1B* mutations (Vasileiou et al., 2015; Wu et al., 2016). We recently showed, however, that *Arid1b* haploinsufficient mice express lower levels of *β-catenin* and its downstream target genes in the ventral telencephalon (Jung et al., 2017), which aligns more with what is seen in a Brg1/Brm-deficient cell line (Barker et al., 2001).

In this study we observe that homozygous deletion of *Arid1b* leads to decreased nuclear localization of β-catenin in vitro and in vivo. We also report that homozygous deletion of *Arid1b* in ventral progenitors leads to ID- and ASD-like behavioral phenotypes, similar to those seen in *Arid1b* haploinsufficient mice (Celen et al., 2017; Jung et al., 2017; Shibutani et al., 2017). Knockout of *Arid1b* in cortical progenitors, in contrast, has very little effect on the mouse behaviors we measured. Taken together, *Arid1b* conditional homozygous deletion has an outsize effect on ventral progenitor proliferation, which is closely linked to animal behavior, whereas homozygous loss of *Arid1b* in cortical progenitors gives rise to comparatively moderate neural and behavioral phenotypes.

2.3 Materials and methods

2.3.1 Generation of conditional Arid1b knockout mice

Knockout-first *Arid1b* mutant mice were developed using a C57BL6 background (Jackson Laboratory, #000058) in the Mouse Genome Engineering Core Facility at the University of Nebraska Medical Center as described previously (Jung et al., 2017). Homozygous floxed mice were crossed with appropriate Cre drivers (Jackson Laboratory, #005628, #023724 and #008661) for tissue-specific *Arid1b* deletion. All mice were housed in cages with 12:12-h light:dark cycles. No more than five mice were housed per cage. Mice were handled according to a protocol approved by the University Nebraska Medical Center Institutional Animal Care and Use Committee.

2.3.2 Immunostaining

Immunostaining of brain sections or dissociated cells was performed as described previously (Ka et al., 2016c; Jung et al., 2017; Ka et al., 2017). Primary antibodies used were mouse anti-ARID1B (Abcam, ab57461; Abnova, H00057492-M02), rabbit anti-cleaved caspase-3 (Cell Signaling Technology, #9664), mouse anti-BrdU (BD Biosciences, #555627), rabbit anti-p-histone-H3 (Cell Signaling Technology, #9701), rabbit anti-Ki67 (Cell Signaling, #9129), rabbit anti-β-catenin (Cell Signaling, #8480) and chicken anti-GFP (Invitrogen, A10262). Appropriate secondary antibodies conjugated with Alexa Fluor dyes (Invitrogen) were used to detect primary antibodies. DAPI (Sigma-Aldrich) was used to stain nuclei.

2.3.3 Stereology

For quantifying numbers of cells, images of 10 different brain sections were taken at periodic distances along the rostrocaudal axis with a Zeiss LSM710 confocal microscope as described previously (Jung et al., 2017; Ka et al., 2017). *N* values for

each experiment are described in figure legends. Mouse cultured neurons were also assessed with this microscope. Cell numbers are described in figure legends. images were analyzed using ZEN (Zeiss) and ImageJ (NIH). The calculated values were averaged, and some results were recalculated as relative changes versus control.

2.3.4 BrdU administration and cell cycle analysis

For proliferation assays, BrdU administration and analysis of cell cycle speed and re-entry were performed as described previously (Kee et al., 2002; Ka et al., 2017). Intraperitoneal injection of BrdU (20 mg per kg body weight, dissolved in 0.9% saline) into pregnant mice at E13.5-15.5. was performed prior to sacrifice. For the analysis of cell cycle re-entry, control and mutant mice were exposed to BrdU for 24 h. Brain slices were then immunostained with antibodies to BrdU and Ki67. The ratio of cells labeled with BrdU and Ki67 to total cells that incorporated BrdU was determined. For the analysis of cell cycle length, the ratio of progenitor cells positive for Ki67 and BrdU to the total Ki67 labeled cells was assessed after a 1 h BrdU pulse.

2.3.5 Cell culture

MGE cells were isolated and cultured from E12.5–E14.5 mice as described previously (Jung et al., 2017). Meninges were removed and MGE cells were dissociated with trituration after trypsin/EDTA treatment. The cells were plated onto poly-D-lysine/laminin-coated coverslips and cultured in a medium containing Neurobasal medium (Invitrogen), 2 mM glutamine, 2% (v/v) B27 supplement (Invitrogen), 1% (v/v) N2 supplement (Invitrogen), and 50 U/mL penicillin/streptomycin (Invitrogen).

2.3.6 Colocalization

Object-corrected fluorescence colocalization was performed as described by Moser et al. (Moser et al., 2017). Briefly, 10 sequential, individual Z stack images, spaced approximately 4 μm apart, were captured using a Zeiss LSM710 confocal microscope and analyzed for colocalization between DAPI and β-catenin using ImageJ (NIH) software with the macro described in the above reference (Moser et al., 2017). The mean corrected Pearson's coefficient for each sample was recorded and the mean of all samples for each genotype is reported in the results.

2.3.7 Behavioral assays

All behavioral assays were done during the light cycle. Health conditions, including weight, activity, and feeding were checked before assays. 3- to 4-month-old male and female mice were for most behavioral assays. For social behavior assays, we used only male mice as sexual interactions between males and females and estrous cycle timing may interfere with accurate interpretation of social behavior. All behavioral assays were done blind to genotypes, with age-matched littermates of mice.

2.3.8 Novel-object recognition test

A test mouse was first habituated to an open field arena (35 × 42 cm) for 5 min. Following habituation, the test mouse was removed from the arena and two identical objects with size (10.5 × 4.5 × 2.5 cm) were placed in opposite corners of the arena, 7 cm from the side walls. The test mouse was then reintroduced into the center of the arena and allowed to explore the field, including the two novel objects, for 10 min. After 6 h, one object was replaced with another novel object, which was of similar size but different shape and color than the previous object. The same test mouse was placed in the arena to explore the arena and the two objects. The movement of the

mouse was recorded by a camera for 10 min and further analyzed by EthoVision XT 7 video tracking software (Noldus).

2.3.9 Three-chamber test for social interaction and novelty behavior

Social behavior was evaluated as described previously (Jung et al., 2016; Jung et al., 2017). A rectangular, transparent Plexiglas box divided by walls into three equal-sized compartments (Ugobasile) was used. Rectangular holes in the Plexiglas walls provide access between the chambers. For sociability testing, a test mouse was moved to the center chamber (chamber 2) with the entrances to the two connecting chambers blocked. A stimulus mouse (unfamiliar mouse) designated as ‘stranger I’ was placed in a wire enclosure in chamber 1. Then the openings to the flanking two chambers (1 and 3) were opened and the test mouse was allowed to explore the entire apparatus for 10 min. For the social novelty test, the stranger I mouse was randomly placed in one of the enclosures, while the test mouse had the choice of whether to investigate the stranger I mouse or a new novel mouse, designated ‘stranger II’. This second novel mouse was taken from a different home cage and placed into the remaining empty wire enclosure. Time spent sniffing each partner by the test mouse was recorded for 10 min in both sociability and social novelty behavior tests. All apparatus chambers were cleaned with water and dried between trials. At the end of each test day, the apparatus was sprayed with 70% ethanol and wiped clean.

2.3.10 Grooming

A mouse was placed in a clear plastic cage (17 × 32 × 14 cm). The mouse was allowed to freely explore the cage for the entirety of the test. The first 10 min served as a habituation period. The movement of the mouse was recorded by a camera for

30 min. Recorded grooming behaviors included head washing, body grooming, genital/tail grooming, and paw and leg licking.

2.3.11 Elevated plus maze test

The elevated plus maze test was performed as previously described (Jung et al., 2016; Jung et al., 2017). The apparatus (EB Instrument) includes two open arms (35 × 5 cm), two enclosed arms (35 × 5 × 15 cm), and a central platform (5 × 5 cm). The entire apparatus was elevated 45 cm above the floor. A mouse was placed on the central platform, facing the open arms, and allowed to roam freely for 5 min. The number of entries into and the time spent in open and closed arms were recorded.

2.3.12 Open field test

A mouse was placed near the wall-side of a 35 × 42 cm open field arena, and the movement of the mouse was recorded by a camera for 5 min. The recorded video file was further analyzed using EthoVision XT 7.0 (Noldus). The number of entries into and the overall time spent in the center of the arena (15 × 15 cm imaginary square) were measured. The open field arena was cleaned with 70% ethanol and allowed to dry between each trial.

2.3.13 Forced swimming test

A mouse was placed individually into a glass cylinder (20 cm height, 17 cm diameter) filled with water to a depth of 10 cm at 25 °C. After 5 min, the animals were removed from the water, dried, and returned to their home cages. They were again placed in the cylinder 24 h later, and after the initial 1 min acclimatization period, the total duration of immobility was measured for 5 min. Motionless floating was considered immobile behavior.

2.3.14 Tail suspension test

A mouse was suspended from the hook of a tail suspension test box, 60 cm above the surface of a table, using adhesive tape placed 1 cm from the tip of the tail. After 1 min acclimatization, immobility duration was recorded by a camera for 5 min. Mice were considered immobile only when they hung passively and were completely motionless.

2.3.15 Statistical analysis

Normal distribution was tested using the Kolmogorov-Smirnov test and variance was compared. Unless otherwise stated, statistical significance was determined using two-tailed, unpaired Student's *t* tests for two-population comparisons or one-way ANOVA followed by Bonferroni's post hoc test for multiple comparisons. Data were analyzed using GraphPad Prism and presented as means ± SEM *P* values for each comparison are described in the results or figure legends. To determine and confirm sample sizes (*n*), we performed power analysis and/or surveyed the literature. Each experiment in this study was performed blind and randomized. Animals were assigned randomly to the various experimental groups, and data were collected and processed randomly. The allocation, treatment, and handling of animals was the same across study groups. Control animals were selected from the same litter as the test group. The individuals conducting the experiments were blinded to group allocation and allocation sequence. Exclusion criteria for mice were based on abnormal health conditions, including weights below 15 g at 6 weeks of age and noticeably reduced activity or feeding. Statistical data and *n* values for all behavioral assays are described in the figure legends.

2.4 Results

2.4.1 Cortical progenitor proliferation is decreased in Arid1b$^{LoxP/LoxP}$;Emx1-Cre mice

We first examined the proliferation of cortical neural progenitors in *Arid1b*$^{LoxP/LoxP}$*;Emx1-Cre* mice by immunostaining consecutive cortical sections from E14-E16 mouse embryos with two antibodies. Anti-phosphorylated Histone-H3 (anti-PH3) staining, which is used to determine cells undergoing mitosis (Hans and Dimitrov, 2001), revealed a significant reduction (37.75%) in mitotic cortical neural progenitors in *Arid1b*$^{LoxP/LoxP}$*;Emx1-Cre* mice, compared with controls (Figure 2.1A-B). Staining for Ki67, which is present during all stages of the cell cycle and absent in quiescent (G_0) cells (Bruno and Darzynkiewicz, 1992; Scholzen and Gerdes, 2000; Cuylen et al., 2016), however, shows no significant difference in the number of actively proliferating cells in *Arid1b*$^{LoxP/LoxP}$*;Emx1-Cre* mice, compared with controls (Figure 2.1C-D). We also peritoneally injected pregnant dams with bromodeoxyuridine (BrdU), a thymidine analog that is incorporated into dividing cells during DNA replication (Gratzner, 1982; Nowakowski et al., 1989; Wojtowicz and Kee, 2006), and report a significant decrease (24.32%) in the number of BrdU-positive cortical neural progenitors in *Arid1b*$^{LoxP/LoxP}$*;Emx1-Cre* mice harvested 1 hour post-injection, compared with controls (Figure 2.1E-F).

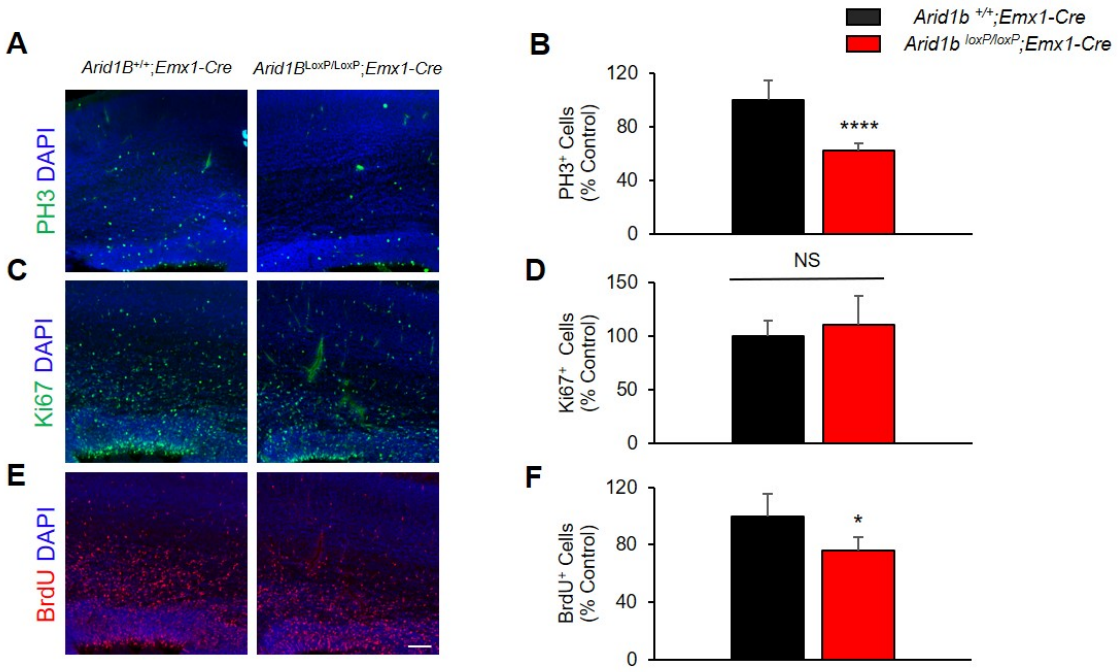

Figure 2.1 *Arid1b* deletion decreases cortical progenitor proliferation

(A), (C), and (E) Immunostaining of coronal cerebral cortical sections from E14-16 control and *Arid1B$^{LoxP/LoxP}$;Emx1-Cre* brains with anti-phosphorylated Histone H3 (PH3), anti-Ki67 or anti-BrdU antibodies with DAPI co-stain. Representative images from both six control and *Arid1B$^{LoxP/LoxP}$;Emx1-Cre* brains for (A) and (E) and five from each genotype for (C). Scale bars: 50μm. (B), (D) and (F) Quantifications of (A), (C) and (E), respectively. N=6 mice for each condition for (B) and (F) and N=5 for each condition for (D). Statistical significance was determined by two-tailed Student's t-test. Error bars show standard error of the mean (SEM). *$p < 0.05$, ***$p < 0.001$.

2.4.2 Ventral progenitor proliferation is impaired in Arid1b$^{LoxP/LoxP}$;Dlx5/6-Cre mice

In E14-E16 *Arid1b$^{LoxP/LoxP}$;Dlx5/6-Cre* mice, we examined ventral neural progenitor proliferation using immunostaining for PH3 and Ki67 in the MGE. We observed a significant decrease (45.32%) in the number of PH3-positive cells (Figure 2.2A-B), as well as a significant decrease (47.20%) in the number of Ki67-positive cells (Figure 2.2C-D), both compared with controls. These indicate large reductions in the numbers of mitotic and actively proliferating ventral neural progenitors in these mice, respectively. *Arid1b$^{LoxP/LoxP}$;Dlx5/6-Cre* embryos removed 1 hour following BrdU injection into pregnant dams display a significant decrease (22.66%) in the number of BrdU-positive cells in the

MGE, compared with controls (Figure 2.2E-F). This can be interpreted to mean a drop in the number of ventral neural progenitors undergoing DNA replication as well as newly-born cells in the MGE.

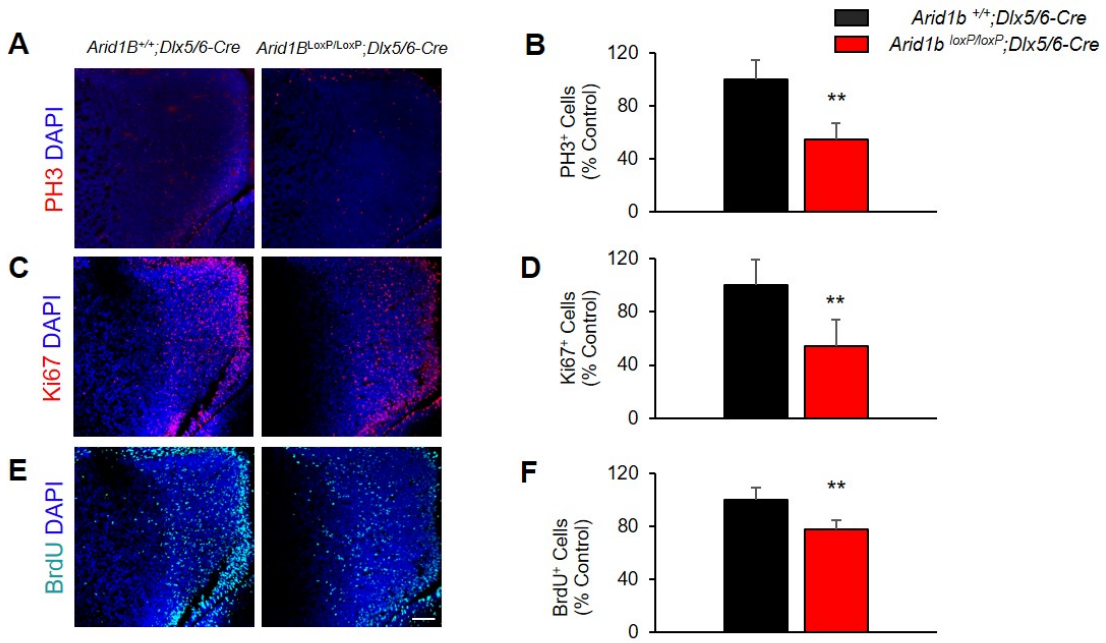

Figure 2.2 *Arid1b* deletion greatly decreases ventral progenitor proliferation

(A), (C), and (E) Immunostaining of coronal cerebral cortical sections from E14-16 control and *Arid1B*$^{LoxP/LoxP}$*;Dlx5/6-Cre* brains with anti-phosphorylated Histone H3 (PH3), anti-Ki67 or anti-BrdU antibodies with DAPI co-stain. Representative images from both six control and *Arid1B*$^{LoxP/LoxP}$*;Dlx5/6-Cre* brains for (A) five from each genotype for (C) and five control and four *Arid1B*$^{LoxP/LoxP}$*;Dlx5/6-Cre* brains for (E). Scale bars: 50μm. (B), (D) and (F) Quantifications of (A), (C) and (E), respectively. N=6 mice for each condition for (B) N=5 for each genotype in (F) and N=5 mice for control and 4 for *Arid1B*$^{LoxP/LoxP}$*;Dlx5/6-Cre* (D). Statistical significance was determined by two-tailed Student's t-test. Error bars show standard error of the mean (SEM). ***p* < 0.01.

2.4.3 ARID1B regulates cell cycle progression in both cortical and ventral neural progenitors

Seeing as homozygous deletion of *Arid1b* leads to impaired neural progenitor proliferation in both cortical and ventral progenitor pools, we next explored the effects of conditional *Arid1b* knockout on the cell cycle. Several BAF subunits have been shown to influence cell cycle progression and cell division (Battaglioli et al., 2002; Olave et al.,

2002; Lessard et al., 2007; Wu et al., 2007; Tuoc et al., 2013; Son and Crabtree, 2014), thus we examined both cell cycle speed and cell cycle re-entry in both *Arid1b*$^{LoxP/LoxP}$*;Emx1-Cre* and *Arid1b*$^{LoxP/LoxP}$*;Dlx5/6-Cre* mice.

Cell cycle speed is assessed by first injecting pregnant dams with BrdU 30 minutes prior to removal of embryos, followed by immunostaining of brain sections using both anti-BrdU and anti-Ki67 antibodies. The ratio of Ki67-BrdU-double-positive cells to the total number of Ki67-positive cells, essentially the proportion of actively proliferating cells that entered S-phase in a 30-minute time span, provides a quantifiable estimate of cell cycle speed (Kee et al., 2002; Ka et al., 2017). Homozygous knockout of *Arid1b* in cortical neural progenitors has no significant impact on cell cycle speed in the developing cerebral cortex (Figure 2.3A-B). In the ventral neural progenitor population, however, *Arid1b* deletion leads to a 50.33% reduction in this measurement of cell cycle speed, compared with control littermates (Figure 2.3E-F).

To quantify cell cycle re-entry, we injected pregnant dams with BrdU 24 hours prior to embryo removal and then co-immunostained with anti-Ki67 and anti-BrdU antibodies. We then calculated the ratio of Ki67-BrdU-double-positive cells to the total number of BrdU-positive cells, which provides a measure of the newborn (in the last 24 hours) cells that are still actively proliferating (Kee et al., 2002; Ka et al., 2017). About 46.06% fewer BrdU-positive cortical neural progenitors also express measurable levels of Ki67 in *Arid1b*$^{LoxP/LoxP}$*;Emx1-Cre* mice, compared with controls, which indicates impaired cell cycle re-entry (Figure 2.3C-D). Cell cycle re-entry is also impaired in ventral neural progenitors, as about 71.48% fewer BrdU-positive ventral neural progenitors are also Ki67-positive in *Arid1b*$^{LoxP/LoxP}$*;Dlx5/6-Cre* mice (Figure 2.3G-H).

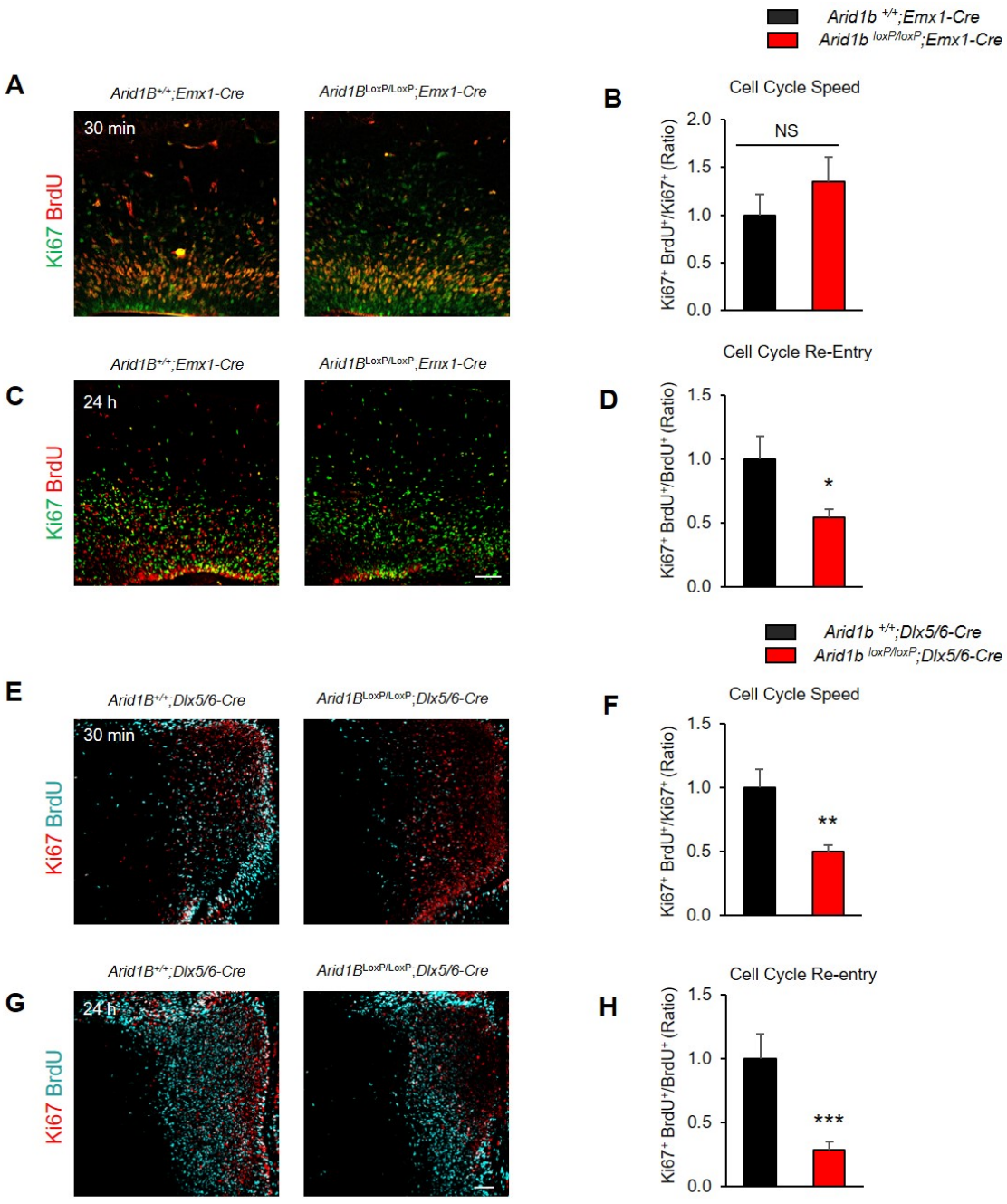

Figure 2.3 ARID1B regulates the cell cycle in neural progenitors

(A) and (E) E14-16 control and *Arid1B*$^{LoxP/LoxP}$*;Emx1-Cre* or *Arid1B*$^{LoxP/LoxP}$*;Dlx/6-Cre* mice were pulse-labeled with BrdU for 30 min, and then brain regions containing the cerebral cortex were collected and immunostained using BrdU and Ki67 antibodies. Scale bar: 50 μm. (B) and (F) Quantification of cell cycle speed from (A) and (E). The cell cycle speed was defined as the fraction of BrdU- and Ki67-double-positive cells in the total Ki67-positive pool in the cerebral cortex. N=6 control and 9 *Arid1B*$^{LoxP/LoxP}$*;Emx1-Cre* mice for (B) and N=10 for each genotype for (F). Statistical significance was determined by two-

tailed Student's t-test. Error bars show SEM. **p < 0.01. (C) and (G) E14-16 control and *Arid1B*$^{LoxP/LoxP}$*;Emx1-Cre* or *Arid1B*$^{LoxP/LoxP}$*;Dlx/6-Cre* mice were pulse-labeled with BrdU for 24 h and then brains were collected for immunostaining with BrdU and Ki67 antibodies. Scale bar: 50μm. (D) and (H) The index of cell cycle re-entry was calculated as the fraction of BrdU- and Ki67-double-positive cells in total BrdU-positive pool. N=9 mice for each genotype from both (D) and (H). Statistical significance was determined by two-tailed Student's t-test. Error bars show SEM. *p < 0.05, ***p<0.001.

2.4.4 Conditional homozygous deletion of Arid1b leads to similar increases in apoptosis in cortical and ventral neural progenitors

In addition to examining the proliferation of cortical and ventral neural progenitors, we assessed apoptotic progenitors in the E14-E16 developing cerebral cortex and ventral telencephalon in conditional *Arid1b* mutants. We used an anti-cleaved-Caspase 3 (anti-cl.-Cas 3) antibody to determine the relative number of apoptotic cells in tissue sections as cl.-Cas 3 is a well-understood marker of cells undergoing apoptosis (Nicholson et al., 1995; Lavrik et al., 2005). In *Arid1b*$^{LoxP/LoxP}$*;Emx1-Cre* mice, the cl.-Cas 3 intensity in the developing cerebral cortex is 138.67% higher than in wild type mice (Figure 2.4A-B). In *Arid1b*$^{LoxP/LoxP}$*;Dlx5/6-Cre* mice, cl.-Cas 3 intensity in the MGE is increased by 165.32%, compared to controls (Figure 2.4C-D). From these results we conclude that homozygous deletion of *Arid1b* leads to a comparable increase in apoptosis among both cortical and ventral neural progenitor populations.

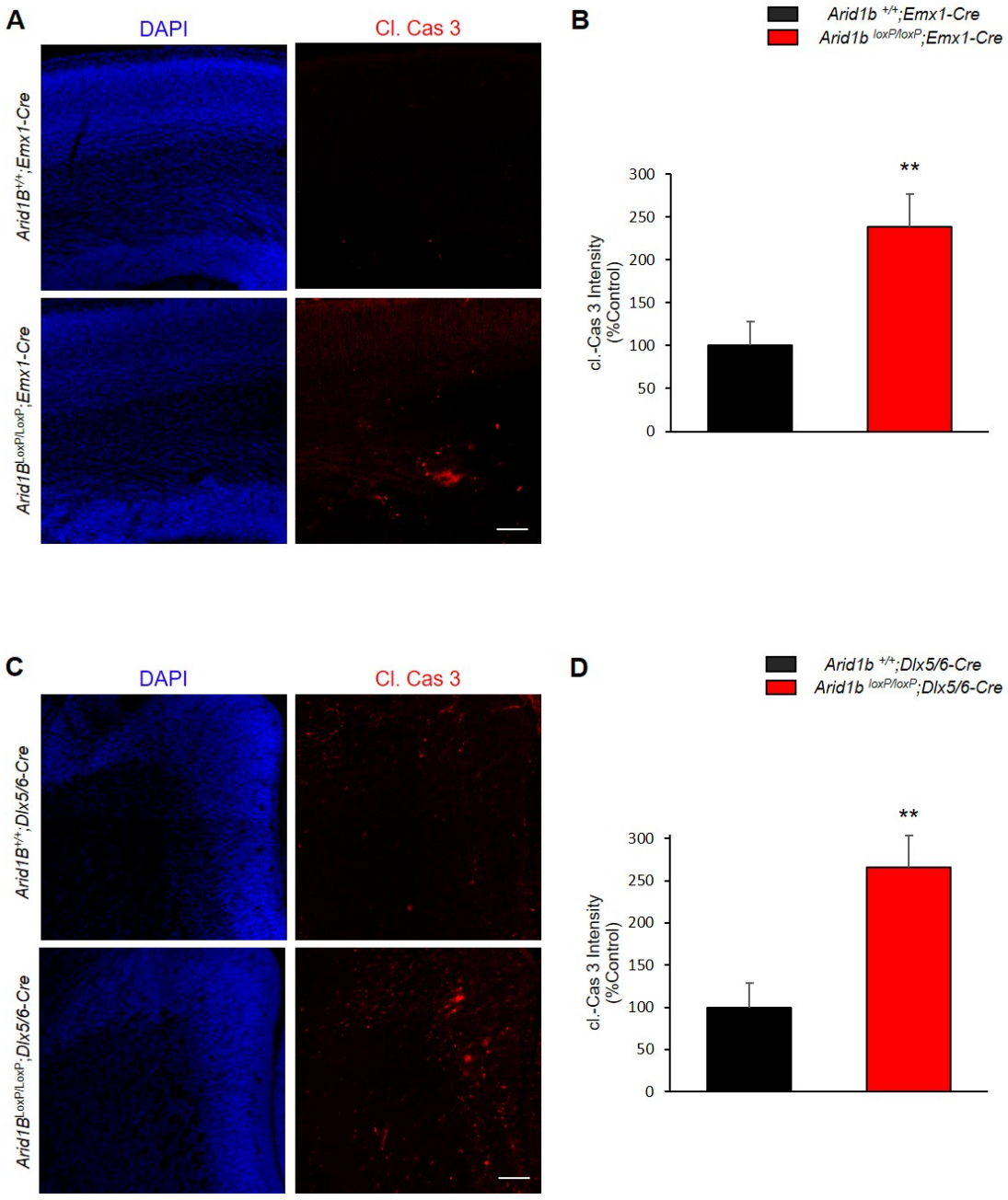

Figure 2.4 *Arid1b* deletion increases apoptosis in cortical and ventral neural progenitor pools

(A) and (C) Cell death was assessed in E14-16 control and *Arid1B$^{LoxP/LoxP}$;Emx1-Cre* or *Arid1B$^{LoxP/LoxP}$;Dlx5/6-Cre* mutant neural progenitors by immunostaining with a cleaved caspase-3 (cl.-Cas 3) antibody. Representative images from both nine control and *Arid1B$^{LoxP/LoxP}$;Emx1-Cre* brains for (A) and (E) and ten from each genotype for (C). Scale bars, 50 μ m. (B) and (D) Quantification of apoptotic cells from (A) and (C), respectively. N=9 mice for each genotype for (A) and N=10 mice for each genotype for (C). Statistical significance was determined by two-tailed Student's t-test. Error bars show SEM. **p<0.01

2.4.5 Arid1b knockout decreases β-catenin nuclear localization in vitro and in vivo

In order to determine the degree to which β-catenin localizes in the nucleus of ARID1B-depleted neurons and neural progenitors, we co-immunostained cultured cells and tissue sections with an anti-β-catenin and the nuclear stain, DAPI. We cultured primary neurons from the MGE of E12.5-E14.5 *Arid1b*$^{+/+}$ and *Arid1b*$^{-/-}$ mouse embryonic brains for six days before fixing cells and immunostaining. Qualitative analysis reveals what appears to be a decrease in overlapping β-catenin and DAPI staining in *Arid1b*$^{-/-}$ cultured neurons, compared with *Arid1b*$^{+/+}$ cultures(2.5A-B). We then determined the object-corrected fluorescence colocalization of β-catenin and DAPI using ImageJ (NIH) software (Moser et al., 2017). The mean Pearson's coefficient for *Arid1b*$^{+/+}$ cultures was 0.61 and 0.20 for *Arid1b*$^{-/-}$ cultures, indicating decreased nuclear β-catenin in the absence of ARID1B (Figure 2.5A-B).

Next, we examined nuclear β-catenin localization in vivo by immunostaining the MGEs of E12-14 *Arid1b*$^{LoxP/LoxP}$*;Dlx5/6-Cre* mice and comparing DAPI-β-catenin colocalization with control MGEs. Similar to what we observed in vitro, we detect less overlapping β-catenin and DAPI staining in *Arid1b*$^{LoxP/LoxP}$*;Dlx5/6-Cre* MGEs than in controls (Figure 2.5C-D). We also report a significantly lower Pearson's coefficient of colocalization in *Arid1b*$^{LoxP/LoxP}$*;Dlx5/6-Cre* mouse MGEs (0.03), compared with controls (0.27) (Figure 2.5C-D). Taken together, we conclude that total loss of *Arid1b* gene expression leads to significant decreases in β-catenin nuclear localization.

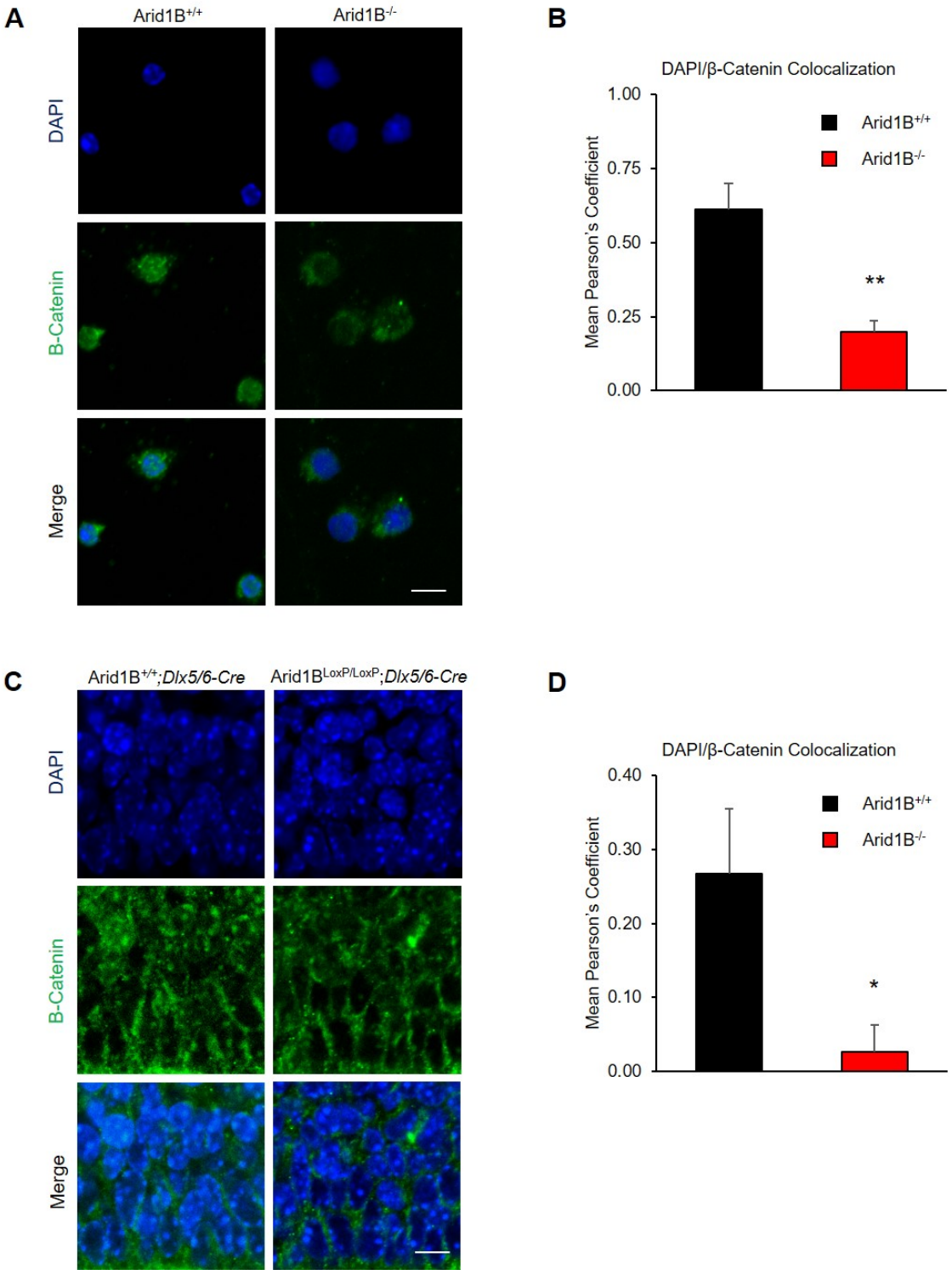

Figure 2.5 Knockout of *Arid1b* reduces β-catenin nuclear localization

(A) And (C) Nuclear localization of β-catenin was assessed in DIV 6 control and *Arid1b*$^{-/-}$ mouse primary neuronal cultures derived from E12.5-E14.5 embryonic MGEs by immunostaining with DAPI and an antibody against β-catenin. Representative images

from N=5 mice from each genotype for (A) and 3 mice from each genotype for (C). Scale bar: 50 μm. (B) and (D) Quantification of (A) and (C), respectively. Mean corrected Pearson's coefficient from object-corrected fluorescence colocalization of DAPI and anti-β-cat is plotted. N=5 mice from each genotype for (B) and 3 mice from each genotype for (D). Statistical significance was determined by two-tailed Student's t-test. Error bars show SEM.

2.4.6 Cortical neural progenitor-specific deletion of Arid1b impairs cognitive function

With the alterations in cortical progenitor proliferation and survival in *Arid1b*$^{LoxP/LoxP}$*;Emx1-Cre* mice more clearly defined, we next examined the behavioral outcomes of homozygous deletion of *Arid1b* within this population in 8-10-week-old animals. Heterozygous deletion of *Arid1b* leads to anxiety-like behaviors in mice (Celen et al., 2017; Jung et al., 2017; Shibutani et al., 2017) and is also present in other mouse models of ID and ASD (1994; Kazdoba et al., 2014). Anxiety is also a frequent comorbid condition with ASD in humans (Wing and Gould, 1979; Gillott et al., 2001; van Steensel and Heeman, 2017). To determine whether *Arid1b*$^{LoxP/LoxP}$*;Emx1-Cre* mice develop anxiety-like behaviors, we performed the elevated plus maze and open field assays. *Arid1b*$^{LoxP/LoxP}$*;Emx1-Cre* mice spent the same amount of time in the open arms of the elevated plus maze as controls (Figure 2.6A) and entered, and spent the same amount of time in, the center portion of the open field apparatus, compared with wild type littermates (Figure 2.6D-E). From these results we concluded that these mutant mice display no appreciable anxiety-like behaviors.

Depression is another condition often seen in individuals with ID and ASD (Wing and Gould, 1979), and *Arid1b* heterozygous mutant mice display significant depression-like behaviors (Jung et al., 2017). To examine depression-like behaviors in this study, we utilized the tail suspension and forced swim tests. We report that *Arid1b*$^{LoxP/LoxP}$*;Emx1-Cre* mice do not spend a discernably different amount of time immobile in either of these assays, compared with control mice (Figure 2.6B-C). Thus, homozygous deletion of

Arid1b in cortical neural progenitors does not appear to engender depression-like symptoms in mice.

Arid1b haploinsufficient mice spend considerably more time grooming than wild type mice, which is considered an appropriate measure of repetitive or stereotyped behaviors in mouse models of ASD (Celen et al., 2017; Jung et al., 2017). *Arid1b*$^{LoxP/LoxP}$*;Emx1-Cre* mice, however, do not demonstrate a significant increase in the amount of time they spend grooming during a 10-minute period (Figure 2.6F).

We have previously reported that heterozygous deletion of *Arid1b* leads to impaired recognition memory in mice (Jung et al., 2017). Therefore, we examined the effects of homozygous *Arid1b* deletion in cortical neural progenitors on performance in the novel object recognition task. *Arid1b*$^{LoxP/LoxP}$*;Emx1-Cre* mice exhibit a recognition index of 48.05% in this task, which indicates no real preference for a novel object versus a familiar one in an otherwise empty open field. *Arid1b*$^{+/+}$*;Emx1-Cre* littermates, on the other hand, display a recognition index of 70.88%, indicative of a stronger preference for interaction with the novel object (Figure 2.6G). *Arid1b*$^{LoxP/LoxP}$*;Emx1-Cre* mice also show no real preference for a second stranger mouse in the three-chamber social behavior assay, while controls do (Figure 2.6H). Their overall sociability, also measured in the three-chamber behavior assay, however, is similar to what we observe with their wild type littermates (Figure 2.6H). We conclude from these results that *Arid1b*$^{LoxP/LoxP}$*;Emx1-Cre* mice develop cognitive impairments specifically related to recognition memory.

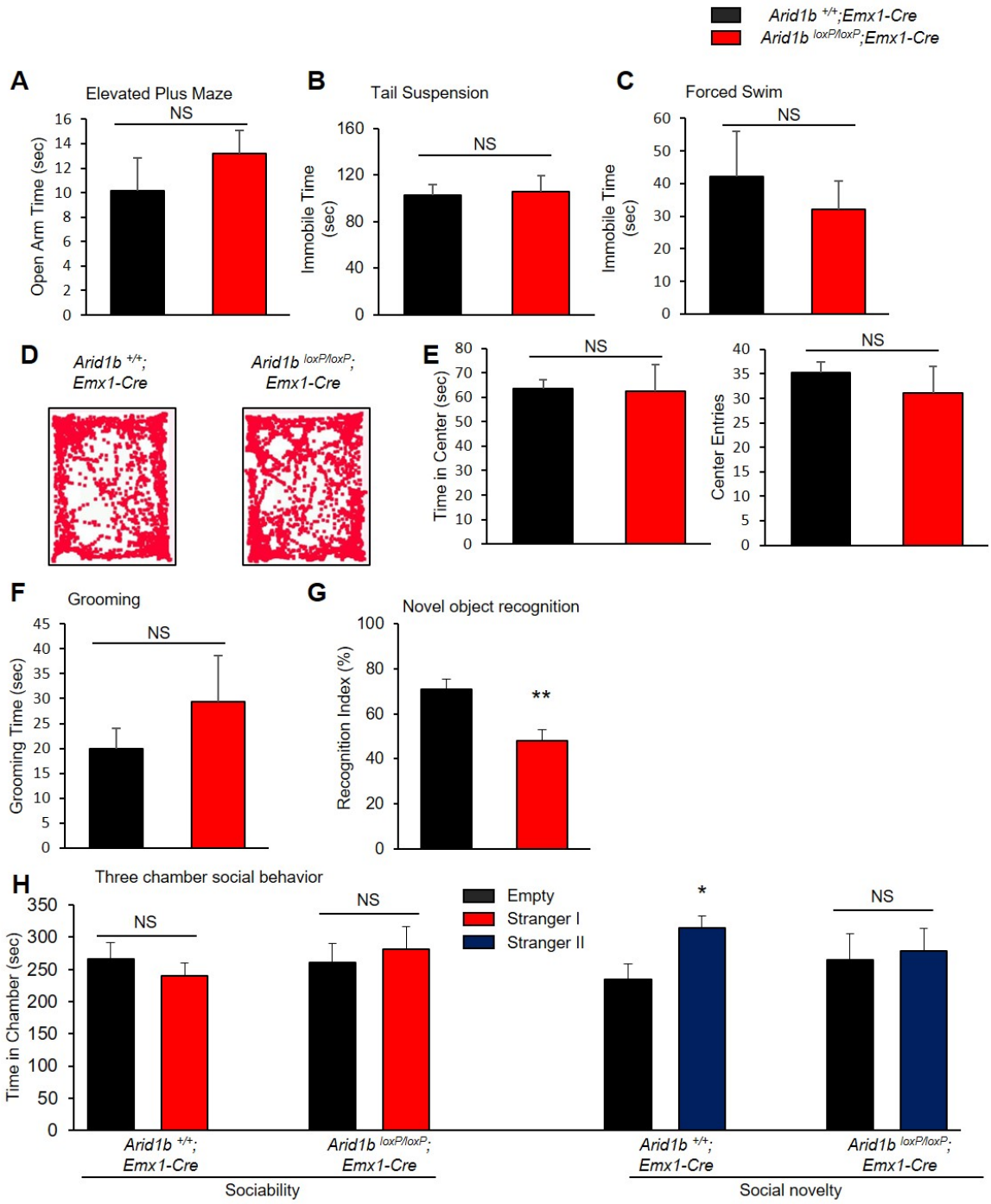

Figure 2.6 Effects of conditional deletion of *Arid1b* in cortical neural progenitors on behavior

(A) In the elevated plus maze, *Arid1B$^{LoxP/LoxP}$;Emx1-Cre* mice spent spend the same amount of time in the open arm as controls. N = 6 mice for control and N=7 mice for *Arid1B$^{LoxP/LoxP}$;Emx1-Cre*. Statistical significance was determined by two-tailed Student's t-test. Error bars show SEM. (B) No significant difference in immobility times in the tail suspension test between controls and *Arid1B$^{LoxP/LoxP}$;Emx1-Cre* mice. N= 6 mice for

control and N=7 mice for *Arid1B$^{LoxP/LoxP}$;Emx1-Cre*. Statistical significance was determined by two-tailed Student's t-test. Error bars show SEM. (C) In the forced swim test there was no significant difference in immobility time control and *Arid1B$^{LoxP/LoxP}$;Emx1-Cre* mice. N= 6 mice for control and N=7 mice for *Arid1B$^{LoxP/LoxP}$;Emx1-Cre*. Statistical significance was determined by two-tailed Student's t-test. Error bars show SEM. (D) Representative traces from (E). (E) No significant difference in the total time spent in the center or the number of entries into the center in the open field test. N= 6 mice for control and N=7 mice for *Arid1B$^{LoxP/LoxP}$;Emx1-Cre*. Statistical significance was determined by two-tailed Student's t-test. Error bars show SEM. (F) No significant change in grooming time in a 10-minute session between control and *Arid1B$^{LoxP/LoxP}$;Emx1-Cre* mice. N= 6 mice for control and N=7 mice for *Arid1B$^{LoxP/LoxP}$;Emx1-Cre*. Statistical significance was determined by two-tailed Student's t-test. Error bars show SEM. (G) *Arid1B$^{LoxP/LoxP}$;Emx1-Cre* mice demonstrate impaired novel object recognition. Recognition index indicates the percentage of time the test mouse interacted with a novel object compared to a familiar one. N= 5 mice for control and N=7 mice for *Arid1B$^{LoxP/LoxP}$;Emx1-Cre*. Statistical significance was determined by two-tailed Student's t-test. Error bars show SEM. (H) Slightly abnormal social behavior in *Arid1B$^{LoxP/LoxP}$;Emx1-Cre* mice. *Arid1B$^{LoxP/LoxP}$;Emx1-Cre* and control mice spend the same amount of time in the chamber containing the "stranger 1" mouse as they do in an empty chamber in the sociability trial. In the social novelty trial, control mice spend significantly more time with the novel "stranger 2" but *Arid1B$^{LoxP/LoxP}$;Emx1-Cre* mice do not. N= 6 mice for control and N=7 mice for *Arid1B$^{LoxP/LoxP}$;Emx1-Cre*. Statistical significance was determined by two-tailed Student's t-test. Error bars show SEM.

2.4.7 Conditional knockout of Arid1b in ventral neural progenitors results in multiple ASD-like behavioral phenotypes

We also examined ID- and ASD-like behaviors in 8-10-week-old *Arid1b$^{LoxP/LoxP}$;Dlx5/6-Cre* and *Arid1b$^{LoxP/LoxP}$;Nkx2.1-Cre* mice. On the elevated plus maze, *Arid1b$^{LoxP/LoxP}$;Dlx5/6-Cre* mice spend less time in the open arm than their wild type littermates, but this result is not statistically significant (Figure 2.7A). *Arid1b$^{LoxP/LoxP}$;Nkx2.1-Cre* mice spend the same amount of time in the open arm as controls (Figure 2.8A). In the open field assay, however, *Arid1b$^{LoxP/LoxP}$;Dlx5/6-Cre* mice enter, and spend significantly less time in, the center area of the apparatus, compared to controls (Figure 2.7D-E), which is indicative of anxiety-like behavior. *Arid1b$^{LoxP/LoxP}$;Nkx2.1-Cre*, in contrast, do not exhibit any significant anxiety-like behavior in the open field assay (Figure 2.8D-E).

Arid1b$^{LoxP/LoxP}$*;Dlx5/6-Cre* mice also spend significantly more time immobile in the tail suspension assay, compared with control littermates (Figure 2.7B), but they are not significantly less mobile in the forced swim test (Figure 2.7C). Intriguingly, *Arid1b*$^{LoxP/LoxP}$*;Nkx2.1-Cre* spend more time immobile in the forced swim test than controls, but do not demonstrate any significant differences in immobility time in the tail suspension test (Figure 2.8B-C). These results suggest that deletion of *Arid1b* in ventral neural progenitors may be sufficient to cause depression-like behaviors in mice.

Similar to *Arid1b* haploinsufficient mice (Celen et al., 2017; Jung et al., 2017), *Arid1b*$^{LoxP/LoxP}$*;Dlx5/6-Cre* mice exhibit a strong tendency toward repetitive/stereotyped behaviors, as evidenced by them spending nearly 4 times as much time grooming themselves during a ten-minute window than their wild type littermates (Figure 2.7F). *Arid1b*$^{LoxP/LoxP}$*;Nkx2.1-Cre* mice also spend almost twice as much time grooming as controls (Figure 2.8F).

In the novel object recognition test, neither *Arid1b*$^{LoxP/LoxP}$*;Dlx5/6-Cre* nor *Arid1b*$^{LoxP/LoxP}$*;Nkx2.1-Cre* mice any significance difference in recognition index, compared with controls (Figure 2.7G and Figure 2.8G). While *Arid1b*$^{LoxP/LoxP}$*;Nkx2.1-Cre* mice did not demonstrate any aberrant social behaviors in the three-chamber social assay (Figure 2.8H), *Arid1b*$^{LoxP/LoxP}$*;Dlx5/6-Cre* mice showed no preference for either the first or second stranger mouse, in contrast to controls (Figure 2.7H). Altogether, homozygous deletion of *Arid1b* in the ventral neural progenitor population contributes to multiple ID- and ASD-like behaviors, including depression- and anxiety-like behaviors, repetitive/stereotyped behaviors and social deficits.

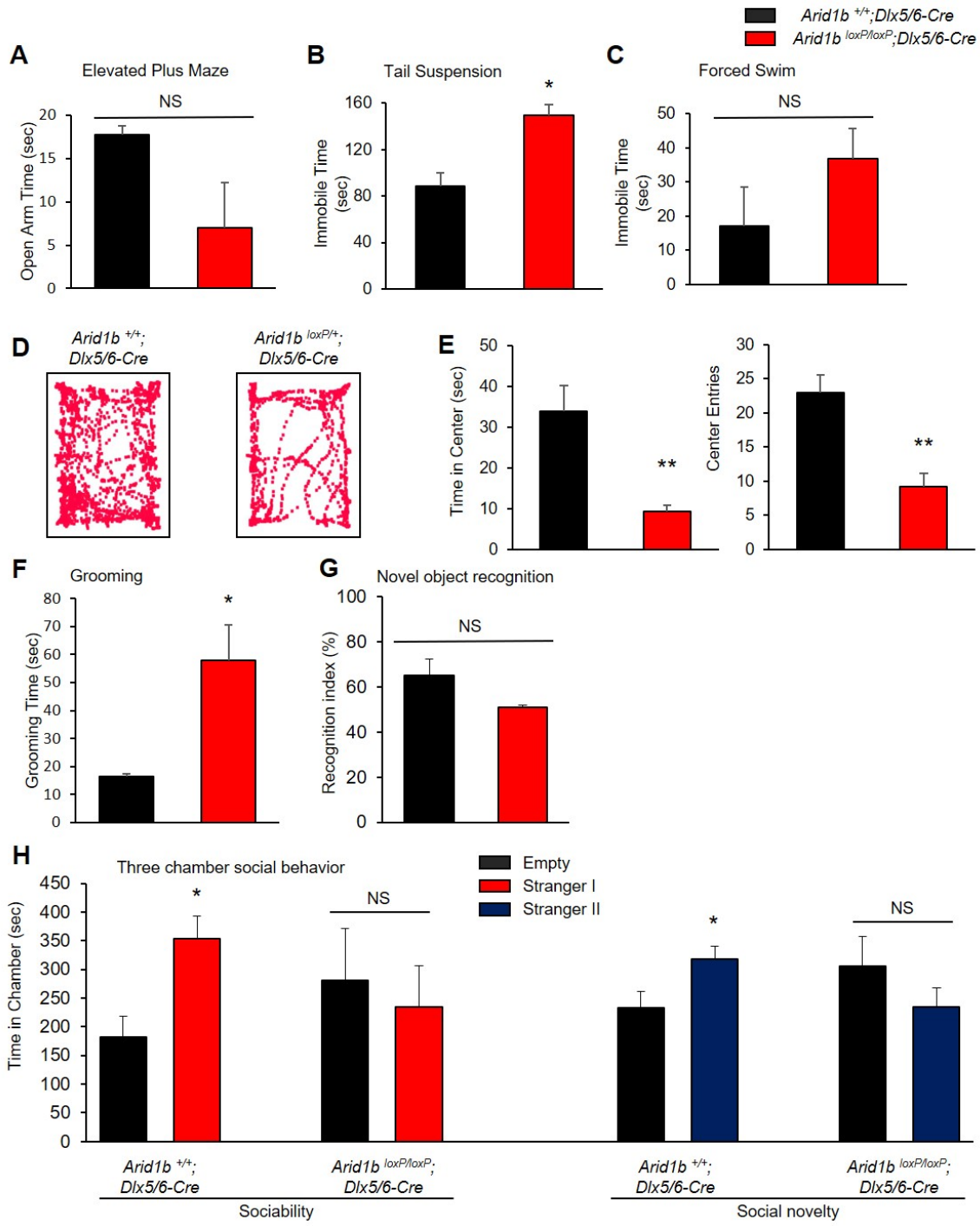

Figure 2.7 Effects of conditional deletion of *Arid1b* in ventral neural progenitors on behavior

(A) In the elevated plus maze, *Arid1B$^{LoxP/LoxP}$;Dlx5/6-Cre* mice spend the same amount of time in the open arm as controls. N = 3 mice from each genotype. Statistical significance was determined by two-tailed Student's t-test. Error bars show SEM. (B) *Arid1B$^{LoxP/LoxP}$;Dlx5/6-Cre* spend significantly more time immobile in the tail suspension test than controls. N= 9 mice for control and N=4 mice for *Arid1B$^{LoxP/LoxP}$;Dlx5/6-Cre*.

Statistical significance was determined by two-tailed Student's t-test. Error bars show SEM. (C) In the forced swim test there was no significant difference in the immobility time of control and *Arid1B*$^{LoxP/LoxP}$*;Dlx5/6-Cre* mice. N= 4 mice for control and N=3 mice for *Arid1B*$^{LoxP/LoxP}$*;Dlx5/6-Cre*. Statistical significance was determined by two-tailed Student's t-test. Error bars show SEM. (D) Representative traces from (E). (E) *Arid1B*$^{LoxP/LoxP}$*;Dlx5/6-Cre* mice spend significantly less total time in the center and enter the center fewer times in the open field test. N= 10 mice for control and N=7 mice for *Arid1B*$^{LoxP/LoxP}$*;Dlx5/6-Cre*. Statistical significance was determined by two-tailed Student's t-test. Error bars show SEM. (F) *Arid1B*$^{LoxP/LoxP}$*;Dlx5/6-Cre* mice spend significantly more time grooming than controls in a 10-minute session. N= 3 mice for control and N=3 mice for *Arid1B*$^{LoxP/LoxP}$*;Dlx5/6-Cre*. Statistical significance was determined by two-tailed Student's t-test. Error bars show SEM. (G) No statistically significant difference in the novel object recognition index between *Arid1B*$^{LoxP/LoxP}$*;Dlx5/6-Cre* and control mice. N=3 mice for each genotype. Statistical significance was determined by two-tailed Student's t-test. Error bars show SEM. (H) *Arid1B*$^{LoxP/LoxP}$*;Dlx5/6-Cre* mice demonstrate significantly impaired sociability and social novelty behaviors compared with controls. N= 4 mice for control and N=5 mice for *Arid1B*$^{LoxP/LoxP}$*;Dlx5/6-Cre*. Statistical significance was determined by two-tailed Student's t-test. Error bars show SEM.

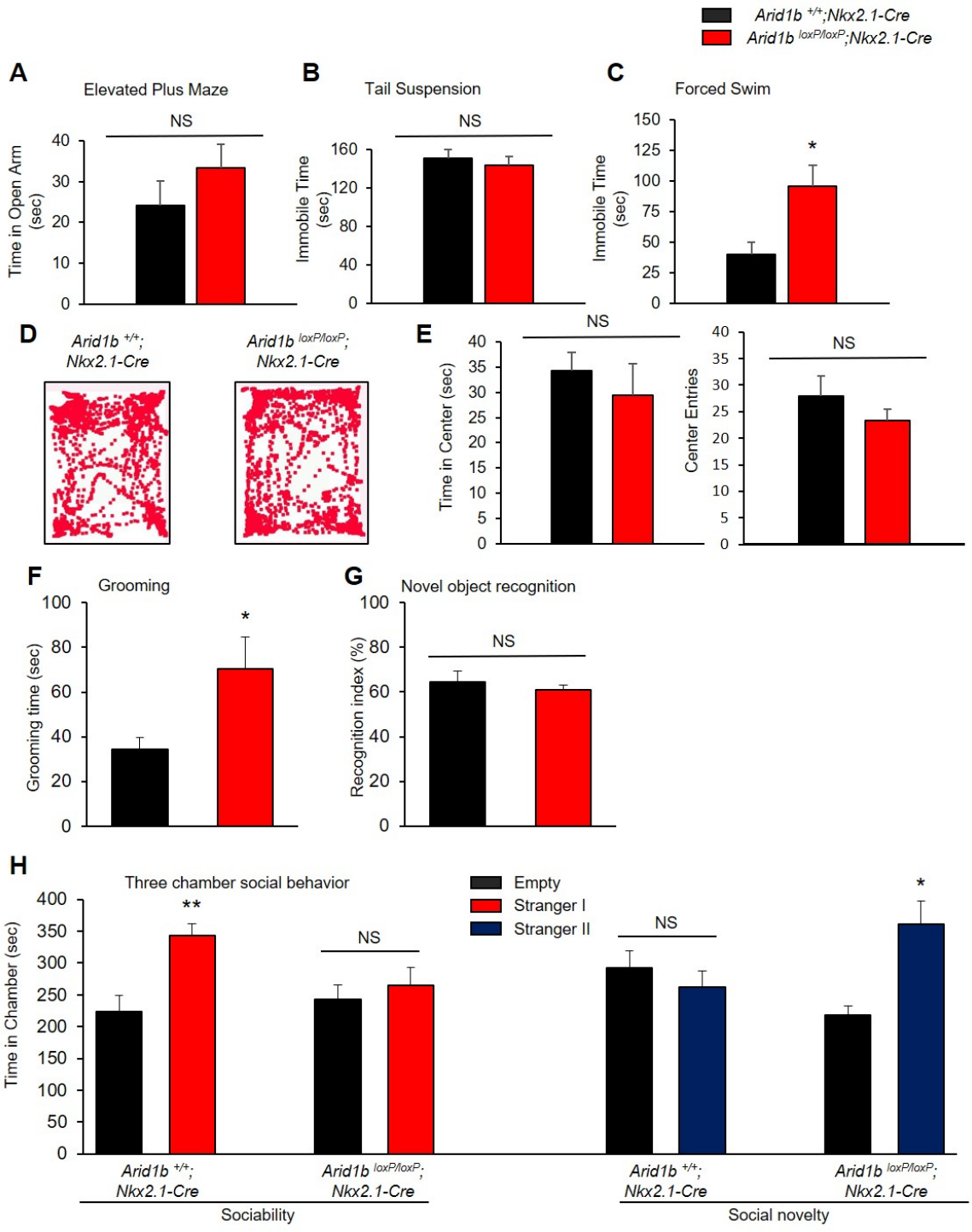

Figure 2.8 Mouse behavior in *Arid1b +/+;Nkx2.1-Cre* mice

(A) In the elevated plus maze, *Arid1B$^{LoxP/LoxP}$;Nkx2.1-Cre* mice spend the same amount of time in the open arm as controls. N = 5 mice for control and N=4 mice for *Arid1B$^{LoxP/LoxP}$;Nkx2.1-Cre*. Statistical significance was determined by two-tailed Student's t-test. Error bars show SEM. (B) In the tail suspension test there was no significant difference in the immobility time of control and *Arid1B$^{LoxP/LoxP}$;Nkx2.1-Cre*

mice. N = 5 mice for control and N=4 mice for *Arid1B*$^{LoxP/LoxP}$*;Nkx2.1-Cre*. Statistical significance was determined by two-tailed Student's t-test. Error bars show SEM. (C) *Arid1B*$^{LoxP/LoxP}$*;Nkx2.1-Cre* mice spend significantly more time immobile in the forced swim test than controls. N = 5 mice for control and N=4 mice for *Arid1B*$^{LoxP/LoxP}$*;Nkx2.1-Cre*. Statistical significance was determined by two-tailed Student's t-test. Error bars show SEM. (D) Representative traces from (E). (E) No significant difference in the total time spent in the center or the number of entries into the center in the open field test. N = 5 mice for control and N=4 mice for *Arid1B*$^{LoxP/LoxP}$*;Nkx2.1-Cre*. Statistical significance was determined by two-tailed Student's t-test. Error bars show SEM. (F) *Arid1B*$^{LoxP/LoxP}$*;Nkx2.1-Cre* mice spend significantly more time grooming than controls in a 10-minute session. N = 5 mice for control and N=4 mice for *Arid1B*$^{LoxP/LoxP}$*;Nkx2.1-Cre*. Statistical significance was determined by two-tailed Student's t-test. Error bars show SEM. (G) No statistically significant difference in the novel object recognition index between *Arid1B*$^{LoxP/LoxP}$*;Nkx2.1-Cre* and control mice N = 5 mice for control and N=4 mice for *Arid1B*$^{LoxP/LoxP}$*;Nkx2.1-Cre*. Statistical significance was determined by two-tailed Student's t-test. Error bars show SEM. (H) *Arid1B*$^{LoxP/LoxP}$*;Nkx2.1-Cre* mice demonstrate significantly impaired sociability and heightened social novelty behaviors compared with controls. N=4 mice for each genotype. Statistical significance was determined by two-tailed Student's t-test. Error bars show SEM.

2.5 Discussion

2.5.1 ARID1B differentially regulates neural progenitor proliferation but has similar effects on cell survival in both cortical and ventral progenitor populations

We recently showed that adult heterozygous *Arid1b* knockout mice display a significant reduction in the overall number of their cortical interneurons with no major changes in cortical pyramidal neurons (Jung et al., 2017). We surmised that this is most likely due to defective proliferation and/or impaired cell survival in the ventral neural progenitor population. Here we show that homozygous knockout of *Arid1b* specifically in these cells leads to an overall decrease in the number of actively proliferating and/or mitotic cells, as well as fewer newborn neurons or neural progenitors in the MGE (Figure 2.2). We also report that loss of *Arid1b* in ventral neural progenitors leads to increased apoptosis in the MGE (Figure 2.3). The defects in proliferation are due, at least in part, to improper cell cycle regulation, as we observe reduced cell cycle speed and a lower rate of cell cycle re-entry in *Arid1b*-deleted ventral neural progenitors.

Somewhat unexpectedly, homozygous deletion of *Arid1b* in cortical neural progenitors also leads to significant defects in cell proliferation and survival (Figures 2.1 and 2.3), though these impairments are not as severe as what we observe with *Arid1b* knockout in the ventral telencephalon. We report no change in active cell cycle participation in *Arid1b*-deleted cortical neural progenitors, however, we do observe a notable drop in the number of mitotic cells and fewer newborn cells in the developing cerebral cortex of these mutant mice. When we examine cell cycle regulation, we also see a significant decrease in cell cycle re-entry amongst cortical neural progenitors with no change in observed cell-cycle speed (Figure 2.3). Overall, it appears that *Arid1b* deletion in this population leads to pre-mitotic cell cycle arrest, as the number of progenitors apparently active in the cell cycle is not altered, but mitosis is decreased and there are fewer newborn cells, as well as decreased cell cycle re-entry. In cortical neural progenitors, at

least, ARID1B seems to play a crucial role in cell cycle progression, which may only be grossly observable with complete depletion of *Arid1b* and its gene product.

Although ARID1B's regulation of the cell cycle and neural progenitor proliferation appears to be cell-type specific, homozygous deletion of *Arid1b* leads to similar increases in apoptosis in both cortical and ventral neural progenitor populations. This indicates that the role of ARID1B in cell survival is likely similar in both progenitor subgroups and potentially elsewhere in the brain or periphery. It is unclear from the current study whether ARID1B's functions in regulating cell proliferation or cell survival is likely to play a larger role in pathology of *ARID1B*-related neurodevelopmental disorders, but we can reasonably conclude that *Arid1b* plays a more substantial role in regulating ventral neural progenitor proliferation and survival than it does in cortical neural progenitors.

2.5.2 Regulation of β-catenin by ARID1B

In this study we report that homozygous deletion of *Arid1b* leads to reduced nuclear localization of β-catenin in ventral neural progenitors. Recently, Vasileiou et al. showed that β-catenin target gene expression is enhanced in peripheral blood lymphocytes taken from human patients with *ARID1B* loss-of-function mutations (Vasileiou et al., 2015). They also examined ARID1B interactions with β-catenin in a human osteosarcoma cell line and concluded that ARID1B-β-catenin interactions are mediated by BRG1 (Vasileiou et al., 2015). Another group demonstrated that shRNA-mediated knockdown of *Arid1b* leads to increased expression of β-catenin target genes in *Stat3* knockout, sciatic-nerve-derived neurofibroma spheres (Wu et al., 2016). A previous report, however, found that the central BAF component, BRG1, enhances β-catenin target gene expression by binding to β-catenin at target gene promoters and, most likely, facilitating chromatin remodeling (Barker et al., 2001). Our recent study involving global heterozygous

knockout of *Arid1b* agrees more with this finding, as we see significant decreases in the mRNA expression levels of several β-catenin target genes in the ventral telencephalon (Jung et al., 2017). Multiple studies have shown broad diversity in the configuration of BAF complexes dependent on cell type and switches in subunit composition play a large role in determining which genes are targeted by BAF complexes and how they mediate transcription (de la Serna et al., 2001; Olave et al., 2002; Lickert et al., 2004; Ohkawa et al., 2006; Cvekl and Duncan, 2007; Lessard et al., 2007; Li et al., 2013; Xiong et al., 2013; Son and Crabtree, 2014; Yu et al., 2015a). For this reason, the effects of *Arid1b* knockdown in non-neural progenitor or non-neuronal populations may be entirely different than what is observed in the brain. It is entirely possible that ARID1B acts to repress β-catenin in a BRG1-dependent manner in peripheral blood lymphocytes and tumor cell lines and enhance β-catenin transcriptional activation in the developing brain. To further illustrate the variable role ARID1B seems to play in different cell types, Vasileiou et al. also report that siRNA-mediated knockdown of *ARID1B* in a human neuroblastoma cell line leads to 48% of cells extending pronounced neurites, compared to 14% of cells in controls, and that this is reversed by concurrently knocking down β-catenin (Vasileiou et al., 2015). Conversely, we have shown that in utero knockdown of *Arid1b* in the cortical ventricular zone leads to impaired neuritogenesis and neurite outgrowth in mouse pyramidal neurons (Ka et al., 2016b).

Overall, these contradictions contribute to the hypothesis that BAF complexes and, by association, ARID1B fulfill different regulatory functions in diverse cell types. As such, the current limited data appears to show that ARID1B enhances the function of β-catenin in the nucleus of neural progenitors. The exact mechanism by which ARID1B influences β-catenin, however, still needs to be elucidated before strong conclusions can be drawn.

2.5.3 Arid1b knockout affects mouse behavior in a cell-type-specific manner

Arid1b haploinsufficient mice demonstrate marked ID- and ASD-like characteristics (Celen et al., 2017; Jung et al., 2017; Shibutani et al., 2017), making them a useful mouse model for studying neurodevelopmental disorders. With the apparent cortical excitatory/inhibitory imbalance we previously observed in *Arid1b* haploinsufficient mice (Jung et al., 2017), we were interested to determine whether ARID1B depletion in cortical or ventral neural progenitors and their progeny contribute individually to specific behavioral phenotypes. We report that homozygous deletion of *Arid1b* in cortical neural progenitors has little to no notable effect on the emotional or social behavior, compared with controls. It does, however, lead to a significant decrease in cognitive function, as evidenced by impaired recognition memory in *Arid1b*$^{LoxP/LoxP}$*;Emx1-Cre* mice (Figure 2.6). Conversely, *Arid1b* deletion in ventral neural progenitors appears to have no effect on cognitive performance but does lead to considerable social and emotional deficits (Figures 2.7 and 2.8).

We previously showed that multiple ASD- and ID-like behaviors can be rescued in *Arid1b* haploinsufficient mice by increasing GABA tone by treating with the GABA positive allosteric modulator, clonazepam. Intriguingly, in that study we saw improvements in both cognitive and emotional aberrant behaviors, although not all behavioral abnormalities were reversed (Jung et al., 2017). This would indicate that GABA signaling does play a role in cognitive function in *Arid1b* haploinsufficiency, even though homozygous deletion of *Arid1b* in GABAergice interneuron precursors leads to no cognitive impairments. Future studies will need to examine specific neuronal subpopulations and circuits related to particular behaviors in *Arid1b* mutant mice to provide a better understanding of the mechanistic link between ARID1B and behavior.

2.5.4 Summary

Arid1b deletion alters neural progenitor proliferation in a cell-type specific manner, but indiscriminately increases apoptosis. The former is partially due to misregulation of the cell cycle in both ventral and cortical neural progenitor pools. ARID1B also plays a role in dictating the subcellular localization of β-catenin, as *Arid1b* deletion leads to decreased levels of β-catenin in the nucleus. Homozygous knockout of *Arid1b* leads to cognitive impairments without deficits in social or emotional behavior, whereas loss of *Arid1b* in ventral neural progenitors results in aberrant social and emotional behaviors and no cognitive dysfunction. Taken together, we conclude that ARID1B plays distinct, yet overlapping roles in cortical and ventral neural progenitors. Future studies will be required to further elucidate the exact mechanisms by which ARID1B independently regulates these cell types. As multiple BAF subunits have been linked to the regulation of cell proliferation and survival (Son and Crabtree, 2014), and the function of BAF complexes can be both cell-type and subunit-composition dependent (Battaglioli et al., 2002; Inoue et al., 2002; Olave et al., 2002; Lickert et al., 2004; Lessard et al., 2007; Wu et al., 2007; Li et al., 2013; Tuoc et al., 2013; Son and Crabtree, 2014; Narayanan et al., 2015; Vasileiou et al., 2015; Hodges et al., 2016), it is likely that ARID1B indeed fulfills different roles in divergent cell populations at different times. This study supports that notion and reiterates that mutations to a single gene can have a broad impact on multiple cell types and regulate diverse functions. In order to better understand and more precisely treat neurodevelopmental disorders such as ID and ASD, we will need to elucidate the specific cell types and circuits associated with aberrant behaviors and symptoms.

CHAPTER 3: MACF1, DELETED IN 1p34.2-p34.3 DELETION SYNDROME, MODULATES RADIAL POLARITY AND CORUPUS CALLOSUM DEVELOPMENT IN THE CEREBRAL CORTEX

Minhan Ka[1,2#], Jeffrey J. Moffat[1#] and Woo-Yang Kim[1]

[1]Developmental Neuroscience, Munroe-Meyer Institute, University of Nebraska Medical Center, Omaha, NE 68198

[2]Research Center for Substance Abuse Pharmacology, Korea Institute of Toxicology, Daejeon 34114, Republic of Korea

# These authors contributed equally to this work

3.1 Abstract

The polarity of radial glial cells, which serve as neural progenitors and as guides for neuronal placement, is crucial for cortical development. Cortical development disorders, such as lissencephaly and Subcortical Band Heterotopia (SBH), are associated with autism and intellectual disability. *MACF1* is the candidate gene for 1p34.2-p34.3 deletion syndrome, a chromosomal deletion disorder characterized by a greatly increased risk for autism and neurodevelopmental delay. Here we show that genetic deletion of *Macf1* in the developing mouse cerebral cortex results in SBH and abnormal neural proliferation. We further show that the abnormal polarity of radial glial progenitors in *Macf1* mutants causes neural proliferation and migration defects through destabilization of actin and microtubules in the developing cortex. Moreover, *Macf1* mutants also show defects in the ciliogenesis of radial glial progenitors in the ventricular zone (VZ) during cortical development. In addition, *Macf1*-mutant mice exhibit significant behavioral deficits. Our findings suggest that defects in microtubule binding components massively affect neural progenitor proliferation and cortical lamination via regulation of radial glial cell polarity in developing cortex, leading to cognitive and behavioral deficits.

3.2 Introduction

Alterations in gene dosage due to the duplication or deletion of specific chromosome regions cause many neurodevelopmental disorders frequently associated with autism spectrum disorders (ASD), mental retardation, intellectual disability (ID), and other related conditions (Lupski and Stankiewicz, 2005; Lee and Lupski, 2006; Geschwind, 2011; Mefford et al., 2012). A de novo 4.1Mb microdeletion at chromosome 1p34.2-p34.3 has been identified by array-based comparative genomic hybridization in a young male with severely delayed development, microcephaly, pronounced hypotonia, and facial dysmorphism (Vermeer et al., 2007). Additionally, a 3.3Mb deletion of 1p34.2-p34.3 was reported in another patient characterized by microcephaly, ID and ASD (Kumar et al., 2010). An unborn fetus with a 2.7Mb de novo deletion of 1p34.3 was diagnosed with developmental delay and micrognathia (Dagklis et al., 2016). Chromosome 1p34.2-p34.3 contains about 43 genes, including Microtubule-Actin Crosslinking Factor 1 (*MACF1*), a gene previously shown to regulate neuronal migration and dendrite outgrowth in the developing cerebral cortex (Kumar et al., 2010; Ka et al., 2014a; Ka and Kim, 2016; Ka et al., 2016a; Moffat et al., 2017).

MACF1 is a cytoskeletal linker protein that interacts with both F-actin and microtubules via an actin-binding domain near its N-terminus and a microtubule-binding domain near its C-terminus (Leung et al., 1999; Sun et al., 2001; Suozzi et al., 2012). MACF1 regulates pyramidal neuronal migration via microtubule dynamics and GSK-3 signaling in the developing cerebral cortex (Ka et al., 2014a). MACF1 is also required for dendrite arborization and axon outgrowth, which are both critical for the establishment of neuronal connections in the developing brain (Ka and Kim, 2016). We have also previously shown that MACF1 plays a critical role in cortical interneuron migration and positioning in the developing brain (Ka et al., 2016a). These findings suggest a potential

role for MACF1 in neuronal differentiation during brain development. However, the role of MACF1 and its associated mechanisms in neural cell proliferation and the interkinetic nuclear migration (INM) of radial glial cells *in vivo* is not known.

The cerebral cortex is a central brain region, which controls complex cognitive behaviors, and cortical size is crucial for normal brain function (Geschwind and Rakic, 2013). The control of cortical size depends on the balanced control of neural progenitor and mature neuron maintenance in developing brain (Chenn and Walsh, 2002). Radial glial cells (RGCs) are the key progenitor cells in the developing cerebral cortex. They can either generate two new RGCs via symmetric division or divide into one intermediate progenitor or post mitotic neuron and one RGC via asymmetric division during development (Gotz and Huttner, 2005; Huttner and Kosodo, 2005). RGCs extend apical radial fibers toward the ventricular zone (VZ) and basal radial fibers toward the marginal zone of the cerebral cortex (Fishell and Kriegstein, 2003; Rakic, 2003). The RGCs in the cortical VZ of the developing brain exhibit INM, in which their nuclei migrate between the apical surface and the basal portion of the polarized radial glial cells in phase with their cell-cycle progression (Frade, 2002; Gotz and Huttner, 2005; Schenk et al., 2009). Immediately following cell division, the nuclei are located at the apical surface, from where they migrate basally for the duration of the G1 phase of the cell cycle and subsequently remain in the basal region of the VZ during S phase. Upon commencement of the G2 phase, the nuclei begin to migrate apically, entering the M phase once they reach the apical surface (Kosodo et al., 2011; Kosodo, 2012). The actin and microtubule cytoskeleton are critical for both INM and neural proliferation (Messier and Auclair, 1973; Gotz and Huttner, 2005), however the regulatory roles for INM of RGCs in neocortical neurogenesis are not fully understood.

Here we investigate the functions and mechanisms of MACF1 in neural proliferation and the INM of radial glial progenitors during cortical development. We employ conditional knockout strategies to target MACF1 specifically in developing neural progenitors and provide evidence that MACF1 is essential for maintaining the neural progenitor pool via regulation of radial glial cell polarity during mouse neocortical development. We also report that loss of MACF1 results in aberrant radial progenitor proliferation and cortical malformation. Furthermore, *Macf1* knockout mice demonstrate social and intellectual behavioral deficits and their brains display SBH. These findings support the proposition that loss of *Macf1* expression is the fundamental cause of at least some of the anatomical and behavioral abnormalities produced by de novo microdeletion of chromosome 1p34.2-p34.3.

3.3 Materials and methods

3.3.1 Mice

Mice were handled according to our animal protocol approved by the University of Nebraska Medical Center. The *Macf1* floxed mouse was described previously (Wu X et al., 2011). The Emx1-Cre mouse (Tronche et al., 1999) was purchased from The Jackson laboratory.

3.3.2 Immunostaining

Immunostaining of brain sections or dissociated neural cells was performed as described previously (Kim et al., 2006; Ka et al., 2016c). The following primary antibodies were used: Rabbit anti-MTOR (Santa Cruz, sc-68430), mouse anti-NeuN (EMD Millipore, MAB337), rat anti-neural cell adhesion molecule L1 (EMD Millipore, MAB5272), rabbit anti-TBR1 (Abcam, ab31940), rabbit anti-CUX1 (Santa Cruz, sc-13024), chicken anti-MAP2 (Abcam, ab5392), rabbit anti-GFAP (Abcam, ab7260), rabbit anti-Ki67 (Cell Signaling, #9129), rabbit anti-phospho-Histone H3 (Cell Signaling, #9701S), mouse anti-BrdU (BD Biosciences, 555627), chicken anti-TBR2 (EMD Millipore, ab15894), rabbit anti-BLBP (Abcam, ab32423), mouse anti-Nestin (PhosphoSolutions, 1435-NES), rabbit anti-ARL13B (Abcam, ab83879), rabbit anti-Acetyl-α-Tubulin (Cell Signaling, #5335), chicken anti-GFP (Thermo Fisher, A10262), rabbit anti-GFP (Thermo Fisher, A11122) and Alexa Fluor568-Phalloidin (Thermo Fisher, A12380). Appropriate secondary antibodies conjugated with Alexa Fluor dyes (Thermo Fisher) were used to detect primary antibodies.

3.3.3 In utero electroporation

In utero electroporation was performed as described previously (Ka et al., 2016b; Ka and

Kim, 2016). Briefly, timed pregnant female mice from E13.5 of gestation were deeply anesthetized, and the uterine horns were gently exposed by laparotomy. The lateral ventricles of an embryonic brain were injected with plasmid DNA (2 μg/μl) and 0.001% fast green (Sigma-Aldrich Corporation, St. Louis, MO, USA) using a Picospritzer II (Parker Hannifin, Hollis, NH, USA). Electroporation was achieved by placing two sterile forceps-type electrodes on opposing sides of the uterine sac around the embryonic head and applying a series of short electrical pulses using a BTX ECM 830 electroporator (Harvard Apparatus, Holliston, MA, USA) (five pulses with 100 ms length separated by 900 ms intervals were applied at 45 V). The small electrical pulses drive charged DNA constructs into surrounding cells in the embryonic brain. Embryos were allowed to develop *in utero* for the indicated time.

3.3.4 Morphometry

Images of brain sections at periodic distances along the rostro-caudal axis were taken with the Zeiss LSM710 confocal microscope and ZEN software. We counted DAPI, BrdU, KI67, phospho-Histone H3, TBR2-positive cells in a field of 0.2 or 0.4 mm^2 throughout the rostro-caudal extent of the cerebral cortex. Ten mice for each experiment (control mice, n= 5; mutant mice, n= 5) were used. Stereological analysis of immunostained cells was performed by analyzing one-in-six series of 40 μm coronal sections (240 μm apart). The images were subjected to software-driven particle analysis with automatic machine-set thresholding in ImageJ, thus eliminating subjective investigator bias. Then, a particle parameter enumeration analysis was followed for size exclusion at minimum of 10 $pixel^2$. The blue channel images were used to assess background cells. For analyzing cultured cells, more than 20 fields scanned horizontally and vertically were examined in each condition. Cell numbers were described in figure legends. The calculated values were averaged, and some results were recalculated as

relative changes versus control.

3.3.5 BrdU administration and cell cycle analysis

BrdU injection and cell cycle analysis were performed as described previously (Ka et al., 2014b; Ka et al., 2017). Intraperitoneal injection of BrdU (20mg per kg body weight) was performed into pregnant mice at E13.5-14.5. For the analysis of cell cycle re-entry, BrdU was administered to control and *Macf1*-cKO mice for 24 h. Brains were fixed with 4% PFA, sliced, and immunostained with antibodies to BrdU and KI67. The ratio of cells labeled with BrdU and KI67 to total cells that incorporated BrdU was determined. For the analysis of cell cycle length, the ratio of progenitor cells positive for KI67 and BrdU to the total KI67 labeled cells was assessed after a 30 min BrdU pulse.

3.3.6 Behavioral assays

All behavioral assays were done during light cycle. Behavior recording and analysis were performed by a researcher blinded to the genotype of each mouse. Health conditions including weights, activity and feeding were checked prior to assays.

3.3.7 Rearing test

A test mouse was placed in a clean 300 ml glass beaker (Fisherbrand) and filmed for 5 minutes. The number of times reared and the total duration of rearing were recorded. A rearing even was only counted when both hindpaws were fully extended. The beaker was cleaned with 70% ethanol between each trail.

3.3.8 Grip strength test

A mouse is suspended upside-down from a wire mesh approximately 60 cm from a

padded surface for a maximum of 2 minutes as described elsewhere (Deacon, 2013). The mean latency to fall for each mouse is recorded in three trials with at least a 30-minute break between trials. The wire mesh was cleaned with 70% ethanol between each trial.

3.3.9 Open field test

A mouse was placed near the wall-side of a 35 × 42 cm open-field arena, and the movement of the mouse was recorded by a camera for 5 min. The recorded video file was further analyzed using EthoVision XT 7.0 software (Noldus). Total distance moved and average velocity of movement were recorded. The number of entries into, and the overall time spent in, the center of the arena (15 × 15 cm imaginary square) were also measured. The open field arena was cleaned with 70% ethanol between each trial.

3.3.10 Novel object recognition test

A test mouse was first habituated to an open field arena (35 × 42 cm) for 5 min. Following habituation, the test mouse was removed from the arena and two identical objects with size (10.5 × 4.5 × 2.5 cm) were placed in the opposite corners of the arena, 7 cm from the side walls. Then the test mouse was reintroduced into the center of the arena and allowed to explore the arena including the two novel objects for 10 min. After 6 h, one object was replaced with another novel object, which was of similar size but different shape and color than the previous object. The same test mouse was placed in the arena to explore the arena and the two objects. The movement of mice was recorded by a camera for 10 min and further analyzed by the video tracking EthoVision XT 7 software (Noldus).

3.3.11 Three-chamber test for social interaction and novelty behavior

Social behavior was evaluated as described previously 41. A rectangular and

transparent Plexiglas box divided by walls into three equal-sized compartments (Ugobasile) was used. Rectangular holes in the Plexiglas walls provide access between the chambers. For sociability testing, the test mouse was moved to the center chamber (chamber 2) with the entrances to the two connecting chambers blocked. A stimulus mouse (unfamiliar mouse) designated as “stranger 1” was placed in a wire enclosure in chamber 1. Then, the openings to the flanking two chambers (1 and 3) were opened and the test mouse was allowed to explore the entire apparatus for 10 min. For the social novelty test, the stranger 1 mouse was randomly placed in one of the enclosures in which the test mouse had the choice of whether to investigate the stranger 1 mouse or a novel mouse, designated “stranger 2”. This novel mouse was taken from a different home cage and placed into the remaining empty wire enclosure. Time spent sniffing each partner by the test mouse was recorded for 10 min in both sociability and social novelty behavior tests. All apparatus chambers were cleaned with water and dried with paper towels between trials. At the end of each test day, the apparatus was sprayed with 70% ethanol and wiped clean with paper towels.

3.3.12 Elevated plus-maze test

The elevated plus-maze test was performed as previously described 41. The apparatus (EB Instrument) includes two open arms (35 × 5 cm), two enclosed arms (35 × 5 × 15 cm), and a central platform (5 × 5 cm). The entire apparatus was elevated 45 cm above the floor. A mouse was placed on the central platform, facing the same open arm and allowed to roam freely for 5 minutes. The number of entries into, and the time spent on open and closed arms were recorded. Percent open arm time was calculated as time spent in the open arms divided by the total time. Rearing frequency was also recorded.

3.3.13 Forced swimming test

A mouse was placed individually into a glass cylinder (20 cm height, 17 cm diameter)

filled with water to a depth of 10 cm at 25°C. After 5 minutes, the animals were removed from the water, dried, and returned to their home cages. They were again placed in the cylinder 24 hr later, and after the initial 1 min acclimatization period, the total duration of immobility was measured for 5 min. Motionless floating was considered immobile behavior.

3.3.14 Tail suspension test

A mouse was suspended from the hook of a tail suspension test box, 60 cm above the surface of a table using adhesive tape placed 1 cm away from the tip of the tail. After 1 min acclimatization, immobility duration was recorded by a camera for 5 minutes. Mice were considered immobile only when they hung passively and were completely motionless.

3.3.15 Statistical analysis

Normal distribution was tested using the Kolmogorov–Smirnov test and variance was compared. Unless otherwise stated, statistical significance was determined by two-tailed unpaired Student's t-test for two-population comparison and one-way analysis of variance followed by Bonferroni correction test for multiple comparisons. Data were analyzed using GraphPad Prism and presented as mean (+/-) SEM. P values are indicated in figure legends.

3.4 Results

3.4.1 Generation and gross anatomy of Macf1$^{F/F}$; Emx1-Cre (Macf1-cKO) mice

To examine the roles of MACF1 in neuronal proliferation during cerebral cortex development, we crossed *Macf1* floxed mice (Goryunov et al., 2010) with an Emx1-Cre mouse line (Tronche et al., 1999). These *Macf1*; *Emx1*-Cre conditional knockout (*Macf1*-cKO) mice express Cre recombinase by embryonic day 9.5 (E9.5) in dorsal neural progenitor cells (Gorski et al., 2002; Iwasato et al., 2004). *Macf1*-cKO mice survive into adulthood, however, they exhibit a reduced survival rate compared to control mice (Figure 3.1A-B). *Macf1*-cKO mice also present with significantly reduced body weight and slightly reduced brain volume and size at 8 weeks of age (Figure 3.1C-D). Interestingly, *Macf1*-cKO mice display an increased brain-to-body-weight ratio (Figure 3.1A, D). In order to further define neuroanatomical abnormalities in these mutant mice, we measured cortical parameters including cortical area, anteroposterior (A-P) length and cortical length in *Macf1*-cKO and control mice (Pucilowska et al., 2015), (Figure 3.1E). *Macf1*-cKO brains show a significant decrease in cortical area, A-P length and cortical length (Figure 3.1C, F). Histological examination of brain sections stained with DAPI reveals that *Macf1*-cKO brains also exhibit thicker cerebral cortices throughout the rostrocaudal axis (Figure 3.1G-H). However, *Macf1*-cKO brains display thinner cortical plates and smaller hippocampal areas, compared with control brains (Figure 3.1G-H). *Macf1*-cKO brains present SBH in the rostrocaudal region of the cerebral cortex, near the hippocampus (Figure 3.1G). Interestingly, *Macf1*-cKO brains do not exhibit any differences in brain size or brain volume at postnatal day 3 (P3) (Figure 3.2A-B). However, histological analysis of *Macf1*-cKO brains displayed SBH throughout the rostrocaudal axis of the cerebral cortex at P3, where we observed a second, ectopic layer of gray and white matter (Figure 3.1I and Figure 3.2B-C).

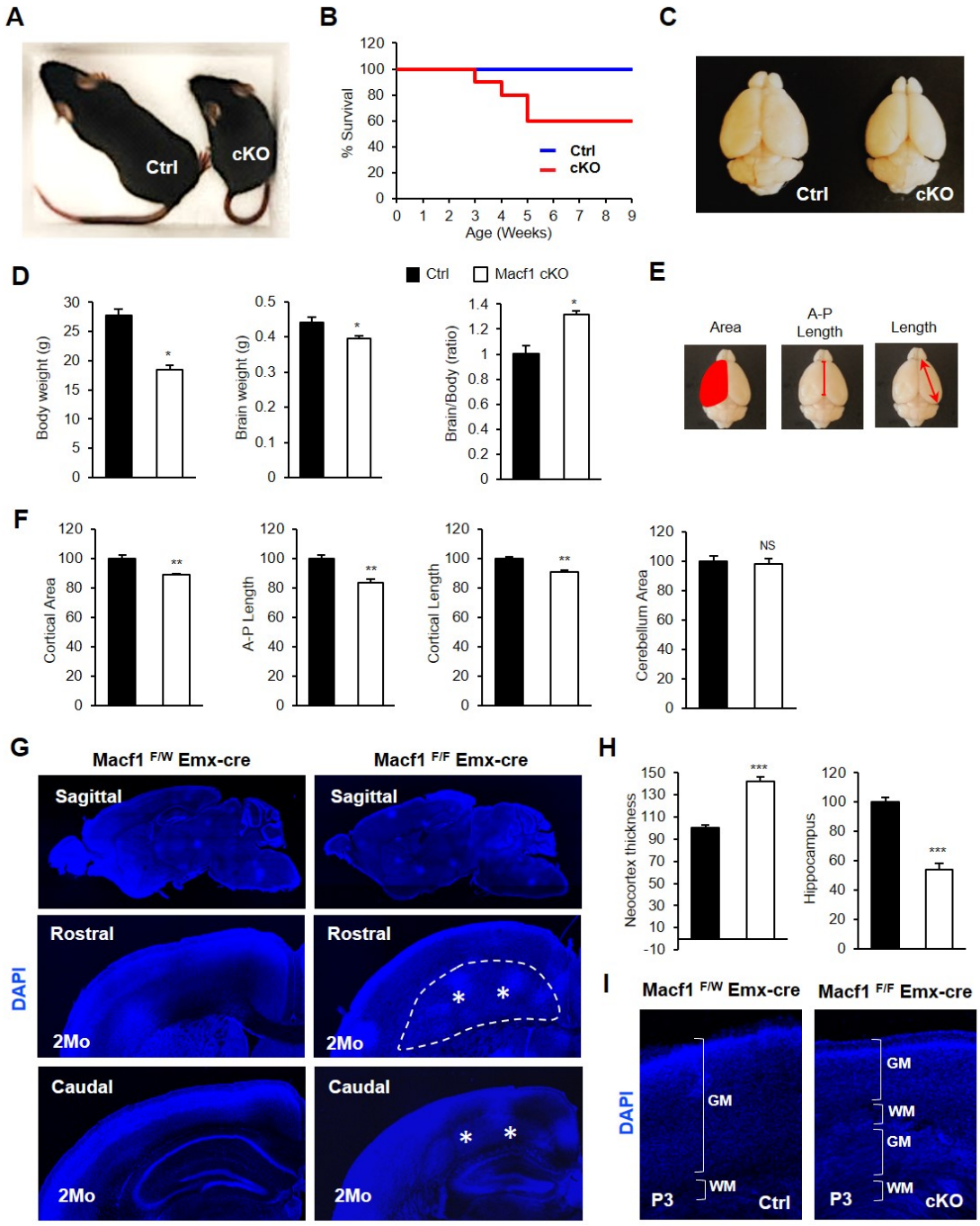

Figure 3.1 Severe brain malformations in *Macf1*$^{LoxP/LoxP}$/*Emx1-Cre* (*Macf1*-cKO) mice

(A) Representative images of control (larger one, left) and Macf1-cKO (smaller one, right) mice at 2-month-old. (B) The survival curve of Macf1-cKO and control mice after the Kaplan-Meier method. The numbers of mice used were 20 for littermate control and 10 for Macf1-cKO mice. (C) Representative images of whole brains control (left) and Macf1-cKO (right) mice at 2-month-old. (D) Quantifications of the body weight and brain weight of the control and Macf1-cKO mice. N=5 mice for each condition. Statistical

significance was determined by two-tailed Student's t-test. Error bars show standard error of the mean (SEM). *p < 0.05. (E), (F) Measured of cortical parameters including cortical area, anteroposterior (A-P) length, cortical length and cerebellum area. N= 5 mice for each condition. Statistical significance was determined by two-tailed Student's t-test. Error bars show standard error of the mean (SEM). **p < 0.01. (G) Histologic appearance of brain sections from 2-month-old control and Macf1-cKO mice were stained with DAPI. Stars indicate SBH. Scale bars: 3mm, 300μm. (H) Quantifications of the thickness of the neocortex and hippocampus of the control and Macf1-cKO mice. N= 5 mice for each condition. Statistical significance was determined by two-tailed Student's t-test. Error bars show standard error of the mean (SEM). ***p < 0.001. (I) Coronal brain sections from P3 of the control and Macf1-cKO mice were stained with DAPI. GM indicates gray matter. WM indicates white matter. Arrows indicate ectopically formed layer of gray matter. Scale bars: 50μm.

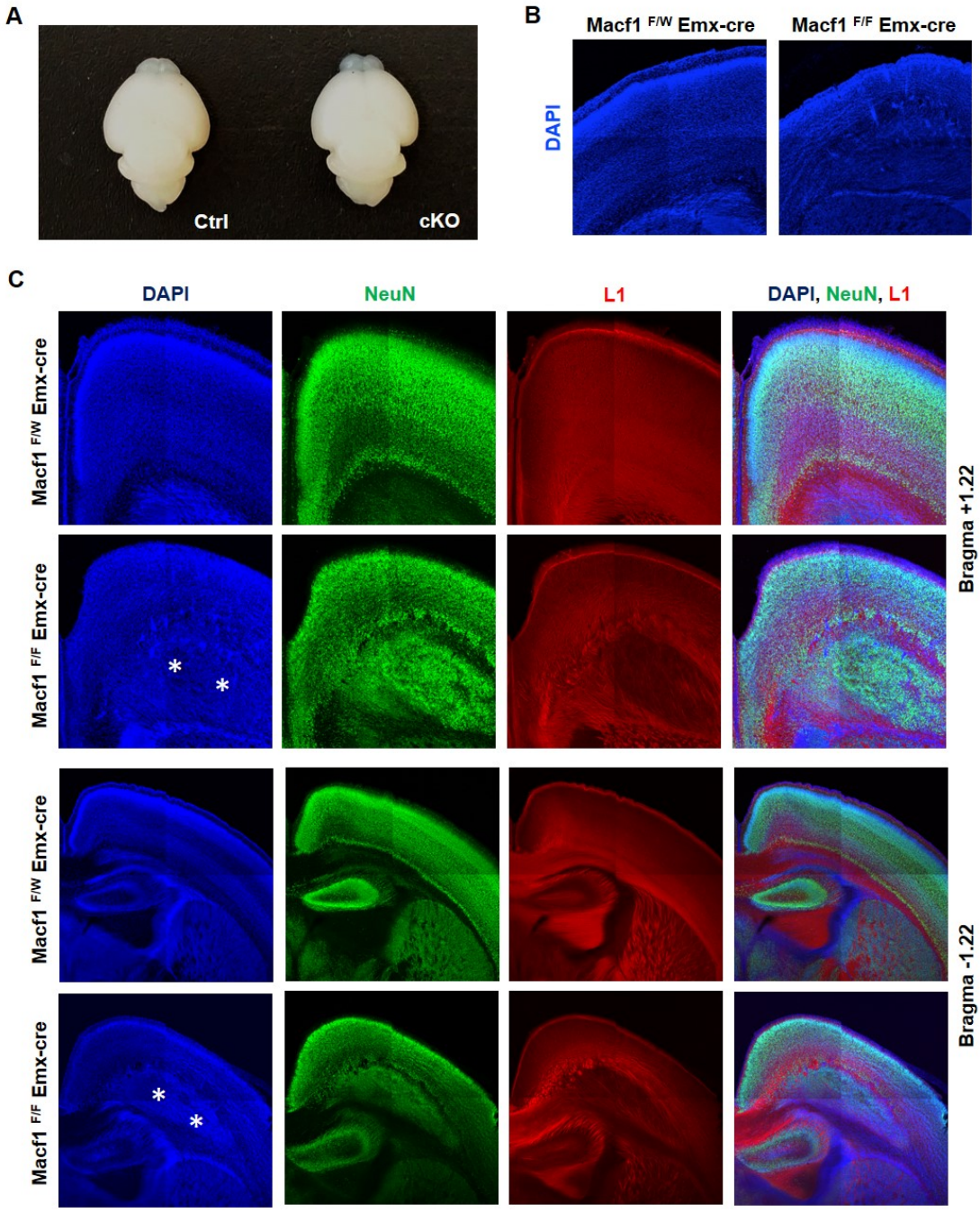

Figure 3.2 *Macf1* cKO causes SBH or double cortex

(A) Representative images of whole brains control (left) and *Macf1*-cKO (right) mice at P3 stage. (B) Measured of cortical parameters including cortical area and cortical length. N= 5 mice for each condition. Statistical significance was determined by two-tailed Student's t-test. Error bars show standard error of the mean (SEM). (C) Immunostaining of coronal cerebral cortical sections from P3 control and *Macf1*-cKO brains with anti-NeuroN (NeuN) and anti-L1 antibodies. Stars indicate SBH. Representative images from both three control and *Macf1*-cKO brains. Scale bars: 300μm.

3.4.2 Cortical malformations in Macf1-cKO brains

To examine the roles of MACF1 in neuronal positioning within the cerebral cortex, we immunostained for NeuN, a marker for differentiated neurons, and L1, a neural cell adhesion molecule. In P3 control mice, NeuN-positive cells were localized to the cortical plate, above L1-positive areas, which lined the neuronal axon tracts and the corpus callosum and make up the white matter of cerebral cortex (Figure 3.3A and Figure 3.2C). Conversely, *Macf1*-cKO mice exhibited a thin layer of NeuN-positive neurons in the cortical plate and periventricular heterotopia. Moreover, *Macf1*-cKO brains displayed abnormal L1-positive axon tracts surrounding ectopic neuronal nodules (Figure 3.3A and Figure 3.2C). These results demonstrate that deletion of *Macf1* in the developing cerebral cortex results in the formation of SBH, or double-cortex, and the SBH in *Macf1*-cKO brains is composed of differentiated neurons.

Next, to examine the laminar identity of the heterotopic neurons, we immunostained for TBR1, a marker of deeper-layer cortical neurons, CUX1, a marker of more superficial cortical neurons, MAP2, a marker of neural dendrites and mature neurons, and GFAP, an astrocyte marker, in P3 mice. In control brains, TBR1-positive neurons are mostly restricted to the deeper cortical layer VI, whereas TBR1-positive neurons in *Macf1*-cKO brains appear to be abnormally distributed throughout multiple cortical layers (Figure 3.3B). Similar patterns can be seen with CUX1 immunostaining. CUX1-positive neurons are localized in superficial cortical layers II-IV in control brains, however CUX1-positive neurons in *Macf1*-cKO mice are spread evenly throughout the cortex (Figure 3.3B). MAP2-positive mature neurons are positioned in the cortical plate and not in the IZ of control brains, however, MAP2-positive mature neurons in *Macf1*-cKO brains accumulate in heterotopic nodules (Figure 3.3B). Moreover, GFAP-positive astrocytes are not generally found in the cortical plate of control brains but can be readily observed in heterotopic nodules within the cortical plates of *Macf1*-cKO mice (Figure 3.3B).

In 8-week-old control mice, NeuN-positive cells are positioned within the cortex, above GFAP-positive astrocytes. GFAP-positive astrocytes also accumulate in the white matter of the corpus callosum (Figure 3.3C). Similarly, NeuN-positive neurons are found throughout the cerebral cortex in *Macf1*-cKO mice, however, GFAP-positive astrocytes are ectopically spread throughout the cortex (Figure 3.3C). Interestingly, the number of NeuN-positive neurons in *Macf1*-cKO mice is higher than in control mice (Figure 3.3C). Finally, to examine cortical layering in *Macf1*-cKO mice we immunostained for NeuN and labeled all nuclei with DAPI and assessed brains from cortical layer II-III to the pial surface of cerebral cortex. Control brains display a clear separation between cortical layer II-III and the pial surface. DAPI-positive, non-neuronal cells are densely concentrated in a straight line along the pial surface, while NeuN-negative Cajal–Retzius cells are localized in cortical layer I, and NeuN-positive pyramidal neurons populate cortical layer II-III (Figure 3.3D). In *Macf1*-cKO brains, however, the pial surface is not clearly defined and non-neuronal cells are interspersed with layer I and layer II-III neurons (Figure 3.3D). Together, these results suggest that dorsal neural progenitor specific *Macf1*-cKO mice display abnormal neural placement and develop pronounced malformations of the cerebral cortex.

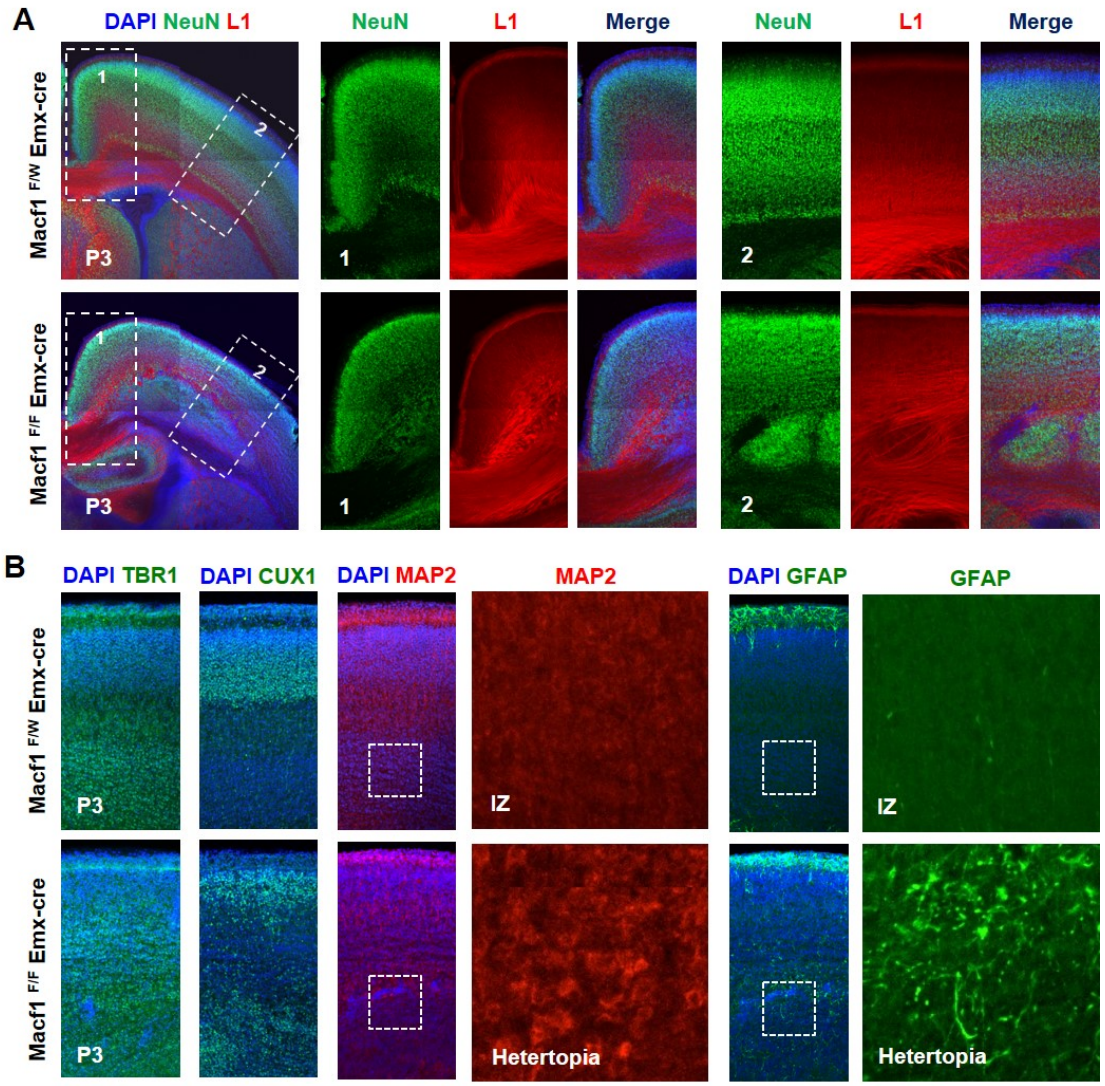
A
DAPI NeuN L1
NeuN
L1
Merge
NeuN
L1
Merge
Macf1 F/W Emx-cre
Macf1 F/F Emx-cre
P3
1
2
B
DAPI TBR1
DAPI CUX1
DAPI MAP2
MAP2
DAPI GFAP
GFAP
IZ
Hetertopia

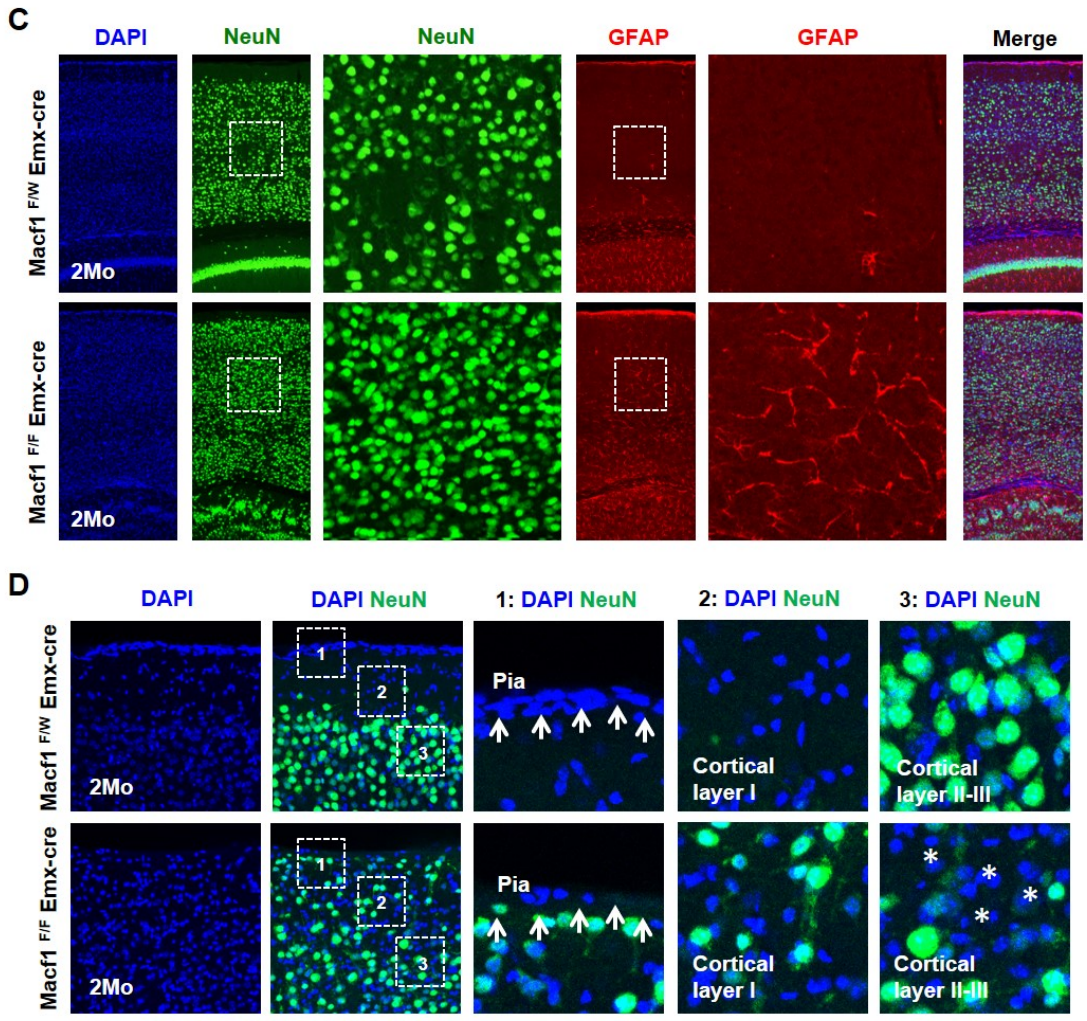

Figure 3.3 Cortical malformation of *Macf1*-cKO brains

(A) Immunostaining of coronal cerebral cortical sections from P3 control and *Macf1*-cKO brains with anti-NeuroN (NeuN) and anti-L1 antibodies. Representative images from both three control and *Macf1*-cKO brains. Scale bars: 300μm, 50μm. (B) Immunostaining of coronal cerebral cortical sections from P3 control and *Macf1*-cKO brains with anti-TBR1, anti-CUX1, anti-MAP2 or anti-GFAP antibodies. Representative images from both five control and *Macf1*-cKO brains. Scale bars: 50μm, 20μm. (D) Immunostaining of coronal cerebral cortical sections from 2-month-old control and *Macf1*-cKO brains with anti-NeuN and anti-GFAP antibodies. Representative images from both three control and *Macf1*-cKO brains. Scale bars: 50μm, 20μm. (D) Immunostaining of coronal cerebral cortical sections control and *Macf1*-cKO brains with anti-NeuN antibody. Arrows indicate Cajal-Retzius cells in pia surface and stars indicate non-neuronal cells in II-III cortical layers. Representative images from both three control and *Macf1*-cKO brains. Scale bars: 20μm, 10μm.

3.4.3 Progenitor proliferation in the Macf1-cKO cerebral cortex

We next attempted to delineate how *Macf1*-cKO mice develop such distinct SBH during development. DAPI staining reveals that *Macf1*-cKO brains exhibit thicker cerebral cortices, compared with control brains, while control mice present with thicker cortical plates all along the rostrocaudal axis (Figure 3.4A-B). Ki67 immunostaining generally labels actively proliferating cells. At E14.5, the number of KI67-positive progenitor cells in *Macf1*-cKO brains is increased by 92%, compared with control brains (Figure 3.4C and Figure 3.5A-B). In addition, KI67-positive proliferating cells accumulate in the subventricular zone (SVZ) and VZ of control brains (Figure 3.4C and Figure 3.5A-C), while KI67-positive progenitor cells in *Macf1*-cKO brains are abnormally scattered between the SVZ/VZ, intermediate zone (IZ) and cortical plate (Figure 3.4C and Figure 3.5A-C). We assessed cells in the mitotic phase by immunostaining for phospho-histone H3. Similar to our Ki67 results, there is a 116% increase in the number of phospho-histone H3-positive mitotic cells in *Macf1*-cKO brains, compared with controls (Figure 3.4D and Figure 3.5D, E). Likewise, phospho-histone H3-positive mitotic cells in control brains accumulate in the VZ, but phospho-histone H3-positive mitotic cells in *Macf1*-cKO brains appear to be abnormally spread throughout all cortical layers (Figure 3.4D and Figure 3.5D, F). Finally, we immunostained cerebral cortex sections with an antibody to Tbr2, a marker for intermediate neural progenitors (Sessa et al., 2008). The number of Tbr2-positive intermediate progenitors in the *Macf1*-cKO cerebral cortex is 98% higher than in control brains (Figure 3.4E and Figure 3.5G-H). In control cortices, Tbr2-positive intermediate progenitors localize within the SVZ, whereas Tbr2-positive cells in *Macf1*-cKO mice are spread out evenly throughout the cortex (Figure 3.4E and Figure 3.5G, I). Together, these results demonstrate that MACF1 plays an important role in radial progenitor proliferation during cortical development. In addition, MACF1 plays a crucial role in regulating proliferation in a region-specific manner within cerebral cortex.

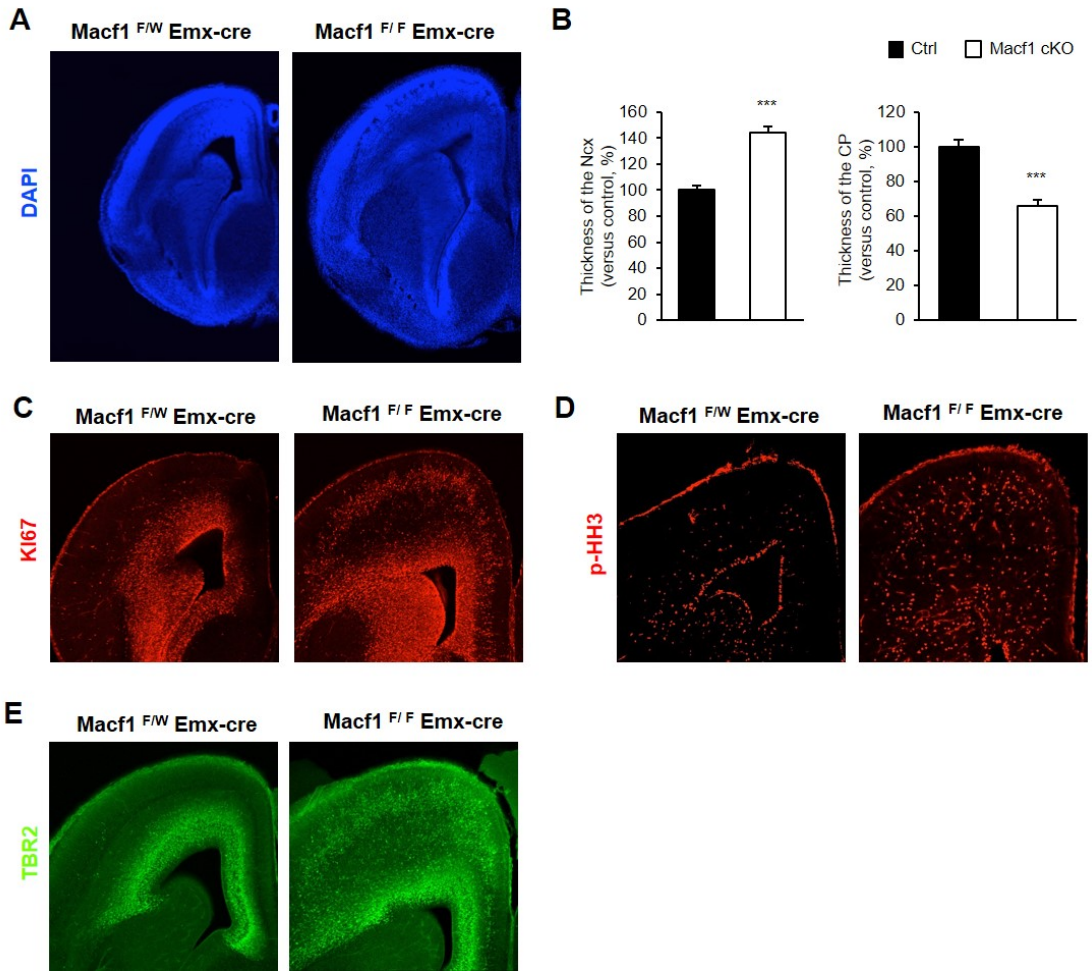

Figure 3.4 *Macf1*-cKO causes abnormal proliferation in developing cerebral cortex

(A) Histologic appearance of coronal brain sections from E14.5 of the control and *Macf1*-cKO mice were stained with DAPI. Scale bars: 300μm. (B) Quantifications of the thickness of the neocortex and CP of the control and *Macf1*-cKO mice. N= 5 mice for each condition. Statistical significance was determined by two-tailed Student's t-test. Error bars show standard error of the mean (SEM). ***$p < 0.001$. (C), (D), (E) Immunostaining of coronal cerebral cortical sections from E14.5 control and *Macf1*-cKO brains with anti-KI67, anti-phospho Histone H3 (p-HH3) or anti-TBR2 antibodies. Representative images from both three control and *Macf1*-cKO brains. Scale bars: 100μm.

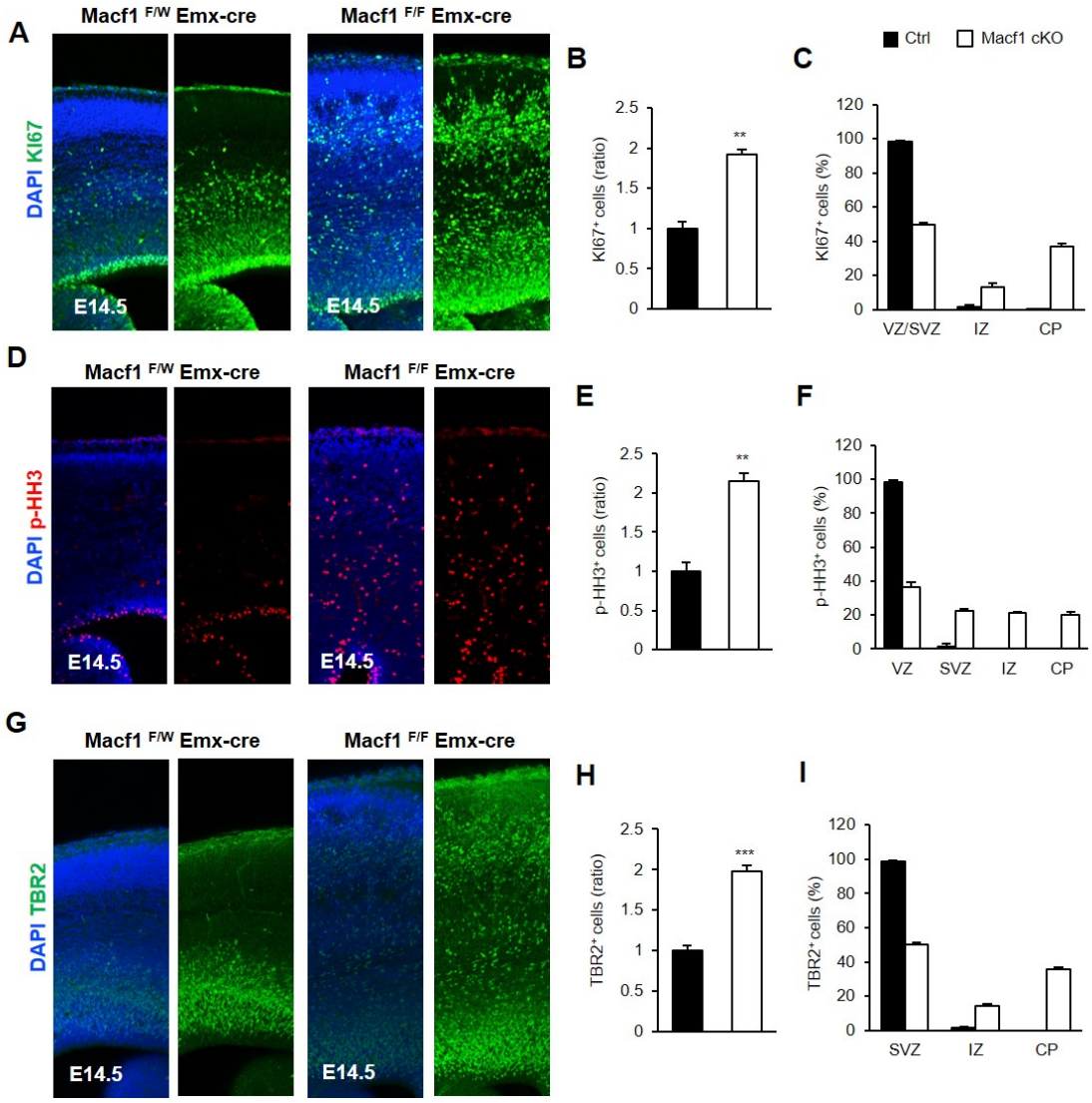

Figure 3.5 Proliferation in the *Macf1*-cKO developing cerebral cortex

(A), (D), (G) Immunostaining of coronal cerebral cortical sections from E14.5 control and *Macf1*-cKO brains with anti-KI67, anti-phospho Histone H3 (p-HH3) or anti-TBR2 antibodies. Representative images from both three control and *Macf1*-cKO brains. Scale bars: 50μm. (B), (E), (H) Quantifications of the KI67$^+$, p-HH3$^+$ or TBR2$^+$ of the control and *Macf1*-cKO brains. N=5 mice for each condition. Statistical significance was determined by two-tailed Student's t-test. Error bars show standard error of the mean (SEM). $^{**}p < 0.01$, $^{***}p < 0.001$. (C), (F), (I) Quantification of KI67$^+$, p-HH3$^+$ or TBR2$^+$ cells throughout the cerebral cortex. N=5 mice for each condition. Statistical significance was determined by multiple t-tests with Bonferroni correction test. Error bars show standard error of the mean SEM. $^{*}p < 0.05$, $^{***}p < 0.001$.

3.4.4 Cell cycle speed and re-entry of Macf1-cKO radial progenitors

To identify the underlying cause of the increase in radial progenitor proliferation in the *Macf1*-cKO cerebral cortex we first examined cell cycle speed, because a prolonged cell cycle could lead to the observed decrease in proliferation. We immunostained control and *Macf1*-cKO brains with Ki67 and BrdU antibodies and assessed Ki67/BrdU double-positive cells divided by the total number of Ki67-positive cells after a 30min BrdU pulse. This method has been established as a way to calculate the cell cycle speed index of neural progenitors (Chenn and Walsh, 2002; Ka et al., 2014b; Ka et al., 2017). This cell cycle speed index is increased by 60% in the *Macf1*-cKO cerebral cortex compared with controls (Figure 3.6A-B). Next, to investigate whether conditional *Macf1* deletion causes changes in cell cycle re-entry, we assessed the proportion of cells that re-enter the cell cycle after a 24 h BrdU pulse, which is calculated by dividing the number of Ki67/BrdU double-positive cells by the total number of BrdU-positive cells (Ka et al., 2014b; Ka et al., 2017). The number of progenitors re-entering cell cycle is 46% higher in the *Macf1*-cKO cerebral cortex than in controls (Figure 3.6C-D and Figure 3.7). These results indicate that both an increase in cell cycle re-entry and an increase in cell cycle speed induce radial progenitor self-renewal, leading to the marked growth of radial progenitor pools in the *Macf1*-cKO cerebral cortex.

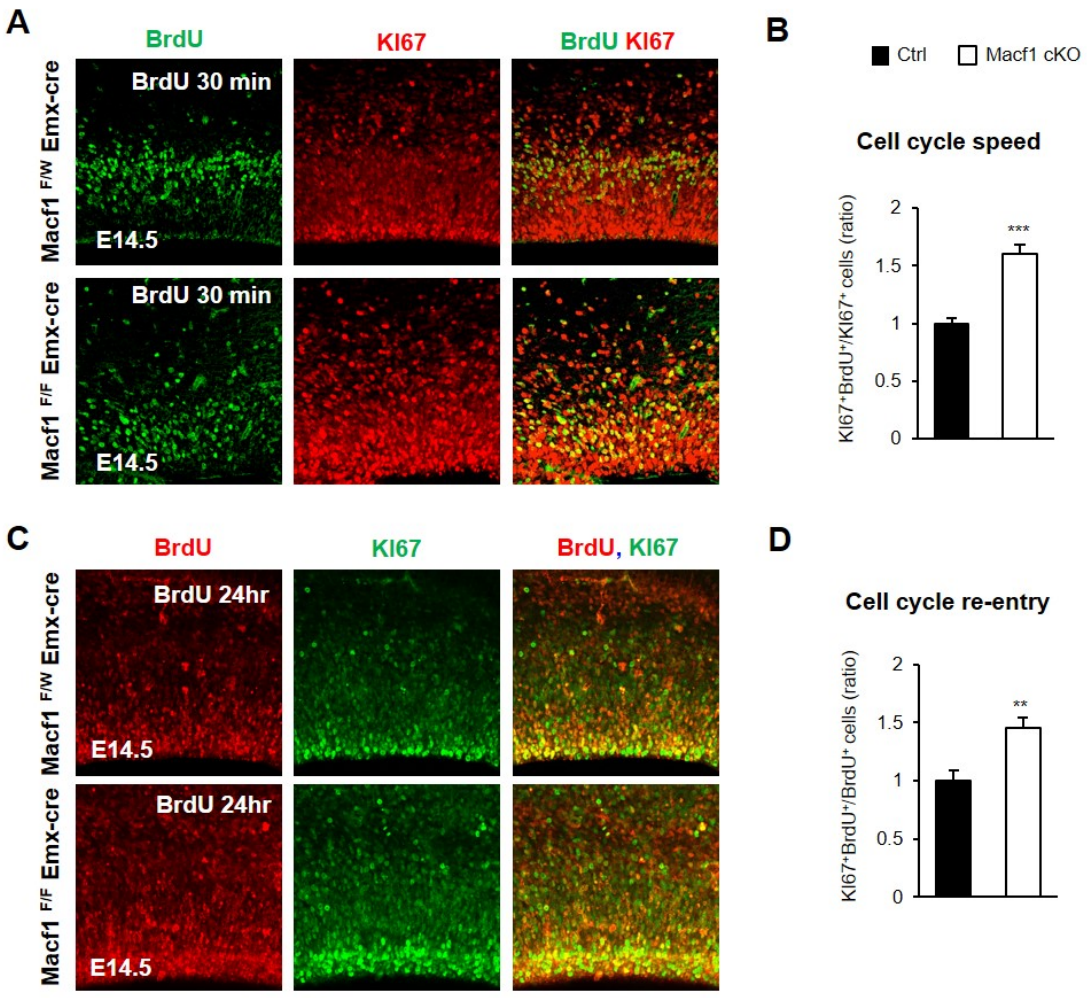

Figure 3.6 Altered cell cycle progression in the *Macf1*-cKO developing cerebral cortex

(A) E14.5 control and *Macf1*-cKO mice were pulse-labeled with BrdU for 30 min, and then brain regions containing the cerebral cortex were collected and immunostained using BrdU and Ki67 antibodies. Scale bar: 20μm. (B) Quantification of cell cycle speed. The cell cycle speed was defined as the fraction of $BrdU^+$ and $Ki67^+$ cells in total $Ki67^+$ cells in the cerebral cortex. N=5 mice for each condition. Statistical significance was determined by two-tailed Student's t-test. Error bars show SEM. ***$p < 0.001$. (C) E13.5 control and *Macf1*-cKO mice were pulse-labeled with BrdU for 24 h and then brains were collected for immunostaining with BrdU and Ki67 antibodies. Scale bar: 20μm. (D) The index of cell cycle re-entry was calculated as the fractions of both $BrdU^+$ and $Ki67^+$ cells in total $BrdU^+$ cells. N=5 mice for each condition. Statistical significance was determined by two-tailed Student's t-test. Error bars show SEM. **$p < 0.01$.

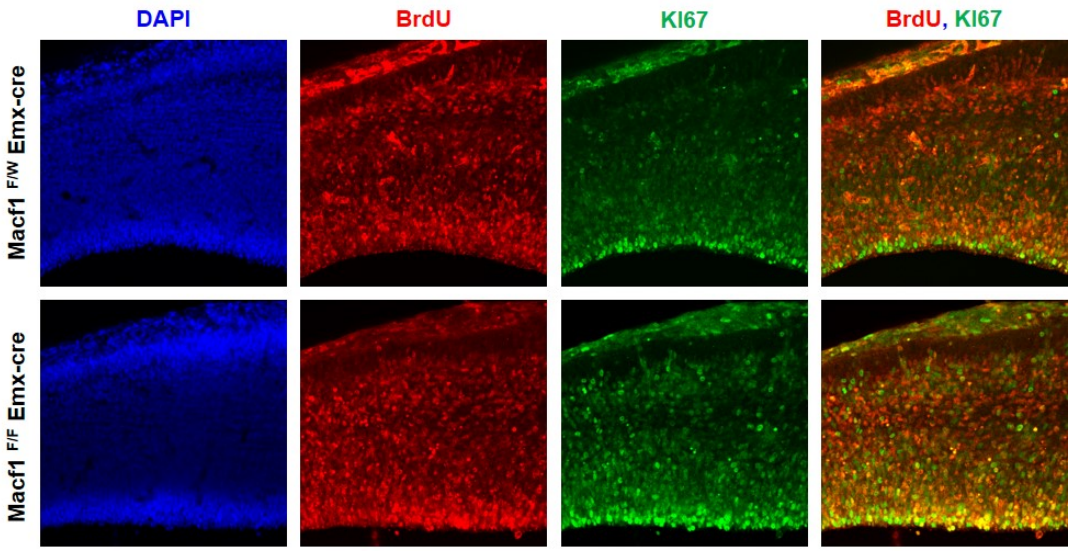

Figure 3.7 *Macf1*-cKO causes abnormal cell cycle progression

E13.5 control and *Macf1*-cKO mice were pulse-labeled with BrdU for 24 h and then brains were collected for immunostaining with BrdU and Ki67 antibodies. Scale bar: 50μm.

3.4.5 Abnormal radial glial development in Macf1-cKO brains

In order to understand the abnormal positioning of proliferating cells in *Macf1*-cKO mice, we first examined the role of MACF1 in radial glial development and corticogenesis. We immunostained cerebral cortex sections at E14.5 with an antibody reactive to BLBP, a radial glial neural progenitor marker. The number of BLBP-positive radial glial cells in *Macf1*-cKO brains is 55% higher than in control brains (Figure 3.8A-B). Furthermore, BLBP-positive radial glial cells in control brains are positioned within the SVZ and VZ (Figure 3.8A-C), while BLBP-positive radial glial cells in *Macf1*-cKO brains are abnormally spread throughout the SVZ/VZ, intermediate zone (IZ) and cortical plate (Figure 3.8A-C). Radial progenitors extend apical radial fibers toward the ventricular zone (VZ) and basal radial fibers toward the marginal zone of the cerebral cortex (Fishell and Kriegstein, 2003; Rakic, 2003). We examined the basal glial fibers in mutant and control developing cerebral cortices. In control brains, BLBP-positive radial glial cells

develop straight, linear basal radial fibers attached at the pial surface (Figure 3.8D). BLBP-positive radial glial cells in *Macf1*-cKO brains, on the other hand, develop abnormal basal radial fibers and do not attach at the pial surface (Figure 3.8D). The intensity of BLBP staining on the *Macf1*-cKO pial surface is 33% lower, when compared with control brains. (Figure 3.8D-E). Moreover, it appears that all radial glial cells in the VZ of control brains are BLBP-positive, while BLBP-staining in *Macf1*-cKO brain VZs is sparser (Figure 3.8F). Finally, to more clearly define the role of MACF1 in radial glial fiber development during corticogenesis, we used *in utero* electroporation to express EGFP under the control of the BLBP promoter in mouse embryonic radial glia neural progenitors (Ka et al., 2016b). We introduced a plasmid encoding the BLBP promoter-EGFP construct into the ventricles of E13.5 brains using *in utero* electroporation. 24 hours after electroporation (E14.5), Most EGFP-labeled radial glial cells are localized in the VZ in control brain sections (Figure 3.8G). However, EGFP-labeled radial glial cells in *Macf1*-cKO brains are spread throughout the developing cortex from the VZ to the cortical plate (Figure 3.8G). We next examined the apical glial fibers of EGFP-labeled radial glial cells at the VZ surface. In control brains, EGFP-labeled radial glial cells develop the linear apical glial fibers that attach to the VZ surface (Figure 3.8G). EGFP-labeled radial glial cells in *Macf1*-cKO brains do not develop prominent apical glial fibers VZ surface attachments (Figure 3.8G). Similar patterns exist on the basal surface, with the basal glial fibers of control radial glial cells robustly anchored to the basal surface, while *Macf1*-cKO basal glial fibers and basal surface attachments are difficult to detect (Figure 3.8G). Together, these results suggest that MACF1 is important for the proper maintenance and placement of radial progenitors during cortical development. Above all, MACF1 plays a crucial role in apical and basal fiber polarity in radial glial cells during corticogenesis.

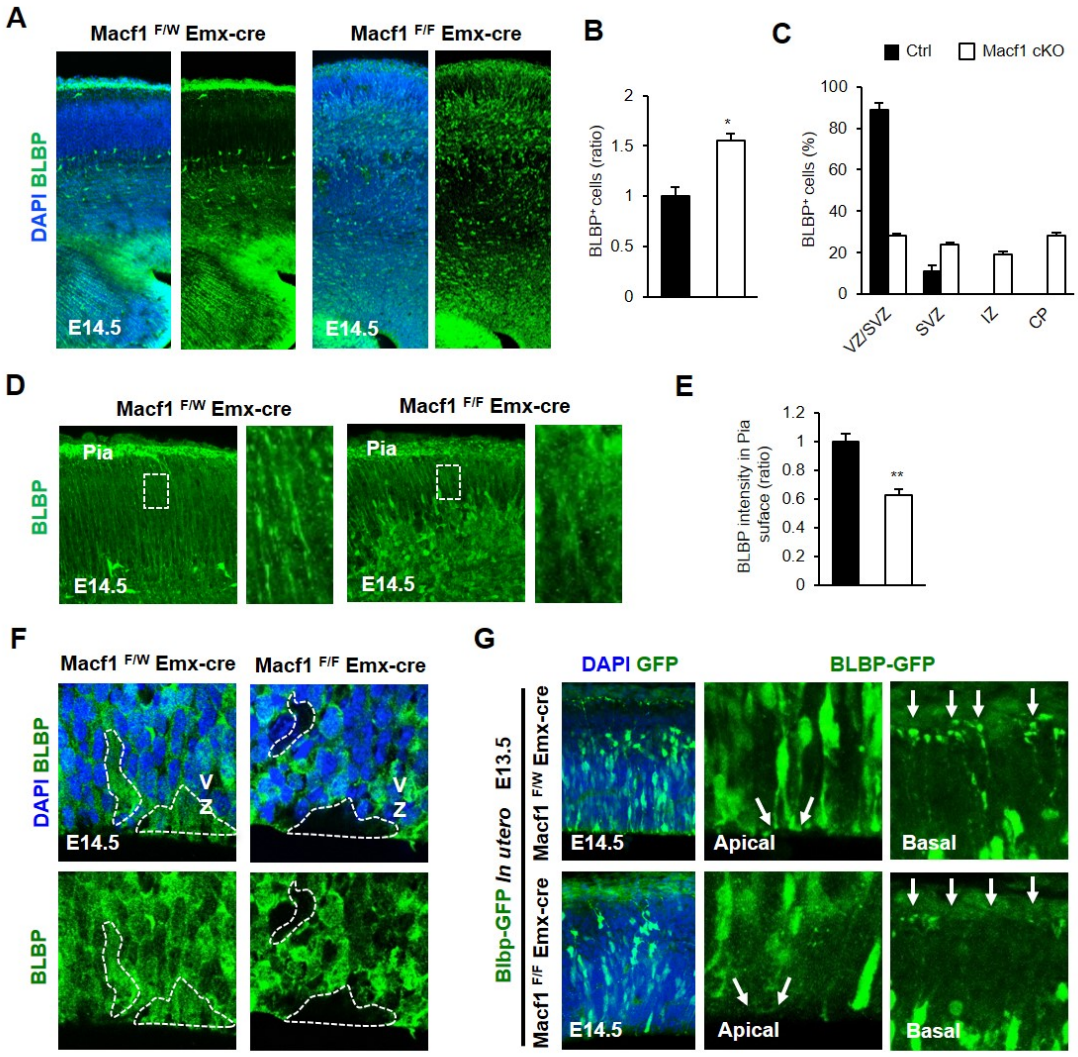

Figure 3.8 Abnormal radial glial development in *Macf1*-cKO developing cortex

(A) Immunostaining of coronal cerebral cortical sections from E14.5 control and *Macf1*-cKO brains with anti-BLBP antibody. Representative images from both five control and *Macf1*-cKO brains. Scale bars: 50μm. (B) Quantifications of the $BLBP^+$ cells of the control and *Macf1*-cKO brains. N=5 mice for each condition. Statistical significance was determined by two-tailed Student's t-test. Error bars show standard error of the mean (SEM). $^{**}p < 0.01$, $^{***}p < 0.001$. (C) Quantification of $BLBP^+$ cells throughout the cerebral cortex. N=5 mice for each condition. Statistical significance was determined by multiple t-tests with Bonferroni correction test. Error bars show standard error of the mean SEM. $^{*}p < 0.05$, $^{***}p < 0.001$. (D) High magnification images of pia to CP in (A). Representative images from both three control and *Macf1*-cKO brains. Scale bars: 20 μm, 5 μm. (E) Quantifications of the intensity of the pia surface of the control and *Macf1*-cKO brains. N=5 mice for each condition. Statistical significance was determined by two-tailed Student's t-test. Error bars show standard error of the mean (SEM). $^{**}p < 0.01$. (F) High magnification images of VZ in (A). Representative images from both three control

and *Macf1*-cKO brains. Scale bars: 10 μm. (G) E13.5 control and *Macf1*-cKO mice brains were electroporated *in utero* with a BLBP-EGFP construct to target radial glial progenitor cells and electroporated brains were collected after 24 hours. Arrows indicate the radial glial fibers of radial glial progenitor cells. Representative images from both three control and *Macf1*-cKO brains. Scale bars: 50 μm, 10 μm.

3.4.6 Disruption of actin polymerization and microtubule stability in primary cilia in Macf1-cKO brains

In order to understand why the apical polarity of radial glial cells is disrupted in *Macf1*-cKO brains, we performed immunostaining with antibodies against MACF1 and Nestin, a marker of neuronal precursor cells. At E14.5, MACF1 is broadly expressed in the developing cerebral cortex and highly expressed in the VZ and upper cortical areas near the MZ (Figure 3.9A). MACF1 also colocalizes with Nestin in the VZ. To identify the role of MACF1 in actin polymerization and cilia formation on the VZ surface, we immunostained cerebral cortex sections at E14.5 with antibodies against Phalloidin, a marker for actin polymerization, and ARL13B, a primary cilia marker. In the control brain Phalloidin is highly expressed on the VZ surface and ARL13B is dotted along the surface of the VZ (Figure 3.9B). In the *Macf1*-cKO brain Phalloidin is broadly expressed throughout the cerebral cortex and ARL13B expression is not restricted to the VZ surface (Figure 3.9B). Finally, to determine the role of MACF1 in microtubule stabilization along the VZ surface, we immunostained cerebral cortex sections at E14.5 stage with antibodies against Acetylated-Tubulin, a marker for microtubule stabilization, and Nestin. In control brains, Acetylated-Tubulin is highly expressed on the VZ surface and colocalizes with Nestin (Figure 3.9C). In *Macf1*-cKO brains, however, Acetylated-Tubulin staining is spread throughout the cerebral cortex (Figure 3.9C). Together, these results demonstrate that MACF1 plays an essential role in actin polymerization, microtubule stabilization and ciliogenesis in the VZ during cortical development.

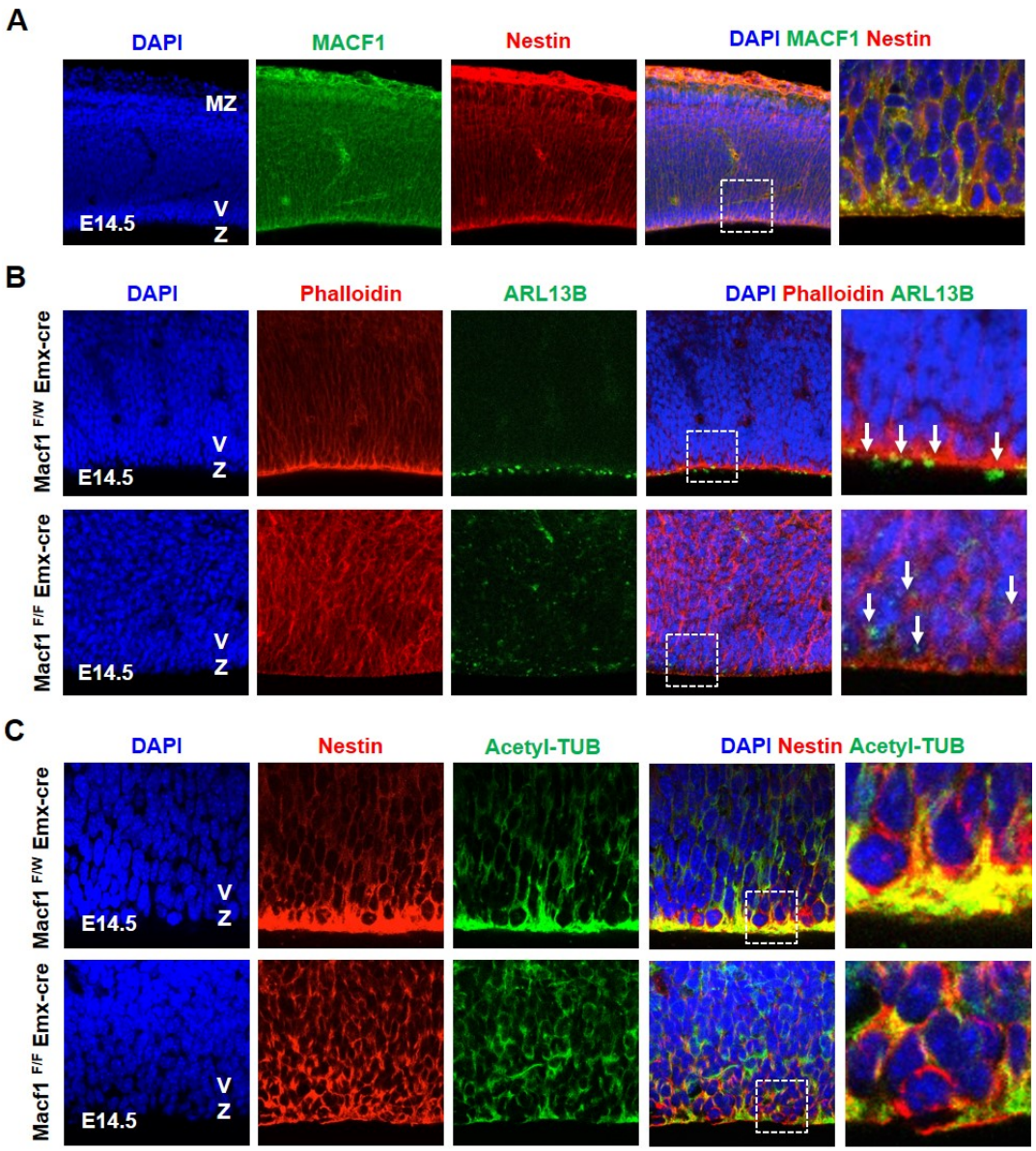

Figure 3.9 Actin polymerization and microtubules stability Is impaired in VZ surface in *Macf1*-cKO brains

(A) Immunostaining of coronal cerebral cortical sections from E14.5 control and *Macf1*-cKO brains with anti-MACF1 and anti-Nestin antibodies. Representative images from both five control and *Macf1*-cKO brains. Scale bars: 50 μm, 10 μm. (B) Immunostaining of coronal cerebral cortical sections from E14.5 control and *Macf1*-cKO brains with anti-Phalloidin and anti-ARL13B antibodies. Representative images from both five control and *Macf1*-cKO brains. Scale bars: 30 μm, 10 μm. (C) Immunostaining of coronal cerebral cortical sections from E14.5 control and *Macf1*-cKO brains with anti-Nestin and anti-Acetyl-TUB antibodies. Representative images from both five control and *Macf1*-cKO brains. Scale bars: 20μm, 5μm.

3.4.7 Hippocampal malformation and abnormal adult neurogenesis in Macf1-cKO mice

To examine the roles of MACF1 in neuronal positioning in the mouse hippocampus, we examined brain sections stained with DAPI, which revealed that *Macf1*-cKO brains exhibit a 34% smaller mean hippocampal area, compared with controls (Figure 3.10A-B). We next immunostained for NeuN and GFAP in 8-week-old mouse brains. In control mice, NeuN-positive cells densely accumulate within the pyramidal cell layer of the dorsal hippocampus. NeuN-positive cells in *Macf1*-cKO mice appear to be abnormally spread between the pyramidal cell layer and the stratum radiatum of the dorsal hippocampus (Figure 3.10C and Figure 3.11A). GFAP-positive cells, on the other hand, are spread evenly throughout the dorsal hippocampus in both the control on mutant hippocampus (Figure 3.10C and Figure 3.11).These results suggest that dorsal neural progenitor-specific *Macf1*-cKO mice develop pronounced hippocampal malformations due to abnormal neural positioning.

To examine adult neurogenesis in the dentate gyrus (DG), we immunostained 2-month-old mouse brains for KI67. In control mice KI67-positive proliferating cells localize to the subgranular zone (SGZ) of the hippocampal dentate gyrus (Figure 3.10D and Figure 3.11B). KI67-positive cells in *Macf1*-cKO brains, however, are abnormally scattered within the hippocampal dentate gyrus (Figure 3.10D and Figure 3.11B). Interestingly, KI67-positive proliferating cells in *Macf1*-cKO brains accumulate within heterotopic clusters in the caudal cerebral cortex (Figure 3.10D). These results support the claim that dorsal neural progenitor-specific *Macf1* knockout leads to abnormal neural positioning resulting in pronounced malformation of the cerebral cortex. Additionally, MACF1 plays a crucial role in regulating adult neurogenesis in a region-specific manner within hippocampus.

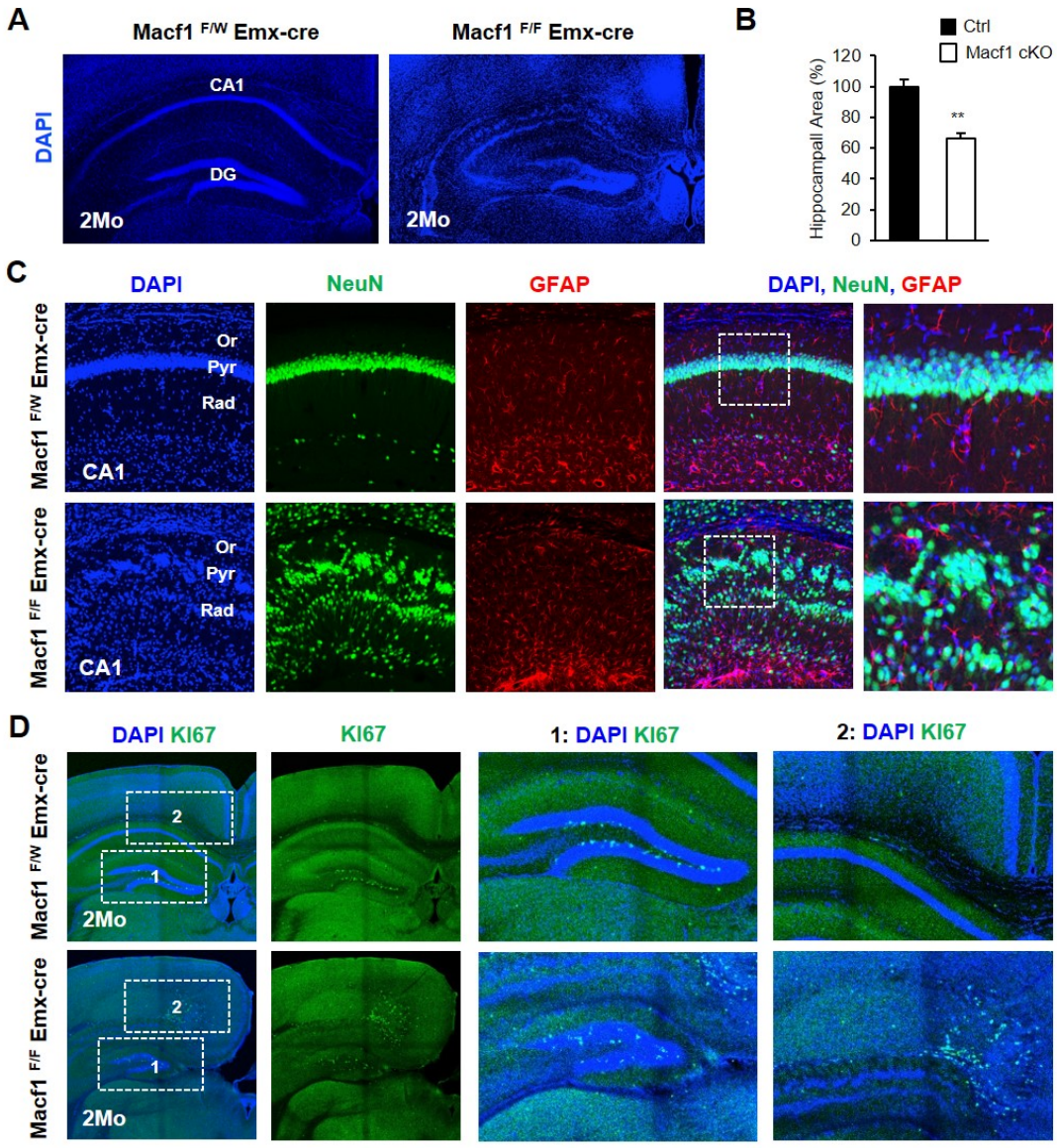

Figure 3.10 Hippocampus malformation and abnormal adult neurogenesis of *Macf1*-cKO brains

(A) Histologic appearance of brain sections from 2-month-old of the control and *Macf1*-cKO mice were stained with DAPI. Scale bars: 500 μm. (B) Quantifications of the area of the hippocampus of the control and *Macf1*-cKO mice. N= 5 mice for each condition. Statistical significance was determined by two-tailed Student's t-test. Error bars show standard error of the mean (SEM). $^{**}p < 0.01$. (C) Immunostaining of the coronal hippocampal sections from 2-month-old control and *Macf1*-cKO brains with anti-NeuN and anti-GFAP antibodies. Representative images from both three control and *Macf1*-cKO brains. Scale bars: 50 μm, 20 μm. (D) Immunostaining of the hippocampal sections from 2-month-old control and *Macf1*-cKO brains with anti-KI67 antibody. Representative images from both three control and *Macf1*-cKO brains. Scale bars: 300 μm, 50 μm.

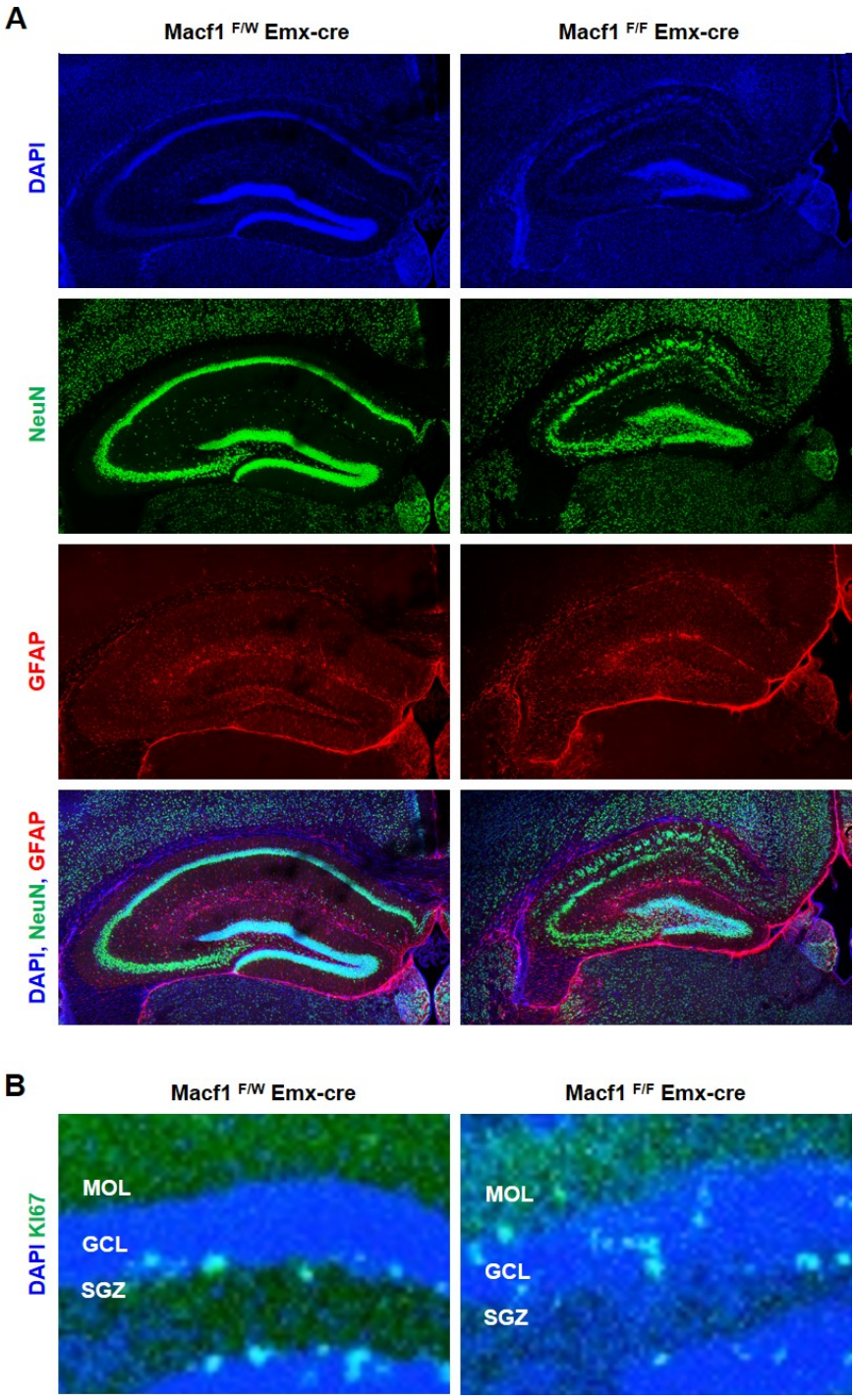

Figure 3.11 *Macf1*-cKO leads to hippocampal malformations and dysregulated adult neurogenesis

(A) Immunostaining of the coronal hippocampal sections from 2-month-old control and *Macf1*-cKO brains with anti-NeuN and anti-GFAP antibodies. Representative images from both three control and *Macf1*-cKO brains. Scale bars: 300μm. (B) Immunostaining

of the hippocampal sections from 2-month-old control and *Macf1*-cKO brains with anti-KI67 antibody. Representative images from both three control and *Macf1*-cKO brains. Scale bars: 20μm.

3.4.8 Agenesis of the corpus callosum in Macf1-cKO brains

Cortical and hippocampal malformations are commonly associated with agenesis of the corpus callosum, both in humans and animal models (Kappeler et al., 2007; Raybaud, 2010; Cid et al., 2014). Therefore, we examined brain sections using Nissl staining and found that *Macf1*-cKO brains exhibit thinner corpus callosums in the rostral cerebral cortex, when compared with control brains (Figure 3.12A). In control brains, callosal axons cross the midline at the rostral extremity of the corpus callosum to varying degrees, while callosal axons in *Macf1*-cKO brains do not cross the midline of the cerebral cortex in the same region (Figure 3.12A). Moreover, in control brains the corpus callosum distinctly separates the caudal cerebral cortex from the dorsal hippocampus. In *Macf1*-cKO brains the caudal cerebral cortex and dorsal hippocampus are difficult to delineate due to corpus callosal abnormalities (Figure 3.12A). We next examined brain sections stained with antibodies specific for NeuN and L1 and confirmed that *Macf1*-cKO brains do indeed exhibit thinner corpus callosums in the rostral cerebral cortex, compared with control brains (Figure 3.12B). Together, these results demonstrated that MACF1 plays a crucial role in corpus callosum development.

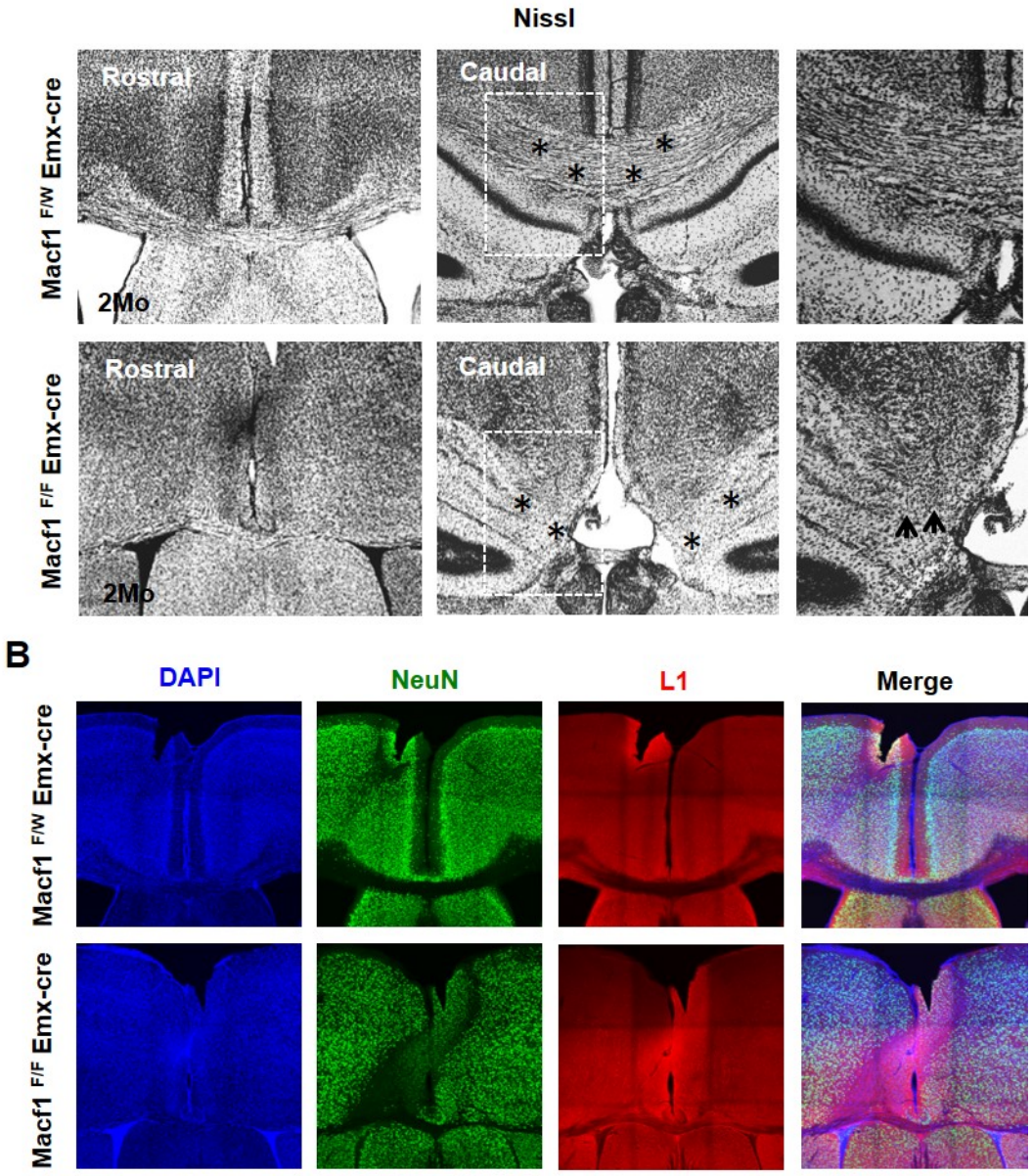

Figure 3.12 Agenesis of the corpus callosum in *Macf1*-cKO brains

(A) Histologic appearance of brains from 2-month-old of the control and *Macf1*-cKO mice. Nissl staining of rostral and caudal areas in the coronal cerebral cortical sections. Stars indicate corpus callosum and arrows indicate agenesis of the corpus callosum. Representative images from both three control and *Macf1*-cKO brains. Scale bars: 50 μm, 30 μm. (B) Immunostaining of coronal cerebral cortical sections from 2-month-old of the control and *Macf1*-cKO brains with anti-NeuN and anti-L1 antibodies. Representative images from both three control and *Macf1*-cKO brains. Scale bars: 100 μm.

3.4.9 Behavioral outcomes of conditional Macf1 deletion

Considering the broad range of neurodevelopmental and neuroanatomical abnormalities we observed in *Macf1*-cKO mice and the severe behavioral phenotypes of individuals with *MACF1* mutations(Vermeer et al., 2007; Kumar et al., 2010; Dagklis et al., 2016), we next performed several assays to determine the behavioral consequences of conditional *Macf1* deletion in mice. In spite of the significant difference in body weight between 8-week-old *Macf1*-cKO and control mice, we do not observe any significant abnormalities in the total distance moved or mean velocity of *Macf1*-cKO mice in the open field (Figure 3.13A-B). 8-week-old *Macf1*-cKO mice also do not exhibit any deficits in hindlimb or grip strength (Figure 3.13C-E). We do, however, observe marked hindlimb clasping and apparent deficits in hindlimb function and grip strength in 4-week-old *Macf1*-cKO mice (Figure 3.14A-D). In the open field, 8-week-old *Macf1*-cKO mice demonstrate unusual exploratory behavior, spending significantly less time in the center of the field and fewer center entries (Figure 3.13F-H). Most of their time appears to be spent seeking possible escape routes from the apparatus. *Macf1*-cKO mice also spend more time in the open arm of the elevated plus maze, compared to controls (Figure 3.13I). In the forced swim test, *Macf1*-cKO mice are immobile for considerably less time than control mice but spend about the same amount of time immobile in the tail suspension test, on average (Figure 3.13J-K).

In the novel object recognition test, *Macf1*-cKO mice and control mice both spend significantly more time exploring a novel object, rather than a familiar one, and show no difference in novel object recognition index (Figure 3.13L). In the three-chamber social interaction assay, we observe no significant differences in sociability between *Macf1*-cKO mice and controls (Figure 3.13M). We do, however, observe deficits in social novelty behavior in *Macf1*-cKO mice, as they spend nearly the same amount of time with the more-familiar “stranger I” mouse as with the novel “stranger II” mouse (Figure

3.13M). To summarize, *Macf1*-cKO mice display multiple abnormal behavioral phenotypes which correspond well with the neurological malformations we observed.

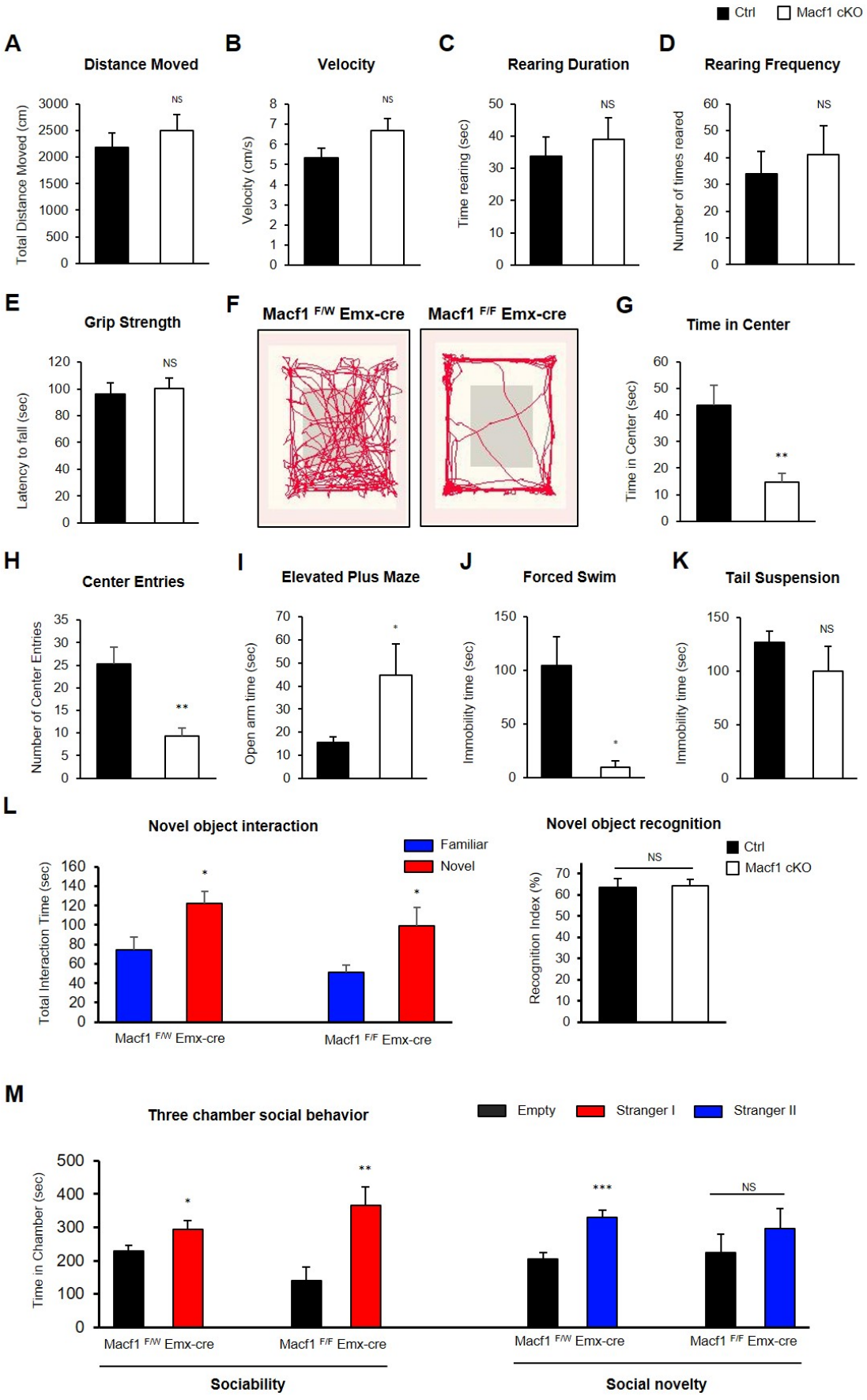
Ctrl
Macf1 cKO
A
Distance Moved
Total Distance Moved (cm)
NS
B
Velocity
Velocity (cm/s)
NS
C
Rearing Duration
Time rearing (sec)
NS
D
Rearing Frequency
Number of times reared
NS
E
Grip Strength
Latency to fall (sec)
NS
F
Macf1 F/W Emx-cre
Macf1 F/F Emx-cre
G
Time in Center
Time in Center (sec)
**
H
Center Entries
Number of Center Entries
**
I
Elevated Plus Maze
Open arm time (sec)
*
J
Forced Swim
Immobility time (sec)
*
K
Tail Suspension
Immobility time (sec)
NS
L
Novel object interaction
Familiar
Novel
Total Interaction Time (sec)
Macf1 F/W Emx-cre
Macf1 F/F Emx-cre
Novel object recognition
Ctrl
Macf1 cKO
NS
Recognition Index (%)
M
Three chamber social behavior
Empty
Stranger I
Stranger II
Time in Chamber (sec)
Macf1 F/W Emx-cre
Macf1 F/F Emx-cre
Sociability
Macf1 F/W Emx-cre
Macf1 F/F Emx-cre
Social novelty
***
NS

Figure 3.13 Behavioral effects of conditional *Macf1* deletion in the cerebral cortex

(A) Total distance moved and (B) mean velocity of movement during the open field test. n = 11 mice for controls and 7 mice for *Macf1*-cKO; two-tailed Student's t test. (C) Total rearing time and (D) number of times reared during the rearing test. n=9 mice for controls and 7 mice for *Macf1*-cKO; two-tailed Student's t test. (E) and (F) Representative traces from panels G and H. (G) Total time spent in the center and (H) the numbers of entries into the center in the open field test. **P < 0.01; n = 11 mice for controls and 7 mice for *Macf1*-cKO; two-tailed Student's t test. (I) In the elevated plus maze, *Macf1*-cKO mice spent more time in the open arms. *P =< 0.05; n = 5 mice for control and 4 mice for *Macf1*-cKO; two-tailed Student's t test. (J) In the forced swim test the immobility time was decreased in *Macf1*-cKO mice. *P < 0.01; n = 5 mice for controls and 4 mice for *Macf1*-cKO; two-tailed Student's t test. (K) No significant difference in immobility times in the tail suspension between controls and *Macf1*-cKO mice. n = 5 mice for controls and 4 mice for *Macf1*-cKO; two-tailed Student's t test. (L) Results of the novel-object recognition test. *P = 0.05; n = 9 mice for controls and 7 mice for *Macf1*-cKO; two-tailed Student's t test. (M) Three-chamber sociability test results for control and *Macf1*-cKO mice. In the social novelty test, *Macf1*-cKO mice spent an equal amount of time with each stranger mouse. *P <0.05, **P < 0.01, ***P < 0.001; n = 9 mice for control and 7 mice for *Macf1*-cKO; two-tailed Student's t test.

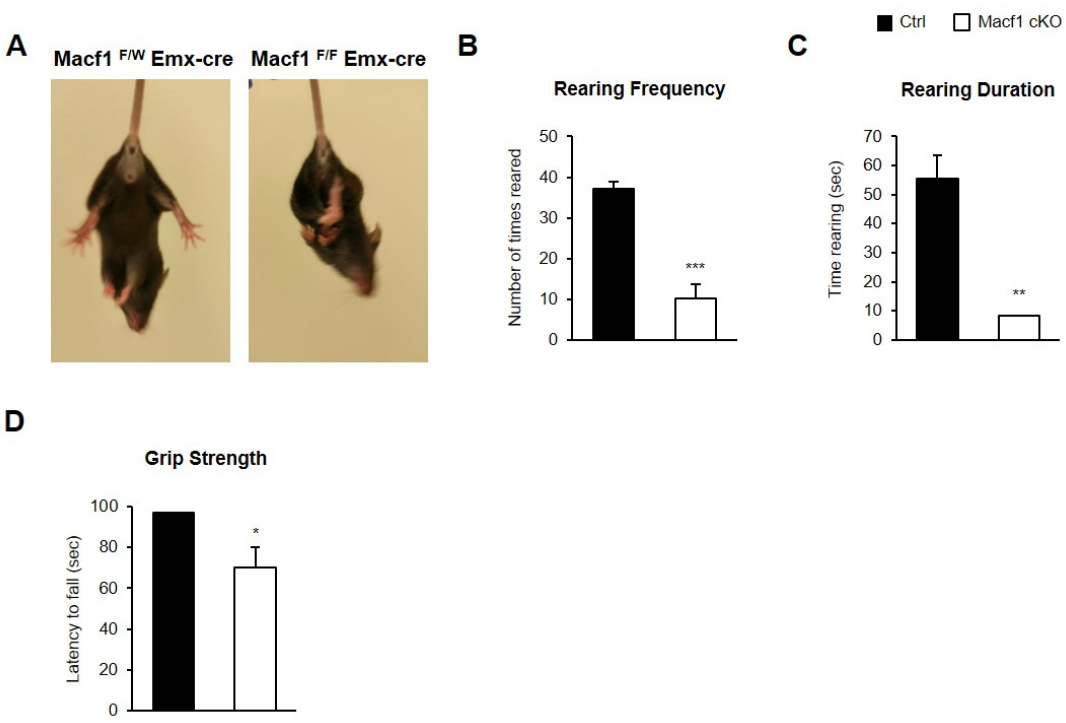

Figure 3.14 Effects of conditional *Macf1* deletion in the cerebral cortex on strength and mobility in 1-month-old mice

(A) 1-month old *Macf1*-cKO mice display hind-limb grasping when lifted by the tail. (B) The total number of times reared and (C) the total time spent rearing during the rearing test and (D) the latency to fall in the grip strength test were significantly lower in 1-month-old *Macf1*-cKO mice. n=4 for controls and 3 for *Macf1*-cKO mice; *P<0.05 ,**P<0.01 and ***P < 0.001; two-tailed Student's t-test.

3.5 Discussion

Using in vivo mouse genetics, we have defined a critical role for MACF1 in radial progenitor regulation in the developing cerebral cortex. A schematic model of radial progenitor polarity and neuronal placement within the cerebral cortex in the absence or presence of MACF1 is presented in Figure 3.15. Deletion of *Macf1* in dorsal neural progenitor cells leads to abnormal neuronal positioning and corresponding malformations of the cerebral cortex via disruption of radial progenitor polarity. More importantly, our results suggest that MACF1 is essential for anchoring radial progenitors in the VZ and that ectopic radial progenitors represent the primary origin of heterotopia in the absence of MACF1. The results of the present study differ from classical forms of SBH, which are likely to be primarily caused by abnormal neuronal migration. We also find that *Macf1* mutants exhibit significant deficits linked to autism-like and anxiety-like behavior. Our findings reveal a novel function of cytoskeleton-related proteins in radial progenitors and suggest a potential pathogenic mechanism for neurodevelopmental disorders associated with SBH, including intellectual disability and autism.

3.5.1 SBH (Double Cortex) and MACF1

SBH, also known as subcortical laminar heterotopia or double cortex syndrome, is a cortical malformation characterized by the presence of bilateral bands of heterotopic grey matter that results from the aberrant migration of neurons during cortical development (Dobyns et al., 1996; Pang et al., 2008). SBH has been largely linked to genetic deletions of microtubule binding components of the cytoskeleton, such as Lis1, Dcx, and a-tubulin (Reiner et al., 1993; Keays et al., 2007; Creppe et al., 2009; Jaglin and Chelly, 2009). Previously, we also reported that MACF1 regulates the neuronal migration and positioning of cortical pyramidal neurons and GABAergic interneurons via its regulation of microtubule stability (Ka et al., 2014a; Ka et al., 2016a). In the present

study, however, we find that loss of MACF1 starting at E9.5 in the developing cerebral cortex results in SBH and abnormal neural proliferation due to disrupted radial glial polarity. This is consistent with a previous report describing the loss of the small GTPase RhoA, which resulted in double cortex and an aberrant scaffold of radial progenitor cells in the developing cerebral cortex (Cappello et al., 2012). While the hypothesis that radial glial cell defects may contribute to SBH disorders has been raised, it has not been demonstrated as of yet (Feng et al., 2006; Sarkisian et al., 2006). The current study suggests that defects in radial glial polarity alter neural proliferation and neuronal migration via destabilization of both the actin and the microtubule cytoskeletons. Considering these observations, we propose that defects in the polarity of radial progenitor cells, rather than strictly neuronal migration defects, may explain some cases of SBH.

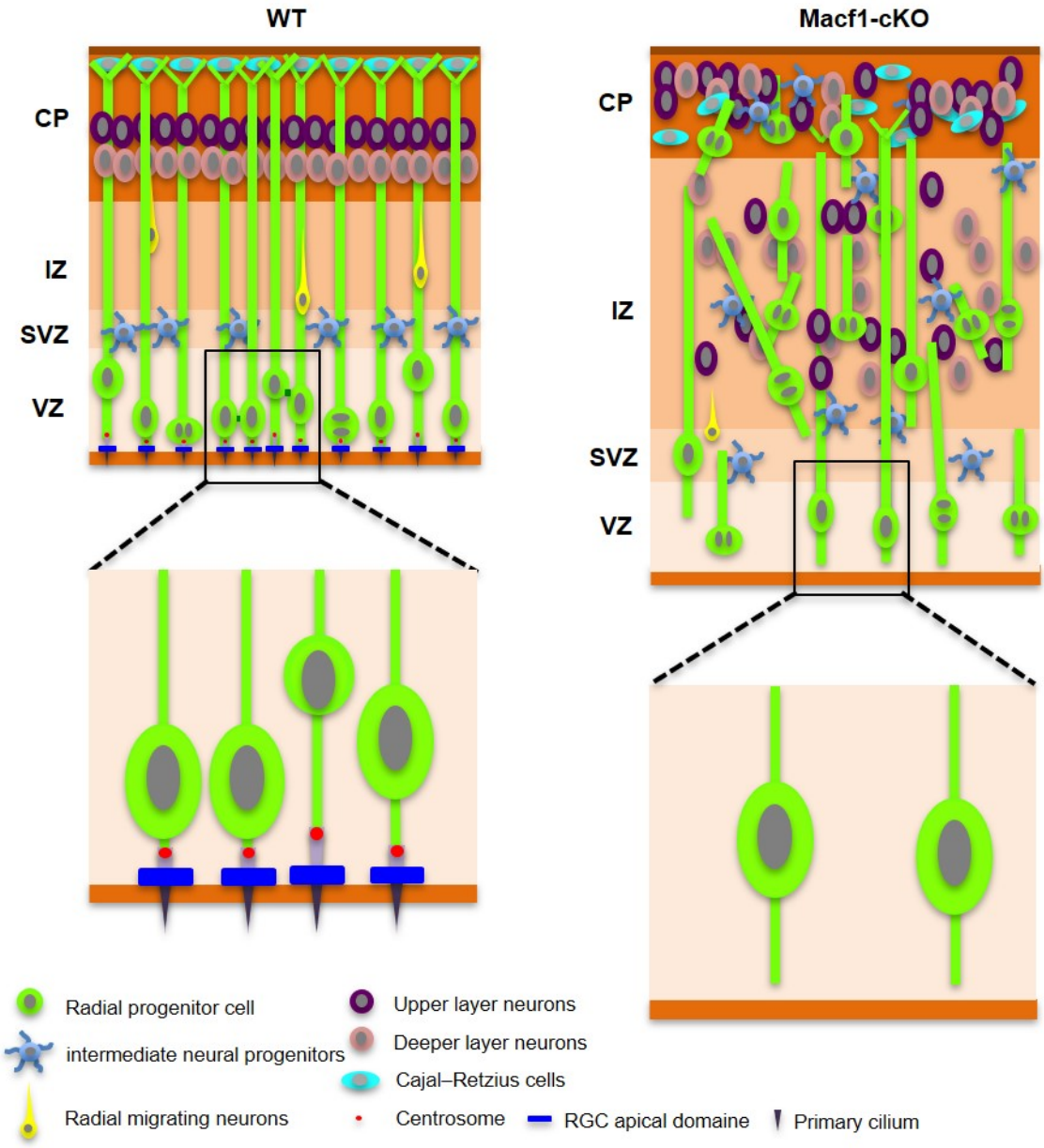

Figure 3.15 Model of cortical malformation and SBH formation in *Macf1*-cKO

MACF1 facilitates the proper neural placement and differentiation via regulation of radial glial fiber polarity. MACF1 regulates the apical polarity and cilliogenesis in the radial progenitor cells during cortex. This is essential for the laminar organization of neurons in the cerebral cortex. In contrast, MACF1 deficiency leads to abnormal cilliogenesis and glial fiber polarity and cause aberrant cortical lamination and SBH.

3.5.2 MACF1 in radial glial neural progenitors

Previous studies have shown that MACF1 regulates the radial migration of pyramidal neurons in the developing brain (Goryunov et al., 2010; Ka et al., 2014a) and, at E12.5, MACF1 is highly expressed at the VZ surface, one of the main proliferative zones during cortical development (Ka et al., 2014a). In spite of the use of a Nestin-cre driver to prevent *Macf1* expression in radial glial neural progenitors at E10.5 (Goryunov et al., 2010), previous studies have failed to clearly define the role of MACF1 in neural proliferation. We hypothesize that normal MACF1 expression is crucial for proper neural proliferation and early cortical development. Radial glial progenitor pools are mainly maintained via self-renewal at early stages of cortical development and begin to actively generate neurons via asymmetric division at later stages (Gotz and Huttner, 2005; Fietz and Huttner, 2011; Shitamukai and Matsuzaki, 2012). Conditional deletion of *Macf1* in mice using an Emx1-cre driver disrupts radial progenitor homeostasis resulting in abnormal neuronal positioning and an increased number of proliferating cells in developing brains. This is similar to 14-3-3, a protein that interacts with MACF1, which, when knocked out, also leads to an aberrant distribution of progenitor cells in the developing cerebral cortex along with an overall increase in their number (Toyo-oka et al., 2014). The first effects of *Macf1* deletion that we observed were major defects in the radial progenitor polarity. Loss of MACF1 at E9.5 disrupted cortical architecture due to aberrations in primary cilia maintenance at the VZ surface and radial glial fiber anchoring defects in the VZ and at the Pia surface. Thus, MACF1 is not only essential for mediating the apical attachment of radial glial primary cilia but also for the development and/or attachment of radial glial fibers. This matches up well with what occurs with loss of MACF1 during retinal development, namely the abolishment of ciliogenesis and disruption of apicobasal polarity (May-Simera et al., 2016). MACF1 is also an important

regulator of apicobasal polarity in mammalian intestinal cells in which radial centrosome-centered microtubule organization inhibits epithelial polarity (Noordstra et al., 2016). This study suggests that depletion of MACF1 during early corticogenesis prevents proper F-actin formation and disrupts microtubules at the VZ surface. Thus, *Macf1* deletion in the VZ causes profound destabilization of the actin and microtubule cytoskeleton in radial progenitor cells resulting in a loss of radial glial processes, anchoring and epithelial architecture, as well as defects in basal radial glial process formation and maintenance. This is consistent with the requirement for acetylated tubulin for proper neuronal migration and process formation in neurons, as we have reported previously (Ka et al., 2014a; Ka et al., 2016a), and implies cell-type-specific effects of MACF1 on the actin and microtubule cytoskeleton. Considering these observations, we propose that actin- and microtubule-interacting cytoskeletal proteins, including MACF1, regulate the polarity of radial progenitor cells during corticogenesis.

3.5.3 Agenesis of the corpus callosum and MACF1

The corpus callosum is one of the largest white matter tracts in the human brain, serving to physically and functionally connect the hemispheres of the cerebral cortex and plays critical roles in normal cognitive function (Tomasch, 1954). In humans, 3–5% of patients with neurodevelopmental disorders present with partial or complete agenesis of the corpus callosum (Jeret et al., 1985; Bodensteiner et al., 1994). Multiple glial assemblages are present at the developing midline and are required for corpus callosum formation (Shu et al., 2003; Smith et al., 2006). The glial wedge is a bilaterally symmetrical structure composed of radial glial cells which regulates callosal axons that have crossed the midline. It repels these axons away from the midline, keeping them in the contralateral hemisphere (Shu and Richards, 2001; Shu et al., 2003). Agenesis of the corpus callosum is associated with 70% cases of SBH (Barkovich et al., 2005). We

find that elimination of MACF1 in the developing cerebral cortex results in agenesis of the corpus callosum leading to abnormal adult neurogenesis and SBH in and around the hippocampal area. This is consistent with mutations of the gene disrupted in schizophrenia 1 (*Disc1*), a MACF1-interacting protein, which may be causally linked to agenesis of the corpus callosum (Paul et al., 2007). LHX2, a LIM-homeodomain transcription factor that has been shown to regulate *Macf1* expression in hair follicles , regulates glial wedge formation, and loss of LHX2 expression causes agenesis of the corpus callosum (Chinn et al., 2015). We conclude that MACF1 plays a critical role in corpus callosum formation and its function in this area may help explain corpus callosal agenesis caused by mutations in related genes.

3.5.4 Abnormal behaviors and MACF1

As may be expected considering the severe behavioral and neurodevelopmental phenotypes in individuals with 1p34.2 and/or 1p34.3 microdeletions (Vermeer et al., 2007; Kumar et al., 2010; Dagklis et al., 2016), *Macf1* cKO mice exhibit distinct and acute behavioral abnormalities. This conditional deletion of *Macf1*, however, considerably reduces the cell types in which *Macf1* is knocked out (Gorski et al., 2002; Iwasato et al., 2004). This could make behavioral comparisons between humans with global reductions in *MACF1* expression and *Macf1*-cKO mice even more likely to be misleading than would be the case with a global or whole brain-specific knockout. A close examination of behavioral differences between control and *Macf1*-cKO mice, on the other hand, demonstrates the profound effect *Macf1* mutations can have on brain function, even though the deletion is restricted to the developing cortex. Adult *Macf1*-cKO animals do not exhibit any obvious physical impairments in spite of their lower body weights. Overall locomotion and limb strength is not significantly affected, but in the open field *Macf1* mutant mice spend the vast majority of their time exploring the

periphery, rarely venturing into the center of the field. This thigmotaxic behavioral pattern has classically been linked to heightened anxiety (Wilson et al., 1976; Crawley, 1999; Belzung and Griebel, 2001; Bailey and Crawley, 2009), though there are multiple critiques regarding the ability to measure anxiety in mice using this method (Belzung and Griebel, 2001; Rodgers, 2007). Interestingly, *Macf1*-cKO mice spent significantly more time in the open arms during the open field test, a result which suggests that these mutants actually have lower levels of baseline anxiety than controls (Handley and Mithani, 1984; Pellow et al., 1985; Belzung and Griebel, 2001). These seemingly confounding findings may be due to the incomplete knockout of *Macf1* in this model or more complex behaviors we are unable to interpret at this time.

In addition to anxiety-like behaviors, we examined depression-like behavior in *Macf1*-cKO mice using the forced-swim and tail suspension tests. In both tests, increased immobility has classically been linked to depression-like phenotypes (Castagne et al., 2011). Although these mutant mice were indistinguishable from controls in the tail suspension test, they spent considerably less time immobile in the forced swim test, indicative of decreased depression-like behavior.

Despite extensive hippocampal anatomical abnormalities and the significant cognitive deficits in human patients (Vermeer et al., 2007; Kumar et al., 2010), *Macf1*-cKO mice did not show any significant deficits in non-spatial memory, as measured using the novel object recognition task (Cohen and Stackman, 2015). In the three chamber social interaction test, *Macf1*-mice did demonstrate deficits in social novelty behavior, but not in overall sociability.

Taken together, these behavioral findings do little to increase our understanding of MACF1 function beyond confirming the profound effect of conditional *Macf1* deletion. As stated above, it may not be surprising that the behavioral effects of *Macf1* deletion in the developing cortex was not sufficient to mirror all of the behavioral defects seen in human

patients. Indeed, the majority of anxiety-like and depression-like behaviors are more strongly linked to deficits in inhibitory interneurons, often in brain regions outside the cerebral cortex, not in the excitatory cortical neurons largely affected by our conditional deletion (Gorski et al., 2002; Dulawa et al., 2004; Iwasato et al., 2004). It is sufficient to conclude that conditional deletion of *Macf1* in radial progenitor cells and their progeny leads to marked behavioral abnormalities and it is reasonable to assume that global deletion of *Macf1* would result in even more severe phenotypes.

3.5.5 Summary

Altogether, we report that conditional deletion of *Macf1* in the mouse dorsal telencephalon starting at E9.5 significantly alters multiple aspects of cortical development, including; SBH, aberrant proliferation, migration, polarity and anchoring. We also report that *Macf1*-cKO mice display stark behavioral abnormalities compared with controls. These findings provide increased understanding of the neurodevelopmental role of MACF1, specifically in radial progenitors. This report also supports the suggestion that loss of *Macf1* gene expression may be largely responsible for the neuroanatomical and behavioral defects observed in patients with 1p34.2 and/or 1p34.3 microdeletions. Further research will be required to understand the role MACF1 plays in the development of other brain structures and their roles in the behavioral phenotypes observed in the aforementioned microdeletions.

CHAPTER 4: CONCLUSIONS AND DISCUSSION

In the preceding pages I have presented two primary research projects investigating the roles of ARID1B and MACF1 in brain development and mouse behavior. In this section I will separately summarize the results and implications from each of these studies and suggest avenues for future research.

We had previously shown that heterozygous deletion of *Arid1b* in mice leads to excitatory/inhibitory balance in the cerebral cortex due to a decrease in the number of GABAergic interneurons. Furthermore, we found that pharmacologically increasing GABA tone was sufficient to rescue a subset of the aberrant behaviors we observed in *Arid1b* haploinsufficient mice (Jung et al., 2017). In the study presented in Chapter 2, we sought to more precisely examine the effects of *Arid1b* deletion in excitatory and inhibitory neural progenitors using a conditional homozygous knockout strategy. Interestingly, deletion of *Arid1b* in excitatory cortical neural progenitors had negative effects on cell proliferation and survival. We concluded that this was due, in part, to impaired cell cycle re-entry, indicative of pre-mitotic cell cycle arrest. The negative impacts of homozygous *Arid1b* knockout was more pronounced in inhibitory neural progenitors in the MGE. In this brain region, these mutant mice exhibit a marked reduction in actively-proliferating and mitotic neural progenitors and newborn neurons, as well as increased apoptosis. In addition to decreased cell cycle re-entry, these conditional mutants also present with slower cell cycle speeds in inhibitory neural progenitors.

In our previous work, we observed that *Arid1b* haploinsufficient mice exhibit reduced expression of β-catenin target genes as well as a decline in the mRNA transcript levels of multiple *Wnt* signaling genes (Jung et al., 2017). This corresponds with other reports that ARID1B and BRG1 interact β-catenin in the nucleus and alter its function as a transcription factor (Barker et al., 2001; Vasileiou et al., 2015). Here we report that homozygous deletion of *Arid1b* in primary neuronal cultures and in inhibitory neural progenitors in vivo leads to a decrease in β-catenin nuclear localization, which could partly explain the lower expression levels of β-catenin target genes.

Finally, we examined the behavioral effects of conditional homozygous deletion of *Arid1b* and found that loss of *Arid1b* expression in excitatory neural progenitors appears to only significantly affect cognitive function or memory, whereas knockout of *Arid1b* in inhibitory neural progenitors substantially alters social and emotional mouse behaviors, but not cognitive function. This leads us to believe that the specific function of *Arid1b* in different neuronal subtypes have likewise specific effects on mouse behavior.

Overall, in this chapter we confirmed that ARID1B indeed plays an outsize role in regulating the proliferation and survival of inhibitory neural progenitors, but, more surprisingly, we also found that *Arid1b* deletion also significantly impairs the survival and proliferation of excitatory neural progenitors. A closer examination reveals that ARID1B regulates cell cycle progression in both neural progenitor pools in a cell type-specific manner. It is likely that ARID1B mediates cell cycle progression via its regulation of Wnt-β-catenin signaling, as β-catenin is known to be a master regulator of neural progenitor proliferation and targets multiple genes related to cell cycle progression (Chenn and Walsh, 2002; Gulacsi and Anderson, 2008).

Perhaps the most intriguing results in this chapter are, however, the distinct behavioral effects of *Arid1b* deletion in excitatory and inhibitory progenitor pools, respectively. As global heterozygous knockout of *Arid1b* alters a wide array of social, emotional and cognitive behaviors while only reducing the number of GABAergic interneurons in the cortex (Jung et al., 2017). Another prior study in our lab, however, found that shRNA-mediated knockdown of *Arid1b* in excitatory neural progenitors does alter neurite outgrowth and dendritic arborization and morphology (Ka et al., 2016b). It is possible that correct “dosage” of ARID1B is required for the survival and proper proliferation and function of both excitatory and inhibitory neurons and their progenitors but that the threshold for measurable ARID1B-related deficiencies is lower in inhibitory neural progenitors and their progeny.

Although we previously found that treatment with a GABA positive allosteric modulator was sufficient to rescue several aberrant behavioral phenotypes seen in *Arid1b* haploinsufficient mice (Jung et al., 2017), the research presented in chapter 2 may help explain why not all behavioral abnormalities can be reversed by increasing GABA tone. While heterozygous deletion of *Arid1b* appears to have the most obvious effects on the GABAergic inhibitory neuron population (Jung et al., 2017), it is clear from the data presented in this study, that ARID1B plays an important role in the development and function of pyramidal neurons as well. For this reason, in part, it will be necessary to determine alternative interventions which target all behavioral symptoms with minimum side effects, if possible. For this to be feasible it will first be necessary to determine in greater detail the mechanisms by which ARID1B regulates brain development and neuronal function, in particular the cell type-specific mechanisms will need more research. One way this could be accomplished is using single-cell RNA sequencing during brain development to compare the differences in gene expression in specific

cellular subtypes following *Arid1b* deletion. Regardless of these potential insights, the most promising potential treatment may be utilizing gene therapy to restore *Arid1b* gene expression, though the success of this tactic is not guaranteed. It is possible that gene therapy would only be effective during a critical developmental period and that restoring *Arid1b* expression in adolescents or adults would yield little or no functional or behavioral rescue.

In chapter 3 we examined the consequences of conditional *Macf1* deletion in the cortical neural progenitor pool. We report that loss of *Macf1* causes SBH and that this is due, at least in part, to destabilization of the cytoskeleton in the cortical VZ. The leads to aberrant migration, positioning and over-proliferation of neural progenitor cells resulting in heterotopic nodules throughout the cortex. The role of MACF1 in regulating the cytoskeleton is also apparent in the severe agenesis of the corpus callosum in conditional *Macf1* mutant brains.

Importantly, conditional deletion of *Macf1* in the developing cortex is sufficient to cause several ASD- and ID-like behavioral phenotypes. This lends credence to the hypothesis that *Macf1* is a gene largely contributing to the behavioral deficits observed in patients with 1p34.2 and/or 1p34.3 microdeletions. At first glance it may appear that the behavioral phenotype of these *Macf1*-cKO mice is not robust, especially considering the contradictory results in social behavior and anxiety tests. It is crucial to keep in mind, however, that conditional deletion of a gene would be unlikely to result in a complete behavioral recapitulation of the human disease phenotype. In this case it is sufficient to conclude that MACF1 is essential in cortical pyramidal neurons and their progenitors for proper mouse behavior. Additional conditional knockout mouse models could be used in

the future to further asses which specific cell types contribute more or less to different behavioral phenotypes related to *Macf1* deletion.

Due to the severe brain malformations present in *Macf1* mutant mice and patients with 1p34.2 and/or 1p34.3 microdeletions (Vermeer et al., 2007; Kumar et al., 2010; Dagklis et al., 2016), it is unlikely that these findings will yield any immediate therapeutic breakthroughs. Future studies should examine the efficacy of individually stimulating or inhibiting specific neural circuits or neuronal subtypes in order to improve behavior. It may also prove beneficial to assess the potential roles MACF1 may play in other neurodevelopmental disorders characterized by heterotopia and corpus callosal agenesis. The identification of convergent pathways in brain development and behavior will greatly improve our understanding of disease pathogenesis and provide avenues for treatment.

Overall, the work presented in this dissertation represents measurable progress toward understanding the pathogenesis of neurodevelopmental disorders such as ID and ASD. These findings also raise several new and exciting questions and directions for future research, as discussed above. Improving our understanding of genes vital for proper neural development will also inspire the conception of novel therapies and enhanced individualized care for patients. As we determine cell types and specific neural circuits regulating pathogenic behaviors in the future, and therapeutic technologies become ever more targeted, treatment with minimal side effects may soon be a reality.

REFERENCES

(1994) Fmr1 knockout mice: a model to study fragile X mental retardation. The Dutch-Belgian Fragile X Consortium. Cell 78:23-33.

Alver BH, Kim KH, Lu P, Wang X, Manchester HE, Wang W, Haswell JR, Park PJ, Roberts CW (2017) The SWI/SNF chromatin remodelling complex is required for maintenance of lineage specific enhancers. Nature communications 8:14648.

Anderson SA, Marin O, Horn C, Jennings K, Rubenstein JL (2001) Distinct cortical migrations from the medial and lateral ganglionic eminences. Development 128:353-363.

Armstrong DD (2005) Neuropathology of Rett syndrome. Journal of child neurology 20:747-753.

Attanasio C, Nord AS, Zhu Y, Blow MJ, Biddie SC, Mendenhall EM, Dixon J, Wright C, Hosseini R, Akiyama JA, Holt A, Plajzer-Frick I, Shoukry M, Afzal V, Ren B, Bernstein BE, Rubin EM, Visel A, Pennacchio LA (2014) Tissue-specific SMARCA4 binding at active and repressed regulatory elements during embryogenesis. Genome Res 24:920-929.

Auerbach BD, Osterweil EK, Bear MF (2011) Mutations causing syndromic autism define an axis of synaptic pathophysiology. Nature 480:63-68.

Bachmann C, Nguyen H, Rosenbusch J, Pham L, Rabe T, Patwa M, Sokpor G, Seong RH, Ashery-Padan R, Mansouri A, Stoykova A, Staiger JF, Tuoc T (2016) mSWI/SNF (BAF) Complexes Are Indispensable for the Neurogenesis and Development of Embryonic Olfactory Epithelium. PLoS genetics 12:e1006274.

Bailey KR, Crawley JN (2009) Anxiety-Related Behaviors in Mice. In: Methods of Behavior Analysis in Neuroscience (nd, Buccafusco JJ, eds). Boca Raton (FL).

Baluch F, Itti L (2011) Mechanisms of top-down attention. Trends Neurosci 34:210-224.

Bandi S, Singh SM, Mallela KM (2015) Interdomain Linker Determines Primarily the Structural Stability of Dystrophin and Utrophin Tandem Calponin-Homology Domains Rather than Their Actin-Binding Affinity. Biochemistry 54:5480-5488.

Bangash MA et al. (2011) Enhanced polyubiquitination of Shank3 and NMDA receptor in a mouse model of autism. Cell 145:758-772.

Bannister AJ, Kouzarides T (2011) Regulation of chromatin by histone modifications. Cell research 21:381-395.

Barker N, Hurlstone A, Musisi H, Miles A, Bienz M, Clevers H (2001) The chromatin remodelling factor Brg-1 interacts with beta-catenin to promote target gene activation. EMBO J 20:4935-4943.

Barkovich AJ, Kuzniecky RI, Jackson GD, Guerrini R, Dobyns WB (2005) A developmental and genetic classification for malformations of cortical development. Neurology 65:1873-1887.

Barkovich AJ, Guerrini R, Kuzniecky RI, Jackson GD, Dobyns WB (2012) A developmental and genetic classification for malformations of cortical development: update 2012. Brain : a journal of neurology 135:1348-1369.

Bartolini G, Ciceri G, Marin O (2013) Integration of GABAergic interneurons into cortical cell assemblies: lessons from embryos and adults. Neuron 79:849-864.

Basu SN, Kollu R, Banerjee-Basu S (2009) AutDB: a gene reference resource for autism research. Nucleic Acids Res 37:D832-836.

Battaglioli E, Andres ME, Rose DW, Chenoweth JG, Rosenfeld MG, Anderson ME, Mandel G (2002) REST repression of neuronal genes requires components of the hSWI.SNF complex. J Biol Chem 277:41038-41045.

Bedogni F, Hodge RD, Elsen GE, Nelson BR, Daza RA, Beyer RP, Bammler TK, Rubenstein JL, Hevner RF (2010) Tbr1 regulates regional and laminar identity of postmitotic neurons in developing neocortex. Proc Natl Acad Sci U S A 107:13129-13134.

Beguin S, Crepel V, Aniksztejn L, Becq H, Pelosi B, Pallesi-Pocachard E, Bouamrane L, Pasqualetti M, Kitamura K, Cardoso C, Represa A (2013) An epilepsy-related ARX polyalanine expansion modifies glutamatergic neurons excitability and morphology without affecting GABAergic neurons development. Cerebral cortex 23:1484-1494.

Belichenko PV, Oldfors A, Hagberg B, Dahlstrom A (1994) Rett syndrome: 3-D confocal microscopy of cortical pyramidal dendrites and afferents. Neuroreport 5:1509-1513.

Belliveau DJ, Bani-Yaghoub M, McGirr B, Naus CC, Rushlow WJ (2006) Enhanced neurite outgrowth in PC12 cells mediated by connexin hemichannels and ATP. J Biol Chem 281:20920-20931.

Belzung C, Griebel G (2001) Measuring normal and pathological anxiety-like behaviour in mice: a review. Behav Brain Res 125:141-149.

Benes FM, Berretta S (2001) GABAergic interneurons: implications for understanding schizophrenia and bipolar disorder. Neuropsychopharmacology 25:1-27.

Bernier G, Mathieu M, De Repentigny Y, Vidal SM, Kothary R (1996) Cloning and characterization of mouse ACF7, a novel member of the dystonin subfamily of actin binding proteins. Genomics 38:19-29.

Bernier G, Pool M, Kilcup M, Alfoldi J, De Repentigny Y, Kothary R (2000) Acf7 (MACF) is an actin and microtubule linker protein whose expression predominates in neural, muscle, and lung development. Developmental dynamics : an official publication of the American Association of Anatomists 219:216-225.

Bielas SL, Gleeson JG (2004) Cytoskeletal-associated proteins in the migration of cortical neurons. Journal of neurobiology 58:149-159.

Bilousova TV, Dansie L, Ngo M, Aye J, Charles JR, Ethell DW, Ethell IM (2009) Minocycline promotes dendritic spine maturation and improves behavioural performance in the fragile X mouse model. Journal of medical genetics 46:94-102.

Bodensteiner J, Schaefer GB, Breeding L, Cowan L (1994) Hypoplasia of the corpus callosum: a study of 445 consecutive MRI scans. Journal of child neurology 9:47-49.

Bourne JN, Harris KM (2008) Balancing structure and function at hippocampal dendritic spines. Annu Rev Neurosci 31:47-67.

Brandao JA, Romcy-Pereira RN (2015) Interplay of environmental signals and progenitor diversity on fate specification of cortical GABAergic neurons. Front Cell Neurosci 9:149.

Bruno S, Darzynkiewicz Z (1992) Cell cycle dependent expression and stability of the nuclear protein detected by Ki-67 antibody in HL-60 cells. Cell Prolif 25:31-40.

Bucan M, Abel T (2002) The mouse: genetics meets behaviour. Nat Rev Genet 3:114-123.

Burgo A, Proux-Gillardeaux V, Sotirakis E, Bun P, Casano A, Verraes A, Liem RK, Formstecher E, Coppey-Moisan M, Galli T (2012) A molecular network for the transport of the TI-VAMP/VAMP7 vesicles from cell center to periphery. Dev Cell 23:166-180.

Butt SJ, Stacey JA, Teramoto Y, Vagnoni C (2017) A role for GABAergic interneuron diversity in circuit development and plasticity of the neonatal cerebral cortex. Current opinion in neurobiology 43:149-155.

Byers TJ, Beggs AH, McNally EM, Kunkel LM (1995) Novel actin crosslinker superfamily member identified by a two step degenerate PCR procedure. FEBS letters 368:500-504.

Calfa G, Percy AK, Pozzo-Miller L (2011) Experimental models of Rett syndrome based on Mecp2 dysfunction. Exp Biol Med (Maywood) 236:3-19.

Callicott JH, Feighery EL, Mattay VS, White MG, Chen Q, Baranger DA, Berman KF, Lu B, Song H, Ming GL, Weinberger DR (2013) DISC1 and SLC12A2 interaction affects human hippocampal function and connectivity. J Clin Invest 123:2961-2964.

Camargo LM, Collura V, Rain JC, Mizuguchi K, Hermjakob H, Kerrien S, Bonnert TP, Whiting PJ, Brandon NJ (2007) Disrupted in Schizophrenia 1 Interactome: evidence for the close connectivity of risk genes and a potential synaptic basis for schizophrenia. Molecular psychiatry 12:74-86.

Cappello S, Bohringer CR, Bergami M, Conzelmann KK, Ghanem A, Tomassy GS, Arlotta P, Mainardi M, Allegra M, Caleo M, van Hengel J, Brakebusch C, Gotz M (2012) A radial glia-specific role of RhoA in double cortex formation. Neuron 73:911-924.

Castagne V, Moser P, Roux S, Porsolt RD (2011) Rodent models of depression: forced swim and tail suspension behavioral despair tests in rats and mice. Curr Protoc Neurosci Chapter 8:Unit 8 10A.

Celen C et al. (2017) Arid1b haploinsufficient mice reveal neuropsychiatric phenotypes and reversible causes of growth impairment. Elife 6.

Cellot G, Cherubini E (2014) GABAergic signaling as therapeutic target for autism spectrum disorders. Front Pediatr 2:70.

Chahrour M, Zoghbi HY (2007) The story of Rett syndrome: from clinic to neurobiology. Neuron 56:422-437.

Chanas-Sacre G, Rogister B, Moonen G, Leprince P (2000) Radial glia phenotype: origin, regulation, and transdifferentiation. J Neurosci Res 61:357-363.

Chao HT, Chen H, Samaco RC, Xue M, Chahrour M, Yoo J, Neul JL, Gong S, Lu HC, Heintz N, Ekker M, Rubenstein JL, Noebels JL, Rosenmund C, Zoghbi HY (2010) Dysfunction in GABA signalling mediates autism-like stereotypies and Rett syndrome phenotypes. Nature 468:263-269.

Chapleau CA, Larimore JL, Theibert A, Pozzo-Miller L (2009) Modulation of dendritic spine development and plasticity by BDNF and vesicular trafficking: fundamental roles in neurodevelopmental disorders associated with mental retardation and autism. J Neurodev Disord 1:185-196.

Chen HJ, Lin CM, Lin CS, Perez-Olle R, Leung CL, Liem RK (2006) The role of microtubule actin cross-linking factor 1 (MACF1) in the Wnt signaling pathway. Genes Dev 20:1933-1945.

Chen RZ, Akbarian S, Tudor M, Jaenisch R (2001) Deficiency of methyl-CpG binding protein-2 in CNS neurons results in a Rett-like phenotype in mice. Nat Genet 27:327-331.

Cheng J, Zhou L, Xie QF, Xie HY, Wei XY, Gao F, Xing CY, Xu X, Li LJ, Zheng SS (2010) The impact of miR-34a on protein output in hepatocellular carcinoma HepG2 cells. Proteomics 10:1557-1572.

Chenn A, Walsh CA (2002) Regulation of cerebral cortical size by control of cell cycle exit in neural precursors. Science 297:365-369.

Chiba H, Muramatsu M, Nomoto A, Kato H (1994) Two human homologues of Saccharomyces cerevisiae SWI2/SNF2 and Drosophila brahma are transcriptional coactivators cooperating with the estrogen receptor and the retinoic acid receptor. Nucleic Acids Res 22:1815-1820.

Chinn GA, Hirokawa KE, Chuang TM, Urbina C, Patel F, Fong J, Funatsu N, Monuki ES (2015) Agenesis of the Corpus Callosum Due to Defective Glial Wedge Formation in Lhx2 Mutant Mice. Cerebral cortex 25:2707-2718.

Choi J, Jeon S, Choi S, Park K, Seong RH (2015) The SWI/SNF chromatin remodeling complex regulates germinal center formation by repressing Blimp-1 expression. Proc Natl Acad Sci U S A 112:E718-727.

Cid E, Gomez-Dominguez D, Martin-Lopez D, Gal B, Laurent F, Ibarz JM, Francis F, Menendez de la Prida L (2014) Dampened hippocampal oscillations and enhanced spindle activity in an asymptomatic model of developmental cortical malformations. Frontiers in systems neuroscience 8:50.

Cohen IL, Fisch GS, Sudhalter V, Wolf-Schein EG, Hanson D, Hagerman R, Jenkins EC, Brown WT (1988) Social gaze, social avoidance, and repetitive behavior in fragile X males: a controlled study. American journal of mental retardation : AJMR 92:436-446.

Cohen SJ, Stackman RW, Jr. (2015) Assessing rodent hippocampal involvement in the novel object recognition task. A review. Behav Brain Res 285:105-117.

Collins RT, Furukawa T, Tanese N, Treisman JE (1999) Osa associates with the Brahma chromatin remodeling complex and promotes the activation of some target genes. EMBO J 18:7029-7040.
Crawley JN (1999) Behavioral phenotyping of transgenic and knockout mice: experimental design and evaluation of general health, sensory functions, motor abilities, and specific behavioral tests. Brain Res 835:18-26.
Creppe C, Malinouskaya L, Volvert ML, Gillard M, Close P, Malaise O, Laguesse S, Cornez I, Rahmouni S, Ormenese S, Belachew S, Malgrange B, Chapelle JP, Siebenlist U, Moonen G, Chariot A, Nguyen L (2009) Elongator controls the migration and differentiation of cortical neurons through acetylation of alpha-tubulin. Cell 136:551-564.
Cuylen S, Blaukopf C, Politi AZ, Muller-Reichert T, Neumann B, Poser I, Ellenberg J, Hyman AA, Gerlich DW (2016) Ki-67 acts as a biological surfactant to disperse mitotic chromosomes. Nature 535:308-312.
Cvekl A, Duncan MK (2007) Genetic and epigenetic mechanisms of gene regulation during lens development. Prog Retin Eye Res 26:555-597.
D'Avino PP, Giansanti MG, Petronczki M (2015) Cytokinesis in animal cells. Cold Spring Harbor perspectives in biology 7:a015834.
da Silva JS, Dotti CG (2002) Breaking the neuronal sphere: regulation of the actin cytoskeleton in neuritogenesis. Nat Rev Neurosci 3:694-704.
Dagklis T, Papageorgiou E, Siomou E, Paspaliaris V, Zerva C, Chatzis P, Thomaidis L, Manolakos E, Papoulidis I (2016) Prenatal diagnosis of 1p34.3 interstitial microdeletion by aCGH in a fetus with jaw bone abnormalities. Molecular cytogenetics 9:77.
Dahlin MG, Amark PE, Nergardh AR (2003) Reduction of seizures with low-dose clonazepam in children with epilepsy. Pediatr Neurol 28:48-52.
de la Serna IL, Carlson KA, Imbalzano AN (2001) Mammalian SWI/SNF complexes promote MyoD-mediated muscle differentiation. Nat Genet 27:187-190.
Deacon RM (2013) Measuring the strength of mice. J Vis Exp.
Declercq J, Brouwers B, Pruniau VP, Stijnen P, de Faudeur G, Tuand K, Meulemans S, Serneels L, Schraenen A, Schuit F, Creemers JW (2015) Metabolic and Behavioural Phenotypes in Nestin-Cre Mice Are Caused by Hypothalamic Expression of Human Growth Hormone. PLoS One 10:e0135502.
Ding Q, Sethna F, Wang H (2014) Behavioral analysis of male and female Fmr1 knockout mice on C57BL/6 background. Behav Brain Res 271:72-78.
Dobkin C, Rabe A, Dumas R, El Idrissi A, Haubenstock H, Brown WT (2000) Fmr1 knockout mouse has a distinctive strain-specific learning impairment. Neuroscience 100:423-429.
Dobyns WB, Andermann E, Andermann F, Czapansky-Beilman D, Dubeau F, Dulac O, Guerrini R, Hirsch B, Ledbetter DH, Lee NS, Motte J, Pinard JM, Radtke RA, Ross ME, Tampieri D, Walsh CA, Truwit CL (1996) X-linked malformations of neuronal migration. Neurology 47:331-339.
Drabek K, van Ham M, Stepanova T, Draegestein K, van Horssen R, Sayas CL, Akhmanova A, Ten Hagen T, Smits R, Fodde R, Grosveld F, Galjart N

(2006) Role of CLASP2 in microtubule stabilization and the regulation of persistent motility. Current biology : CB 16:2259-2264.
Dranovsky A, Hen R (2007) DISC1 puts the brakes on neurogenesis. Cell 130:981-983.
Duan X, Chang JH, Ge S, Faulkner RL, Kim JY, Kitabatake Y, Liu XB, Yang CH, Jordan JD, Ma DK, Liu CY, Ganesan S, Cheng HJ, Ming GL, Lu B, Song H (2007) Disrupted-In-Schizophrenia 1 regulates integration of newly generated neurons in the adult brain. Cell 130:1146-1158.
Dulawa SC, Holick KA, Gundersen B, Hen R (2004) Effects of chronic fluoxetine in animal models of anxiety and depression. Neuropsychopharmacology 29:1321-1330.
Eberharter A, Becker PB (2002) Histone acetylation: a switch between repressive and permissive chromatin. Second in review series on chromatin dynamics. EMBO reports 3:224-229.
Etienne-Manneville S (2004) Actin and microtubules in cell motility: which one is in control? Traffic 5:470-477.
Evsyukova I, Plestant C, Anton ES (2013) Integrative mechanisms of oriented neuronal migration in the developing brain. Annual review of cell and developmental biology 29:299-353.
Feng J (2006) Microtubule: a common target for parkin and Parkinson's disease toxins. Neuroscientist 12:469-476.
Feng Y, Walsh CA (2001) Protein-protein interactions, cytoskeletal regulation and neuronal migration. Nat Rev Neurosci 2:408-416.
Feng Y, Chen MH, Moskowitz IP, Mendonza AM, Vidali L, Nakamura F, Kwiatkowski DJ, Walsh CA (2006) Filamin A (FLNA) is required for cell-cell contact in vascular development and cardiac morphogenesis. Proc Natl Acad Sci U S A 103:19836-19841.
Ferreira JG, Pereira AL, Maiato H (2014) Microtubule plus-end tracking proteins and their roles in cell division. International review of cell and molecular biology 309:59-140.
Fiala JC, Spacek J, Harris KM (2002) Dendritic spine pathology: cause or consequence of neurological disorders? Brain Res Brain Res Rev 39:29-54.
Fietz SA, Huttner WB (2011) Cortical progenitor expansion, self-renewal and neurogenesis-a polarized perspective. Current opinion in neurobiology 21:23-35.
Fishell G, Kriegstein AR (2003) Neurons from radial glia: the consequences of asymmetric inheritance. Current opinion in neurobiology 13:34-41.
Frade JM (2002) Interkinetic nuclear movement in the vertebrate neuroepithelium: encounters with an old acquaintance. Progress in brain research 136:67-71.
Franco SJ, Muller U (2013) Shaping our minds: stem and progenitor cell diversity in the mammalian neocortex. Neuron 77:19-34.
Gabriele M, Lopez Tobon A, D'Agostino G, Testa G (2018) The chromatin basis of neurodevelopmental disorders: Rethinking dysfunction along the

molecular and temporal axes. Prog Neuropsychopharmacol Biol Psychiatry 84:306-327.
Galichet C, Lovell-Badge R, Rizzoti K (2010) Nestin-Cre mice are affected by hypopituitarism, which is not due to significant activity of the transgene in the pituitary gland. PLoS One 5:e11443.
Gao R, Penzes P (2015) Common mechanisms of excitatory and inhibitory imbalance in schizophrenia and autism spectrum disorders. Current molecular medicine 15:146-167.
Gatto CL, Broadie K (2010) Genetic controls balancing excitatory and inhibitory synaptogenesis in neurodevelopmental disorder models. Front Synaptic Neurosci 2:4.
Gauthier J, Spiegelman D, Piton A, Lafreniere RG, Laurent S, St-Onge J, Lapointe L, Hamdan FF, Cossette P, Mottron L, Fombonne E, Joober R, Marineau C, Drapeau P, Rouleau GA (2009) Novel de novo SHANK3 mutation in autistic patients. Am J Med Genet B Neuropsychiatr Genet 150B:421-424.
Geschwind DH (2011) Genetics of autism spectrum disorders. Trends in cognitive sciences 15:409-416.
Geschwind DH, Rakic P (2013) Cortical evolution: judge the brain by its cover. Neuron 80:633-647.
Ghashghaei HT, Lai C, Anton ES (2007) Neuronal migration in the adult brain: are we there yet? Nat Rev Neurosci 8:141-151.
Gillott A, Furniss F, Walter A (2001) Anxiety in high-functioning children with autism. Autism 5:277-286.
Giusti SA, Vercelli CA, Vogl AM, Kolarz AW, Pino NS, Deussing JM, Refojo D (2014) Behavioral phenotyping of Nestin-Cre mice: implications for genetic mouse models of psychiatric disorders. J Psychiatr Res 55:87-95.
Gleeson JG, Walsh CA (2000) Neuronal migration disorders: from genetic diseases to developmental mechanisms. Trends Neurosci 23:352-359.
Gogolla N, Leblanc JJ, Quast KB, Sudhof TC, Fagiolini M, Hensch TK (2009) Common circuit defect of excitatory-inhibitory balance in mouse models of autism. J Neurodev Disord 1:172-181.
Gong TW, Besirli CG, Lomax MI (2001) MACF1 gene structure: a hybrid of plectin and dystrophin. Mammalian genome : official journal of the International Mammalian Genome Society 12:852-861.
Goode BL, Drubin DG, Barnes G (2000) Functional cooperation between the microtubule and actin cytoskeletons. Current opinion in cell biology 12:63-71.
Gorski JA, Talley T, Qiu M, Puelles L, Rubenstein JL, Jones KR (2002) Cortical excitatory neurons and glia, but not GABAergic neurons, are produced in the Emx1-expressing lineage. J Neurosci 22:6309-6314.
Goryunov D, He CZ, Lin CS, Leung CL, Liem RK (2010) Nervous-tissue-specific elimination of microtubule-actin crosslinking factor 1a results in multiple developmental defects in the mouse brain. Molecular and cellular neurosciences 44:1-14.

Gotz M, Huttner WB (2005) The cell biology of neurogenesis. Nature reviews Molecular cell biology 6:777-788.
Gratzner HG (1982) Monoclonal antibody to 5-bromo- and 5-iododeoxyuridine: A new reagent for detection of DNA replication. Science 218:474-475.
Greenspan RJ (2008) The origins of behavioral genetics. Current biology : CB 18:R192-198.
Greig LC, Woodworth MB, Galazo MJ, Padmanabhan H, Macklis JD (2013) Molecular logic of neocortical projection neuron specification, development and diversity. Nat Rev Neurosci 14:755-769.
Guerrini R, Filippi T (2005) Neuronal migration disorders, genetics, and epileptogenesis. Journal of child neurology 20:287-299.
Guerrini R, Parrini E (2010) Neuronal migration disorders. Neurobiology of disease 38:154-166.
Gulacsi AA, Anderson SA (2008) Beta-catenin-mediated Wnt signaling regulates neurogenesis in the ventral telencephalon. Nat Neurosci 11:1383-1391.
Gupta T, Marlow FL, Ferriola D, Mackiewicz K, Dapprich J, Monos D, Mullins MC (2010) Microtubule actin crosslinking factor 1 regulates the Balbiani body and animal-vegetal polarity of the zebrafish oocyte. PLoS genetics 6:e1001073.
Guy J, Hendrich B, Holmes M, Martin JE, Bird A (2001) A mouse Mecp2-null mutation causes neurological symptoms that mimic Rett syndrome. Nat Genet 27:322-326.
Halgren C et al. (2012) Corpus callosum abnormalities, intellectual disability, speech impairment, and autism in patients with haploinsufficiency of ARID1B. Clinical genetics 82:248-255.
Han S, Tai C, Jones CJ, Scheuer T, Catterall WA (2014) Enhancement of inhibitory neurotransmission by GABAA receptors having alpha2,3-subunits ameliorates behavioral deficits in a mouse model of autism. Neuron 81:1282-1289.
Handley SL, Mithani S (1984) Effects of alpha-adrenoceptor agonists and antagonists in a maze-exploration model of 'fear'-motivated behaviour. Naunyn Schmiedebergs Arch Pharmacol 327:1-5.
Hans F, Dimitrov S (2001) Histone H3 phosphorylation and cell division. Oncogene 20:3021-3027.
Harno E, Cottrell EC, White A (2013) Metabolic pitfalls of CNS Cre-based technology. Cell Metab 18:21-28.
Harris KM, Kater SB (1994) Dendritic spines: cellular specializations imparting both stability and flexibility to synaptic function. Annu Rev Neurosci 17:341-371.
Harris SW, Hessl D, Goodlin-Jones B, Ferranti J, Bacalman S, Barbato I, Tassone F, Hagerman PJ, Herman H, Hagerman RJ (2008) Autism profiles of males with fragile X syndrome. American journal of mental retardation : AJMR 113:427-438.
Harrison PJ, Weinberger DR (2005) Schizophrenia genes, gene expression, and neuropathology: on the matter of their convergence. Molecular psychiatry 10:40-68; image 45.

Hartfuss E, Galli R, Heins N, Gotz M (2001) Characterization of CNS precursor subtypes and radial glia. Dev Biol 229:15-30.

Hatton BA, Knoepfler PS, Kenney AM, Rowitch DH, de Alboran IM, Olson JM, Eisenman RN (2006) N-myc is an essential downstream effector of Shh signaling during both normal and neoplastic cerebellar growth. Cancer research 66:8655-8661.

Hayashi-Takagi A, Takaki M, Graziane N, Seshadri S, Murdoch H, Dunlop AJ, Makino Y, Seshadri AJ, Ishizuka K, Srivastava DP, Xie Z, Baraban JM, Houslay MD, Tomoda T, Brandon NJ, Kamiya A, Yan Z, Penzes P, Sawa A (2010) Disrupted-in-Schizophrenia 1 (DISC1) regulates spines of the glutamate synapse via Rac1. Nature neuroscience 13:327-332.

Heidenreich M, Zhang F (2016) Applications of CRISPR-Cas systems in neuroscience. Nat Rev Neurosci 17:36-44.

Higginbotham HR, Gleeson JG (2007) The centrosome in neuronal development. Trends Neurosci 30:276-283.

Ho L, Crabtree GR (2010) Chromatin remodelling during development. Nature 463:474-484.

Hodges C, Kirkland JG, Crabtree GR (2016) The Many Roles of BAF (mSWI/SNF) and PBAF Complexes in Cancer. Cold Spring Harb Perspect Med 6.

Homem CC, Repic M, Knoblich JA (2015) Proliferation control in neural stem and progenitor cells. Nat Rev Neurosci 16:647-659.

Horwitz R, Webb D (2003) Cell migration. Current biology : CB 13:R756-759.

Hossain MM, Hwang DY, Huang QQ, Sasaki Y, Jin JP (2003) Developmentally regulated expression of calponin isoforms and the effect of h2-calponin on cell proliferation. American journal of physiology Cell physiology 284:C156-167.

Howard J, Hyman AA (2007) Microtubule polymerases and depolymerases. Current opinion in cell biology 19:31-35.

Hoyer J, Ekici AB, Endele S, Popp B, Zweier C, Wiesener A, Wohlleber E, Dufke A, Rossier E, Petsch C, Zweier M, Gohring I, Zink AM, Rappold G, Schrock E, Wieczorek D, Riess O, Engels H, Rauch A, Reis A (2012) Haploinsufficiency of ARID1B, a member of the SWI/SNF-a chromatin-remodeling complex, is a frequent cause of intellectual disability. Am J Hum Genet 90:565-572.

Hu L, Su P, Li R, Yan K, Chen Z, Shang P, Qian A (2015) Knockdown of microtubule actin crosslinking factor 1 inhibits cell proliferation in MC3T3-E1 osteoblastic cells. BMB reports 48:583-588.

Hu L, Su P, Li R, Yin C, Zhang Y, Shang P, Yang T, Qian A (2016) Isoforms, structures, and functions of versatile spectraplakin MACF1. BMB reports 49:37-44.

Hurlstone AF, Olave IA, Barker N, van Noort M, Clevers H (2002) Cloning and characterization of hELD/OSA1, a novel BRG1 interacting protein. Biochem J 364:255-264.

Huttenlocher PR (1974) Dendritic development in neocortex of children with mental defect and infantile spasms. Neurology 24:203-210.

Huttner WB, Kosodo Y (2005) Symmetric versus asymmetric cell division during neurogenesis in the developing vertebrate central nervous system. Current opinion in cell biology 17:648-657.

Imai T, Hattori H, Miyazaki M, Higuchi Y, Adachi S, Nakahata T (2001) Dandy-Walker variant in Coffin-Siris syndrome. Am J Med Genet 100:152-155.

Inoue H, Furukawa T, Giannakopoulos S, Zhou S, King DS, Tanese N (2002) Largest subunits of the human SWI/SNF chromatin-remodeling complex promote transcriptional activation by steroid hormone receptors. J Biol Chem 277:41674-41685.

Irwin SA, Idupulapati M, Gilbert ME, Harris JB, Chakravarti AB, Rogers EJ, Crisostomo RA, Larsen BP, Mehta A, Alcantara CJ, Patel B, Swain RA, Weiler IJ, Oostra BA, Greenough WT (2002) Dendritic spine and dendritic field characteristics of layer V pyramidal neurons in the visual cortex of fragile-X knockout mice. Am J Med Genet 111:140-146.

Ishizuka K, Kamiya A, Oh EC, Kanki H, Seshadri S, Robinson JF, Murdoch H, Dunlop AJ, Kubo K, Furukori K, Huang B, Zeledon M, Hayashi-Takagi A, Okano H, Nakajima K, Houslay MD, Katsanis N, Sawa A (2011) DISC1-dependent switch from progenitor proliferation to migration in the developing cortex. Nature 473:92-96.

Iwasato T, Nomura R, Ando R, Ikeda T, Tanaka M, Itohara S (2004) Dorsal telencephalon-specific expression of Cre recombinase in PAC transgenic mice. Genesis 38:130-138.

Jaglin XH, Chelly J (2009) Tubulin-related cortical dysgeneses: microtubule dysfunction underlying neuronal migration defects. Trends in genetics : TIG 25:555-566.

Jan YN, Jan LY (2010) Branching out: mechanisms of dendritic arborization. Nat Rev Neurosci 11:316-328.

Jefferson JJ, Ciatto C, Shapiro L, Liem RK (2007) Structural analysis of the plakin domain of bullous pemphigoid antigen1 (BPAG1) suggests that plakins are members of the spectrin superfamily. Journal of molecular biology 366:244-257.

Jentarra GM, Olfers SL, Rice SG, Srivastava N, Homanics GE, Blue M, Naidu S, Narayanan V (2010) Abnormalities of cell packing density and dendritic complexity in the MeCP2 A140V mouse model of Rett syndrome/X-linked mental retardation. BMC Neurosci 11:19.

Jeret JS, Serur D, Wisniewski K, Fisch C (1985) Frequency of agenesis of the corpus callosum in the developmentally disabled population as determined by computerized tomography. Pediatric neuroscience 12:101-103.

Jorgensen LH, Mosbech MB, Faergeman NJ, Graakjaer J, Jacobsen SV, Schroder HD (2014) Duplication in the microtubule-actin cross-linking factor 1 gene causes a novel neuromuscular condition. Scientific reports 4:5180.

Jung EM, Ka M, Kim WY (2016) Loss of GSK-3 Causes Abnormal Astrogenesis and Behavior in Mice. Mol Neurobiol 53:3954-3966.

Jung EM, Moffat JJ, Liu J, Dravid SM, Gurumurthy CB, Kim WY (2017) Arid1b haploinsufficiency disrupts cortical interneuron development and mouse behavior. Nat Neurosci 20:1694-1707.

Ka M, Kim WY (2016) Microtubule-Actin Crosslinking Factor 1 Is Required for Dendritic Arborization and Axon Outgrowth in the Developing Brain. Mol Neurobiol 53:6018-6032.

Ka M, Moffat JJ, Kim WY (2016a) MACF1 Controls Migration and Positioning of Cortical GABAergic Interneurons in Mice. Cerebral cortex.

Ka M, Smith AL, Kim WY (2017) MTOR controls genesis and autophagy of GABAergic interneurons during brain development. Autophagy 13:1348-1363.

Ka M, Jung EM, Mueller U, Kim WY (2014a) MACF1 regulates the migration of pyramidal neurons via microtubule dynamics and GSK-3 signaling. Dev Biol 395:4-18.

Ka M, Condorelli G, Woodgett JR, Kim WY (2014b) mTOR regulates brain morphogenesis by mediating GSK3 signaling. Development 141:4076-4086.

Ka M, Chopra DA, Dravid SM, Kim WY (2016b) Essential Roles for ARID1B in Dendritic Arborization and Spine Morphology of Developing Pyramidal Neurons. J Neurosci 36:2723-2742.

Ka M, Kook YH, Liao K, Buch S, Kim WY (2016c) Transactivation of TrkB by Sigma-1 receptor mediates cocaine-induced changes in dendritic spine density and morphology in hippocampal and cortical neurons. Cell Death Dis 7:e2414.

Kamiya A, Kubo K, Tomoda T, Takaki M, Youn R, Ozeki Y, Sawamura N, Park U, Kudo C, Okawa M, Ross CA, Hatten ME, Nakajima K, Sawa A (2005) A schizophrenia-associated mutation of DISC1 perturbs cerebral cortex development. Nature cell biology 7:1167-1178.

Kang E, Burdick KE, Kim JY, Duan X, Guo JU, Sailor KA, Jung DE, Ganesan S, Choi S, Pradhan D, Lu B, Avramopoulos D, Christian K, Malhotra AK, Song H, Ming GL (2011) Interaction between FEZ1 and DISC1 in regulation of neuronal development and risk for schizophrenia. Neuron 72:559-571.

Kappeler C, Dhenain M, Phan Dinh Tuy F, Saillour Y, Marty S, Fallet-Bianco C, Souville I, Souil E, Pinard JM, Meyer G, Encha-Razavi F, Volk A, Beldjord C, Chelly J, Francis F (2007) Magnetic resonance imaging and histological studies of corpus callosal and hippocampal abnormalities linked to doublecortin deficiency. J Comp Neurol 500:239-254.

Karakesisoglou I, Yang Y, Fuchs E (2000) An epidermal plakin that integrates actin and microtubule networks at cellular junctions. The Journal of cell biology 149:195-208.

Katayama Y, Nishiyama M, Shoji H, Ohkawa Y, Kawamura A, Sato T, Suyama M, Takumi T, Miyakawa T, Nakayama KI (2016) CHD8 haploinsufficiency results in autistic-like phenotypes in mice. Nature 537:675-679.

Kaufmann WE, Moser HW (2000) Dendritic anomalies in disorders associated with mental retardation. Cerebral cortex 10:981-991.

Kazdoba TM, Leach PT, Silverman JL, Crawley JN (2014) Modeling fragile X syndrome in the Fmr1 knockout mouse. Intractable Rare Dis Res 3:118-133.

Keays DA, Tian G, Poirier K, Huang GJ, Siebold C, Cleak J, Oliver PL, Fray M, Harvey RJ, Molnar Z, Pinon MC, Dear N, Valdar W, Brown SD, Davies KE, Rawlins JN, Cowan NJ, Nolan P, Chelly J, Flint J (2007) Mutations in alpha-tubulin cause abnormal neuronal migration in mice and lissencephaly in humans. Cell 128:45-57.

Kee N, Sivalingam S, Boonstra R, Wojtowicz JM (2002) The utility of Ki-67 and BrdU as proliferative markers of adult neurogenesis. J Neurosci Methods 115:97-105.

Keeler CE, Sutcliffe E, Chaffee EL (1928) Normal and "Rodless" Retinae of the House Mouse with Respect to the Electromotive Force Generated through Stimulation by Light. Proc Natl Acad Sci U S A 14:477-484.

Kelly OG, Pinson KI, Skarnes WC (2004) The Wnt co-receptors Lrp5 and Lrp6 are essential for gastrulation in mice. Development 131:2803-2815.

Kelsom C, Lu W (2013) Development and specification of GABAergic cortical interneurons. Cell & bioscience 3:19.

Kenny EM, Cormican P, Furlong S, Heron E, Kenny G, Fahey C, Kelleher E, Ennis S, Tropea D, Anney R, Corvin AP, Donohoe G, Gallagher L, Gill M, Morris DW (2014) Excess of rare novel loss-of-function variants in synaptic genes in schizophrenia and autism spectrum disorders. Molecular psychiatry 19:872-879.

Kim SY, Burris J, Bassal F, Koldewyn K, Chattarji S, Tassone F, Hessl D, Rivera SM (2014) Fear-specific amygdala function in children and adolescents on the fragile x spectrum: a dosage response of the FMR1 gene. Cerebral cortex 24:600-613.

Kim WY, Wang X, Wu Y, Doble BW, Patel S, Woodgett JR, Snider WD (2009) GSK-3 is a master regulator of neural progenitor homeostasis. Nat Neurosci 12:1390-1397.

Kim WY, Zhou FQ, Zhou J, Yokota Y, Wang YM, Yoshimura T, Kaibuchi K, Woodgett JR, Anton ES, Snider WD (2006) Essential roles for GSK-3s and GSK-3-primed substrates in neurotrophin-induced and hippocampal axon growth. Neuron 52:981-996.

Kioussi C, Briata P, Baek SH, Rose DW, Hamblet NS, Herman T, Ohgi KA, Lin C, Gleiberman A, Wang J, Brault V, Ruiz-Lozano P, Nguyen HD, Kemler R, Glass CK, Wynshaw-Boris A, Rosenfeld MG (2002) Identification of a Wnt/Dvl/beta-Catenin --> Pitx2 pathway mediating cell-type-specific proliferation during development. Cell 111:673-685.

Kodama A, Karakesisoglou I, Wong E, Vaezi A, Fuchs E (2003) ACF7: an essential integrator of microtubule dynamics. Cell 115:343-354.

Kogan MD, Blumberg SJ, Schieve LA, Boyle CA, Perrin JM, Ghandour RM, Singh GK, Strickland BB, Trevathan E, van Dyck PC (2009) Prevalence of parent-reported diagnosis of autism spectrum disorder among children in the US, 2007. Pediatrics 124:1395-1403.

Koleske AJ (2013) Molecular mechanisms of dendrite stability. Nat Rev Neurosci 14:536-550.
Koludrovic D, Laurette P, Strub T, Keime C, Le Coz M, Coassolo S, Mengus G, Larue L, Davidson I (2015) Chromatin-Remodelling Complex NURF Is Essential for Differentiation of Adult Melanocyte Stem Cells. PLoS genetics 11:e1005555.
Konno D, Shioi G, Shitamukai A, Mori A, Kiyonari H, Miyata T, Matsuzaki F (2008) Neuroepithelial progenitors undergo LGN-dependent planar divisions to maintain self-renewability during mammalian neurogenesis. Nature cell biology 10:93-101.
Korobova F, Svitkina T (2010) Molecular architecture of synaptic actin cytoskeleton in hippocampal neurons reveals a mechanism of dendritic spine morphogenesis. Molecular biology of the cell 21:165-176.
Kosodo Y (2012) Interkinetic nuclear migration: beyond a hallmark of neurogenesis. Cellular and molecular life sciences : CMLS 69:2727-2738.
Kosodo Y, Suetsugu T, Suda M, Mimori-Kiyosue Y, Toida K, Baba SA, Kimura A, Matsuzaki F (2011) Regulation of interkinetic nuclear migration by cell cycle-coupled active and passive mechanisms in the developing brain. EMBO J 30:1690-1704.
Kreienkamp HJ (2008) Scaffolding proteins at the postsynaptic density: shank as the architectural framework. Handb Exp Pharmacol:365-380.
Kumar RA, Sudi J, Babatz TD, Brune CW, Oswald D, Yen M, Nowak NJ, Cook EH, Christian SL, Dobyns WB (2010) A de novo 1p34.2 microdeletion identifies the synaptic vesicle gene RIMS3 as a novel candidate for autism. Journal of medical genetics 47:81-90.
Kurdistani SK, Grunstein M (2003) Histone acetylation and deacetylation in yeast. Nature reviews Molecular cell biology 4:276-284.
Larkum ME (2013) The yin and yang of cortical layer 1. Nat Neurosci 16:114-115.
Lauffenburger DA, Horwitz AF (1996) Cell migration: a physically integrated molecular process. Cell 84:359-369.
Lavrik IN, Golks A, Krammer PH (2005) Caspases: pharmacological manipulation of cell death. J Clin Invest 115:2665-2672.
Lawrence M, Daujat S, Schneider R (2016) Lateral Thinking: How Histone Modifications Regulate Gene Expression. Trends in genetics : TIG 32:42-56.
Lawrence YA, Kemper TL, Bauman ML, Blatt GJ (2010) Parvalbumin-, calbindin-, and calretinin-immunoreactive hippocampal interneuron density in autism. Acta neurologica Scandinavica 121:99-108.
Lee JA, Lupski JR (2006) Genomic rearrangements and gene copy-number alterations as a cause of nervous system disorders. Neuron 52:103-121.
Lee JH, Huynh M, Silhavy JL, Kim S, Dixon-Salazar T, Heiberg A, Scott E, Bafna V, Hill KJ, Collazo A, Funari V, Russ C, Gabriel SB, Mathern GW, Gleeson JG (2012) De novo somatic mutations in components of the PI3K-AKT3-mTOR pathway cause hemimegalencephaly. Nat Genet 44:941-945.

Lessard J, Wu JI, Ranish JA, Wan M, Winslow MM, Staahl BT, Wu H, Aebersold R, Graef IA, Crabtree GR (2007) An essential switch in subunit composition of a chromatin remodeling complex during neural development. Neuron 55:201-215.

Leung CL, Sun D, Zheng M, Knowles DR, Liem RK (1999) Microtubule actin cross-linking factor (MACF): a hybrid of dystonin and dystrophin that can interact with the actin and microtubule cytoskeletons. The Journal of cell biology 147:1275-1286.

Levinson DF et al. (2011) Copy number variants in schizophrenia: confirmation of five previous findings and new evidence for 3q29 microdeletions and VIPR2 duplications. The American journal of psychiatry 168:302-316.

Li F, Wan M, Zhang B, Peng Y, Zhou Y, Pi C, Xu X, Ye L, Zhou X, Zheng L (2018) Bivalent Histone Modifications and Development. Current stem cell research & therapy 13:83-90.

Li W, Xiong Y, Shang C, Twu KY, Hang CT, Yang J, Han P, Lin CY, Lin CJ, Tsai FC, Stankunas K, Meyer T, Bernstein D, Pan M, Chang CP (2013) Brg1 governs distinct pathways to direct multiple aspects of mammalian neural crest cell development. Proc Natl Acad Sci U S A 110:1738-1743.

Lickert H, Takeuchi JK, Von Both I, Walls JR, McAuliffe F, Adamson SL, Henkelman RM, Wrana JL, Rossant J, Bruneau BG (2004) Baf60c is essential for function of BAF chromatin remodelling complexes in heart development. Nature 432:107-112.

Liebner S, Corada M, Bangsow T, Babbage J, Taddei A, Czupalla CJ, Reis M, Felici A, Wolburg H, Fruttiger M, Taketo MM, von Melchner H, Plate KH, Gerhardt H, Dejana E (2008) Wnt/beta-catenin signaling controls development of the blood-brain barrier. The Journal of cell biology 183:409-417.

Lin CM, Chen HJ, Leung CL, Parry DA, Liem RK (2005) Microtubule actin crosslinking factor 1b: a novel plakin that localizes to the Golgi complex. Journal of cell science 118:3727-3738.

Liu JS (2011) Molecular genetics of neuronal migration disorders. Current neurology and neuroscience reports 11:171-178.

Liu P, Wakamiya M, Shea MJ, Albrecht U, Behringer RR, Bradley A (1999) Requirement for Wnt3 in vertebrate axis formation. Nat Genet 22:361-365.

Lodato S, Rouaux C, Quast KB, Jantrachotechatchawan C, Studer M, Hensch TK, Arlotta P (2011) Excitatory projection neuron subtypes control the distribution of local inhibitory interneurons in the cerebral cortex. Neuron 69:763-779.

Lupski JR, Stankiewicz P (2005) Genomic disorders: molecular mechanisms for rearrangements and conveyed phenotypes. PLoS genetics 1:e49.

Luskin MB (1993) Restricted proliferation and migration of postnatally generated neurons derived from the forebrain subventricular zone. Neuron 11:173-189.

Machado-Salas JP (1984) Abnormal dendritic patterns and aberrant spine development in Bourneville's disease--a Golgi survey. Clin Neuropathol 3:52-58.

Malagelada C, Lopez-Toledano MA, Willett RT, Jin ZH, Shelanski ML, Greene LA (2011) RTP801/REDD1 regulates the timing of cortical neurogenesis and neuron migration. J Neurosci 31:3186-3196.
Margaron Y, Fradet N, Cote JF (2013) ELMO recruits actin cross-linking family 7 (ACF7) at the cell membrane for microtubule capture and stabilization of cellular protrusions. J Biol Chem 288:1184-1199.
Mariani J, Coppola G, Zhang P, Abyzov A, Provini L, Tomasini L, Amenduni M, Szekely A, Palejev D, Wilson M, Gerstein M, Grigorenko EL, Chawarska K, Pelphrey KA, Howe JR, Vaccarino FM (2015) FOXG1-Dependent Dysregulation of GABA/Glutamate Neuron Differentiation in Autism Spectrum Disorders. Cell 162:375-390.
Marin-Padilla M (1976) Pyramidal cell abnormalities in the motor cortex of a child with Down's syndrome. A Golgi study. J Comp Neurol 167:63-81.
Martini FJ, Valiente M, Lopez Bendito G, Szabo G, Moya F, Valdeolmillos M, Marin O (2009) Biased selection of leading process branches mediates chemotaxis during tangential neuronal migration. Development 136:41-50.
May-Simera HL, Gumerson JD, Gao C, Campos M, Cologna SM, Beyer T, Boldt K, Kaya KD, Patel N, Kretschmer F, Kelley MW, Petralia RS, Davey MG, Li T (2016) Loss of MACF1 Abolishes Ciliogenesis and Disrupts Apicobasal Polarity Establishment in the Retina. Cell Rep 17:1399-1413.
Mayr MI, Hummer S, Bormann J, Gruner T, Adio S, Woehlke G, Mayer TU (2007) The human kinesin Kif18A is a motile microtubule depolymerase essential for chromosome congression. Current biology : CB 17:488-498.
McKinney BC, Grossman AW, Elisseou NM, Greenough WT (2005) Dendritic spine abnormalities in the occipital cortex of C57BL/6 Fmr1 knockout mice. Am J Med Genet B Neuropsychiatr Genet 136B:98-102.
McNaughton CH, Moon J, Strawderman MS, Maclean KN, Evans J, Strupp BJ (2008) Evidence for social anxiety and impaired social cognition in a mouse model of fragile X syndrome. Behav Neurosci 122:293-300.
Mefford HC, Batshaw ML, Hoffman EP (2012) Genomics, intellectual disability, and autism. The New England journal of medicine 366:733-743.
Mehnert JM, Kelly WK (2007) Histone deacetylase inhibitors: biology and mechanism of action. Cancer journal 13:23-29.
Messier PE, Auclair C (1973) Inhibition of nuclear migration in the absence of microtubules in the chick embryo. Journal of embryology and experimental morphology 30:661-671.
Ming GL, Song H (2009) DISC1 partners with GSK3beta in neurogenesis. Cell 136:990-992.
Miyata T, Okamoto M, Shinoda T, Kawaguchi A (2014) Interkinetic nuclear migration generates and opposes ventricular-zone crowding: insight into tissue mechanics. Front Cell Neurosci 8:473.
Moffat JJ, Ka M, Jung EM, Smith AL, Kim WY (2017) The role of MACF1 in nervous system development and maintenance. Seminars in cell & developmental biology.
Molyneaux BJ, Arlotta P, Menezes JR, Macklis JD (2007) Neuronal subtype specification in the cerebral cortex. Nat Rev Neurosci 8:427-437.

Monory K et al. (2006) The endocannabinoid system controls key epileptogenic circuits in the hippocampus. Neuron 51:455-466.
Mora-Bermudez F, Huttner WB (2015) Novel insights into mammalian embryonic neural stem cell division: focus on microtubules. Molecular biology of the cell 26:4302-4306.
Mora-Bermudez F, Matsuzaki F, Huttner WB (2014) Specific polar subpopulations of astral microtubules control spindle orientation and symmetric neural stem cell division. Elife 3.
Moser B, Hochreiter B, Herbst R, Schmid JA (2017) Fluorescence colocalization microscopy analysis can be improved by combining object-recognition with pixel-intensity-correlation. Biotechnol J 12.
Moulding DA, Blundell MP, Spiller DG, White MR, Cory GO, Calle Y, Kempski H, Sinclair J, Ancliff PJ, Kinnon C, Jones GE, Thrasher AJ (2007) Unregulated actin polymerization by WASp causes defects of mitosis and cytokinesis in X-linked neutropenia. The Journal of experimental medicine 204:2213-2224.
Munemasa Y, Chang CS, Kwong JM, Kyung H, Kitaoka Y, Caprioli J, Piri N (2012) The neuronal EGF-related gene Nell2 interacts with Macf1 and supports survival of retinal ganglion cells after optic nerve injury. PLoS One 7:e34810.
Nagl NG, Jr., Wang X, Patsialou A, Van Scoy M, Moran E (2007) Distinct mammalian SWI/SNF chromatin remodeling complexes with opposing roles in cell-cycle control. EMBO J 26:752-763.
Narayanan R, Pirouz M, Kerimoglu C, Pham L, Wagener RJ, Kiszka KA, Rosenbusch J, Seong RH, Kessel M, Fischer A, Stoykova A, Staiger JF, Tuoc T (2015) Loss of BAF (mSWI/SNF) Complexes Causes Global Transcriptional and Chromatin State Changes in Forebrain Development. Cell Rep 13:1842-1854.
Nelson SB, Valakh V (2015) Excitatory/Inhibitory Balance and Circuit Homeostasis in Autism Spectrum Disorders. Neuron 87:684-698.
Nicholson DW, Ali A, Thornberry NA, Vaillancourt JP, Ding CK, Gallant M, Gareau Y, Griffin PR, Labelle M, Lazebnik YA, et al. (1995) Identification and inhibition of the ICE/CED-3 protease necessary for mammalian apoptosis. Nature 376:37-43.
Noctor SC, Flint AC, Weissman TA, Dammerman RS, Kriegstein AR (2001) Neurons derived from radial glial cells establish radial units in neocortex. Nature 409:714-720.
Noordstra I, Liu Q, Nijenhuis W, Hua S, Jiang K, Baars M, Remmelzwaal S, Martin M, Kapitein LC, Akhmanova A (2016) Control of apico-basal epithelial polarity by the microtubule minus-end-binding protein CAMSAP3 and spectraplakin ACF7. Journal of cell science 129:4278-4288.
Nord AS, Roeb W, Dickel DE, Walsh T, Kusenda M, O'Connor KL, Malhotra D, McCarthy SE, Stray SM, Taylor SM, Sebat J, Network SP, King B, King MC, McClellan JM (2011) Reduced transcript expression of genes affected by inherited and de novo CNVs in autism. Eur J Hum Genet 19:727-731.

Nowakowski RS, Lewin SB, Miller MW (1989) Bromodeoxyuridine immunohistochemical determination of the lengths of the cell cycle and the DNA-synthetic phase for an anatomically defined population. J Neurocytol 18:311-318.

Ohkawa Y, Marfella CG, Imbalzano AN (2006) Skeletal muscle specification by myogenin and Mef2D via the SWI/SNF ATPase Brg1. EMBO J 25:490-501.

Okamoto K, Nagai T, Miyawaki A, Hayashi Y (2004) Rapid and persistent modulation of actin dynamics regulates postsynaptic reorganization underlying bidirectional plasticity. Nat Neurosci 7:1104-1112.

Okuda T, Matsuda S, Nakatsugawa S, Ichigotani Y, Iwahashi N, Takahashi M, Ishigaki T, Hamaguchi M (1999) Molecular cloning of macrophin, a human homologue of Drosophila kakapo with a close structural similarity to plectin and dystrophin. Biochemical and biophysical research communications 264:568-574.

Olave I, Wang W, Xue Y, Kuo A, Crabtree GR (2002) Identification of a polymorphic, neuron-specific chromatin remodeling complex. Genes Dev 16:2509-2517.

Ortega E, Manso JA, Buey RM, Carballido AM, Carabias A, Sonnenberg A, de Pereda JM (2016) The Structure of the Plakin Domain of Plectin Reveals an Extended Rod-like Shape. The Journal of biological chemistry 291:18643-18662.

Palazzo AF, Gundersen GG (2002) Microtubule-actin cross-talk at focal adhesions. Science's STKE : signal transduction knowledge environment 2002:pe31.

Pang T, Atefy R, Sheen V (2008) Malformations of cortical development. The neurologist 14:181-191.

Paradee W, Melikian HE, Rasmussen DL, Kenneson A, Conn PJ, Warren ST (1999) Fragile X mouse: strain effects of knockout phenotype and evidence suggesting deficient amygdala function. Neuroscience 94:185-192.

Pascual J, Pfuhl M, Walther D, Saraste M, Nilges M (1997) Solution structure of the spectrin repeat: a left-handed antiparallel triple-helical coiled-coil. Journal of molecular biology 273:740-751.

Paul LK, Brown WS, Adolphs R, Tyszka JM, Richards LJ, Mukherjee P, Sherr EH (2007) Agenesis of the corpus callosum: genetic, developmental and functional aspects of connectivity. Nat Rev Neurosci 8:287-299.

Peca J, Feliciano C, Ting JT, Wang W, Wells MF, Venkatraman TN, Lascola CD, Fu Z, Feng G (2011) Shank3 mutant mice display autistic-like behaviours and striatal dysfunction. Nature 472:437-442.

Peier AM, McIlwain KL, Kenneson A, Warren ST, Paylor R, Nelson DL (2000) (Over)correction of FMR1 deficiency with YAC transgenics: behavioral and physical features. Human molecular genetics 9:1145-1159.

Pellow S, Chopin P, File SE, Briley M (1985) Validation of open:closed arm entries in an elevated plus-maze as a measure of anxiety in the rat. J Neurosci Methods 14:149-167.

Penagarikano O, Abrahams BS, Herman EI, Winden KD, Gdalyahu A, Dong H, Sonnenblick LI, Gruver R, Almajano J, Bragin A, Golshani P, Trachtenberg JT, Peles E, Geschwind DH (2011) Absence of CNTNAP2 leads to epilepsy, neuronal migration abnormalities, and core autism-related deficits. Cell 147:235-246.

Penzes P, Rafalovich I (2012) Regulation of the actin cytoskeleton in dendritic spines. Advances in experimental medicine and biology 970:81-95.

Penzes P, Cahill ME, Jones KA, VanLeeuwen JE, Woolfrey KM (2011) Dendritic spine pathology in neuropsychiatric disorders. Nat Neurosci 14:285-293.

Perou R et al. (2013) Mental health surveillance among children--United States, 2005-2011. Morbidity and mortality weekly report Surveillance summaries 62 Suppl 2:1-35.

Pietropaolo S, Guilleminot A, Martin B, D'Amato FR, Crusio WE (2011) Genetic-background modulation of core and variable autistic-like symptoms in Fmr1 knock-out mice. PLoS One 6:e17073.

Pizzarelli R, Cherubini E (2011) Alterations of GABAergic signaling in autism spectrum disorders. Neural plasticity 2011:297153.

Pleasure SJ, Anderson S, Hevner R, Bagri A, Marin O, Lowenstein DH, Rubenstein JL (2000) Cell migration from the ganglionic eminences is required for the development of hippocampal GABAergic interneurons. Neuron 28:727-740.

Powell EM, Campbell DB, Stanwood GD, Davis C, Noebels JL, Levitt P (2003) Genetic disruption of cortical interneuron development causes region- and GABA cell type-specific deficits, epilepsy, and behavioral dysfunction. J Neurosci 23:622-631.

Provenzano G, Zunino G, Genovesi S, Sgado P, Bozzi Y (2012) Mutant mouse models of autism spectrum disorders. Dis Markers 33:225-239.

Pucilowska J, Vithayathil J, Tavares EJ, Kelly C, Karlo JC, Landreth GE (2015) The 16p11.2 deletion mouse model of autism exhibits altered cortical progenitor proliferation and brain cytoarchitecture linked to the ERK MAPK pathway. J Neurosci 35:3190-3200.

Purpura G, Fulceri F, Puglisi V, Masoni P, Contaldo A (2016) Motor coordination impairment in children with autism spectrum disorder: a pilot study using Movement Assessment Battery for Children-2 Checklist. Minerva pediatrica.

Rakic P (1972) Mode of cell migration to the superficial layers of fetal monkey neocortex. J Comp Neurol 145:61-83.

Rakic P (1978) Neuronal migration and contact guidance in the primate telencephalon. Postgraduate medical journal 54 Suppl 1:25-40.

Rakic P (2003) Developmental and evolutionary adaptations of cortical radial glia. Cerebral cortex 13:541-549.

Rakic P (2009) Evolution of the neocortex: a perspective from developmental biology. Nat Rev Neurosci 10:724-735.

Raybaud C (2010) The corpus callosum, the other great forebrain commissures, and the septum pellucidum: anatomy, development, and malformation. Neuroradiology 52:447-477.

Reiner O, Carrozzo R, Shen Y, Wehnert M, Faustinella F, Dobyns WB, Caskey CT, Ledbetter DH (1993) Isolation of a Miller-Dieker lissencephaly gene containing G protein beta-subunit-like repeats. Nature 364:717-721.
Riviere JB et al. (2012) De novo germline and postzygotic mutations in AKT3, PIK3R2 and PIK3CA cause a spectrum of related megalencephaly syndromes. Nat Genet 44:934-940.
Roberts DA, Balderson D, Pickering-Brown SM, Deakin JF, Owen F (1996) The relative abundance of dopamine D4 receptor mRNA in post mortem brains of schizophrenics and controls. Schizophr Res 20:171-174.
Rodgers RJ (2007) More haste, considerably less speed. J Psychopharmacol 21:141-143.
Rodriguez OC, Schaefer AW, Mandato CA, Forscher P, Bement WM, Waterman-Storer CM (2003) Conserved microtubule-actin interactions in cell movement and morphogenesis. Nature cell biology 5:599-609.
Roidl D, Hacker C (2014) Histone methylation during neural development. Cell and tissue research 356:539-552.
Ronan JL, Wu W, Crabtree GR (2013) From neural development to cognition: unexpected roles for chromatin. Nat Rev Genet 14:347-359.
Roper K, Gregory SL, Brown NH (2002) The 'spectraplakins': cytoskeletal giants with characteristics of both spectrin and plakin families. Journal of cell science 115:4215-4225.
Rubenstein JL, Merzenich MM (2003) Model of autism: increased ratio of excitation/inhibition in key neural systems. Genes Brain Behav 2:255-267.
Sanai N, Tramontin AD, Quinones-Hinojosa A, Barbaro NM, Gupta N, Kunwar S, Lawton MT, McDermott MW, Parsa AT, Manuel-Garcia Verdugo J, Berger MS, Alvarez-Buylla A (2004) Unique astrocyte ribbon in adult human brain contains neural stem cells but lacks chain migration. Nature 427:740-744.
Sanchez-Soriano N, Travis M, Dajas-Bailador F, Goncalves-Pimentel C, Whitmarsh AJ, Prokop A (2009) Mouse ACF7 and drosophila short stop modulate filopodia formation and microtubule organisation during neuronal growth. Journal of cell science 122:2534-2542.
Santen GW, Aten E, Sun Y, Almomani R, Gilissen C, Nielsen M, Kant SG, Snoeck IN, Peeters EA, Hilhorst-Hofstee Y, Wessels MW, den Hollander NS, Ruivenkamp CA, van Ommen GJ, Breuning MH, den Dunnen JT, van Haeringen A, Kriek M (2012) Mutations in SWI/SNF chromatin remodeling complex gene ARID1B cause Coffin-Siris syndrome. Nat Genet 44:379-380.
Sarkisian MR, Bartley CM, Chi H, Nakamura F, Hashimoto-Torii K, Torii M, Flavell RA, Rakic P (2006) MEKK4 signaling regulates filamin expression and neuronal migration. Neuron 52:789-801.
Scheffler K, Tran PT (2012) Motor proteins: kinesin can replace Myosin. Current biology : CB 22:R52-54.
Schenk J, Wilsch-Brauninger M, Calegari F, Huttner WB (2009) Myosin II is required for interkinetic nuclear migration of neural progenitors. Proc Natl Acad Sci U S A 106:16487-16492.

Scholzen T, Gerdes J (2000) The Ki-67 protein: from the known and the unknown. J Cell Physiol 182:311-322.
Schrier Vergano S, Santen G, Wieczorek D, Wollnik B, Matsumoto N, Deardorff MA (1993) Coffin-Siris Syndrome. In: GeneReviews((R)) (Adam MP, Ardinger HH, Pagon RA, Wallace SE, Bean LJH, Stephens K, Amemiya A, eds). Seattle (WA).
Segarra J, Balenci L, Drenth T, Maina F, Lamballe F (2006) Combined signaling through ERK, PI3K/AKT, and RAC1/p38 is required for met-triggered cortical neuron migration. J Biol Chem 281:4771-4778.
Sessa A, Mao CA, Hadjantonakis AK, Klein WH, Broccoli V (2008) Tbr2 directs conversion of radial glia into basal precursors and guides neuronal amplification by indirect neurogenesis in the developing neocortex. Neuron 60:56-69.
Shahbazian M, Young J, Yuva-Paylor L, Spencer C, Antalffy B, Noebels J, Armstrong D, Paylor R, Zoghbi H (2002) Mice with truncated MeCP2 recapitulate many Rett syndrome features and display hyperacetylation of histone H3. Neuron 35:243-254.
Shahbazian MD, Grunstein M (2007) Functions of site-specific histone acetylation and deacetylation. Annual review of biochemistry 76:75-100.
Sharaf A, Bock HH, Spittau B, Bouche E, Krieglstein K (2013) ApoER2 and VLDLr are required for mediating reelin signalling pathway for normal migration and positioning of mesencephalic dopaminergic neurons. PLoS One 8:e71091.
Sheen VL, Ganesh VS, Topcu M, Sebire G, Bodell A, Hill RS, Grant PE, Shugart YY, Imitola J, Khoury SJ, Guerrini R, Walsh CA (2004) Mutations in ARFGEF2 implicate vesicle trafficking in neural progenitor proliferation and migration in the human cerebral cortex. Nat Genet 36:69-76.
Shibutani M, Horii T, Shoji H, Morita S, Kimura M, Terawaki N, Miyakawa T, Hatada I (2017) Arid1b Haploinsufficiency Causes Abnormal Brain Gene Expression and Autism-Related Behaviors in Mice. Int J Mol Sci 18.
Shinozaki K, Miyagi T, Yoshida M, Miyata T, Ogawa M, Aizawa S, Suda Y (2002) Absence of Cajal-Retzius cells and subplate neurons associated with defects of tangential cell migration from ganglionic eminence in Emx1/2 double mutant cerebral cortex. Development 129:3479-3492.
Shirao T, Gonzalez-Billault C (2013) Actin filaments and microtubules in dendritic spines. Journal of neurochemistry 126:155-164.
Shitamukai A, Matsuzaki F (2012) Control of asymmetric cell division of mammalian neural progenitors. Development, growth & differentiation 54:277-286.
Shu T, Richards LJ (2001) Cortical axon guidance by the glial wedge during the development of the corpus callosum. J Neurosci 21:2749-2758.
Shu T, Puche AC, Richards LJ (2003) Development of midline glial populations at the corticoseptal boundary. Journal of neurobiology 57:81-94.
Siegrist SE, Doe CQ (2007) Microtubule-induced cortical cell polarity. Genes Dev 21:483-496.

Sim JC, White SM, Lockhart PJ (2015) ARID1B-mediated disorders: Mutations and possible mechanisms. Intractable Rare Dis Res 4:17-23.

Simunovic F, Yi M, Wang Y, Macey L, Brown LT, Krichevsky AM, Andersen SL, Stephens RM, Benes FM, Sonntag KC (2009) Gene expression profiling of substantia nigra dopamine neurons: further insights into Parkinson's disease pathology. Brain : a journal of neurology 132:1795-1809.

Singhal N, Graumann J, Wu G, Arauzo-Bravo MJ, Han DW, Greber B, Gentile L, Mann M, Scholer HR (2010) Chromatin-Remodeling Components of the BAF Complex Facilitate Reprogramming. Cell 141:943-955.

Slep KC, Rogers SL, Elliott SL, Ohkura H, Kolodziej PA, Vale RD (2005) Structural determinants for EB1-mediated recruitment of APC and spectraplakins to the microtubule plus end. The Journal of cell biology 168:587-598.

Smith KM, Ohkubo Y, Maragnoli ME, Rasin MR, Schwartz ML, Sestan N, Vaccarino FM (2006) Midline radial glia translocation and corpus callosum formation require FGF signaling. Nat Neurosci 9:787-797.

Sohda M, Misumi Y, Ogata S, Sakisaka S, Hirose S, Ikehara Y, Oda K (2015) Trans-Golgi protein p230/golgin-245 is involved in phagophore formation. Biochemical and biophysical research communications 456:275-281.

Sokpor G, Xie Y, Rosenbusch J, Tuoc T (2017) Chromatin Remodeling BAF (SWI/SNF) Complexes in Neural Development and Disorders. Front Mol Neurosci 10:243.

Son EY, Crabtree GR (2014) The role of BAF (mSWI/SNF) complexes in mammalian neural development. Am J Med Genet C Semin Med Genet 166C:333-349.

Srivastava AK, Schwartz CE (2014) Intellectual disability and autism spectrum disorders: causal genes and molecular mechanisms. Neurosci Biobehav Rev 46 Pt 2:161-174.

Steinecke A, Gampe C, Valkova C, Kaether C, Bolz J (2012) Disrupted-in-Schizophrenia 1 (DISC1) is necessary for the correct migration of cortical interneurons. The Journal of neuroscience : the official journal of the Society for Neuroscience 32:738-745.

Stiles J, Jernigan TL (2010) The basics of brain development. Neuropsychol Rev 20:327-348.

Sultan KT, Brown KN, Shi SH (2013) Production and organization of neocortical interneurons. Front Cell Neurosci 7:221.

Sun D, Leung CL, Liem RK (2001) Characterization of the microtubule binding domain of microtubule actin crosslinking factor (MACF): identification of a novel group of microtubule associated proteins. Journal of cell science 114:161-172.

Suozzi KC, Wu X, Fuchs E (2012) Spectraplakins: master orchestrators of cytoskeletal dynamics. The Journal of cell biology 197:465-475.

Takashima S, Chan F, Becker LE, Kuruta H (1991) Aberrant neuronal development in hemimegalencephaly: immunohistochemical and Golgi studies. Pediatr Neurol 7:275-280.

Tamminga CA, Holcomb HH (2005) Phenotype of schizophrenia: a review and formulation. Molecular psychiatry 10:27-39.
Tan SS, Kalloniatis M, Sturm K, Tam PP, Reese BE, Faulkner-Jones B (1998) Separate progenitors for radial and tangential cell dispersion during development of the cerebral neocortex. Neuron 21:295-304.
Tanenbaum ME, Galjart N, van Vugt MA, Medema RH (2006) CLIP-170 facilitates the formation of kinetochore-microtubule attachments. EMBO J 25:45-57.
Tang BL (2006) Molecular genetic determinants of human brain size. Biochemical and biophysical research communications 345:911-916.
Taniguchi H, He M, Wu P, Kim S, Paik R, Sugino K, Kvitsiani D, Fu Y, Lu J, Lin Y, Miyoshi G, Shima Y, Fishell G, Nelson SB, Huang ZJ (2011) A resource of Cre driver lines for genetic targeting of GABAergic neurons in cerebral cortex. Neuron 71:995-1013.
Taupin P, Gage FH (2002) Adult neurogenesis and neural stem cells of the central nervous system in mammals. J Neurosci Res 69:745-749.
Taverna E, Huttner WB (2010) Neural progenitor nuclei IN motion. Neuron 67:906-914.
Taverna E, Gotz M, Huttner WB (2014) The cell biology of neurogenesis: toward an understanding of the development and evolution of the neocortex. Annual review of cell and developmental biology 30:465-502.
Tian D, Diao M, Jiang Y, Sun L, Zhang Y, Chen Z, Huang S, Ou G (2015) Anillin Regulates Neuronal Migration and Neurite Growth by Linking RhoG to the Actin Cytoskeleton. Current biology : CB 25:1135-1145.
Tomasch J (1954) Size, distribution, and number of fibres in the human corpus callosum. The Anatomical record 119:119-135.
Toyo-oka K, Wachi T, Hunt RF, Baraban SC, Taya S, Ramshaw H, Kaibuchi K, Schwarz QP, Lopez AF, Wynshaw-Boris A (2014) 14-3-3epsilon and zeta regulate neurogenesis and differentiation of neuronal progenitor cells in the developing brain. J Neurosci 34:12168-12181.
Tronche F, Kellendonk C, Kretz O, Gass P, Anlag K, Orban PC, Bock R, Klein R, Schutz G (1999) Disruption of the glucocorticoid receptor gene in the nervous system results in reduced anxiety. Nat Genet 23:99-103.
Tsaneva-Atanasova K, Burgo A, Galli T, Holcman D (2009) Quantifying neurite growth mediated by interactions among secretory vesicles, microtubules, and actin networks. Biophys J 96:840-857.
Tsurusaki Y et al. (2012) Mutations affecting components of the SWI/SNF complex cause Coffin-Siris syndrome. Nat Genet 44:376-378.
Tuoc TC, Boretius S, Sansom SN, Pitulescu ME, Frahm J, Livesey FJ, Stoykova A (2013) Chromatin regulation by BAF170 controls cerebral cortical size and thickness. Dev Cell 25:256-269.
Turner AH, Greenspan KS, van Erp TGM (2016) Pallidum and lateral ventricle volume enlargement in autism spectrum disorder. Psychiatry Res Neuroimaging 252:40-45.
Van Dam D, D'Hooge R, Hauben E, Reyniers E, Gantois I, Bakker CE, Oostra BA, Kooy RF, De Deyn PP (2000) Spatial learning, contextual fear

conditioning and conditioned emotional response in Fmr1 knockout mice. Behav Brain Res 117:127-136.
van Gaal S, Lamme VA (2012) Unconscious high-level information processing: implication for neurobiological theories of consciousness. Neuroscientist 18:287-301.
van Steensel FJA, Heeman EJ (2017) Anxiety Levels in Children with Autism Spectrum Disorder: A Meta-Analysis. J Child Fam Stud 26:1753-1767.
Vasileiou G, Ekici AB, Uebe S, Zweier C, Hoyer J, Engels H, Behrens J, Reis A, Hadjihannas MV (2015) Chromatin-Remodeling-Factor ARID1B Represses Wnt/beta-Catenin Signaling. Am J Hum Genet 97:445-456.
Vecsey CG, Hawk JD, Lattal KM, Stein JM, Fabian SA, Attner MA, Cabrera SM, McDonough CB, Brindle PK, Abel T, Wood MA (2007) Histone deacetylase inhibitors enhance memory and synaptic plasticity via CREB:CBP-dependent transcriptional activation. J Neurosci 27:6128-6140.
Vermeer S, Koolen DA, Visser G, Brackel HJ, van der Burgt I, de Leeuw N, Willemsen MA, Sistermans EA, Pfundt R, de Vries BB (2007) A novel microdeletion in 1(p34.2p34.3), involving the SLC2A1 (GLUT1) gene, and severe delayed development. Developmental medicine and child neurology 49:380-384.
Wade RH (2009) On and around microtubules: an overview. Molecular biotechnology 43:177-191.
Walsh P, Elsabbagh M, Bolton P, Singh I (2011) In search of biomarkers for autism: scientific, social and ethical challenges. Nat Rev Neurosci 12:603-612.
Wang X, Nagl NG, Wilsker D, Van Scoy M, Pacchione S, Yaciuk P, Dallas PB, Moran E (2004) Two related ARID family proteins are alternative subunits of human SWI/SNF complexes. Biochem J 383:319-325.
Wang X, Li N, Xiong N, You Q, Li J, Yu J, Qing H, Wang T, Cordell HJ, Isacson O, Vance JM, Martin ER, Zhao Y, Cohen BM, Buttner EA, Lin Z (2016) Genetic Variants of Microtubule Actin Cross-linking Factor 1 (MACF1) Confer Risk for Parkinson's Disease. Mol Neurobiol.
Watanabe T, Noritake J, Kaibuchi K (2005) Regulation of microtubules in cell migration. Trends in cell biology 15:76-83.
Way M, Pope B, Weeds AG (1992) Evidence for functional homology in the F-actin binding domains of gelsolin and alpha-actinin: implications for the requirements of severing and capping. The Journal of cell biology 119:835-842.
Wegiel J, Kuchna I, Nowicki K, Imaki H, Wegiel J, Marchi E, Ma SY, Chauhan A, Chauhan V, Bobrowicz TW, de Leon M, Louis LA, Cohen IL, London E, Brown WT, Wisniewski T (2010) The neuropathology of autism: defects of neurogenesis and neuronal migration, and dysplastic changes. Acta neuropathologica 119:755-770.
Weinberg P, Flames N, Sawa H, Garriga G, Hobert O (2013) The SWI/SNF chromatin remodeling complex selectively affects multiple aspects of serotonergic neuron differentiation. Genetics 194:189-198.

Wilson RC, Vacek T, Lanier DL, Dewsbury DA (1976) Open-field behavior in muroid rodents. Behav Biol 17:495-506.

Winder SJ, Hemmings L, Maciver SK, Bolton SJ, Tinsley JM, Davies KE, Critchley DR, Kendrick-Jones J (1995) Utrophin actin binding domain: analysis of actin binding and cellular targeting. Journal of cell science 108 (Pt 1):63-71.

Wing L, Gould J (1979) Severe impairments of social interaction and associated abnormalities in children: epidemiology and classification. Journal of autism and developmental disorders 9:11-29.

Wohr M, Orduz D, Gregory P, Moreno H, Khan U, Vorckel KJ, Wolfer DP, Welzl H, Gall D, Schiffmann SN, Schwaller B (2015) Lack of parvalbumin in mice leads to behavioral deficits relevant to all human autism core symptoms and related neural morphofunctional abnormalities. Translational psychiatry 5:e525.

Wojtowicz JM, Kee N (2006) BrdU assay for neurogenesis in rodents. Nat Protoc 1:1399-1405.

Wood KW, Cornwell WD, Jackson JR (2001) Past and future of the mitotic spindle as an oncology target. Current opinion in pharmacology 1:370-377.

Wu J et al. (2016) Insertional Mutagenesis Identifies a STAT3/Arid1b/beta-catenin Pathway Driving Neurofibroma Initiation. Cell Rep 14:1979-1990.

Wu JI, Lessard J, Olave IA, Qiu Z, Ghosh A, Graef IA, Crabtree GR (2007) Regulation of dendritic development by neuron-specific chromatin remodeling complexes. Neuron 56:94-108.

Wu Q, Wang X (2012) Neuronal stem cells in the central nervous system and in human diseases. Protein & cell 3:262-270.

Wu Q, Li Y, Xiao B (2013) DISC1-related signaling pathways in adult neurogenesis of the hippocampus. Gene 518:223-230.

Wu X, Kodama A, Fuchs E (2008) ACF7 regulates cytoskeletal-focal adhesion dynamics and migration and has ATPase activity. Cell 135:137-148.

Wu X, Shen QT, Oristian DS, Lu CP, Zheng Q, Wang HW, Fuchs E (2011) Skin stem cells orchestrate directional migration by regulating microtubule-ACF7 connections through GSK3beta. Cell 144:341-352.

Xie Z, Samuels BA, Tsai LH (2006) Cyclin-dependent kinase 5 permits efficient cytoskeletal remodeling--a hypothesis on neuronal migration. Cerebral cortex 16 Suppl 1:i64-68.

Xiong Y, Li W, Shang C, Chen RM, Han P, Yang J, Stankunas K, Wu B, Pan M, Zhou B, Longaker MT, Chang CP (2013) Brg1 governs a positive feedback circuit in the hair follicle for tissue regeneration and repair. Dev Cell 25:169-181.

Xu Q, Tam M, Anderson SA (2008) Fate mapping Nkx2.1-lineage cells in the mouse telencephalon. J Comp Neurol 506:16-29.

Yabe I, Soma H, Takei A, Fujik N, Sasaki H (2004) No association between FMR1 premutations and multiple system atrophy. J Neurol 251:1411-1412.

Yan Y, Winograd E, Viel A, Cronin T, Harrison SC, Branton D (1993) Crystal structure of the repetitive segments of spectrin. Science 262:2027-2030.

Yan Z, Wang Z, Sharova L, Sharov AA, Ling C, Piao Y, Aiba K, Matoba R, Wang W, Ko MS (2008) BAF250B-associated SWI/SNF chromatin-remodeling complex is required to maintain undifferentiated mouse embryonic stem cells. Stem Cells 26:1155-1165.

Yarm F, Sagot I, Pellman D (2001) The social life of actin and microtubules: interaction versus cooperation. Current opinion in microbiology 4:696-702.

Yingling J, Youn YH, Darling D, Toyo-Oka K, Pramparo T, Hirotsune S, Wynshaw-Boris A (2008) Neuroepithelial stem cell proliferation requires LIS1 for precise spindle orientation and symmetric division. Cell 132:474-486.

Yu Y, Yao R, Wang L, Fan Y, Huang X, Hirschhorn J, Dauber A, Shen Y (2015a) De novo mutations in ARID1B associated with both syndromic and non-syndromic short stature. BMC Genomics 16:701.

Yu Y, Yao R, Wang L, Fan Y, Huang X, Hirschhorn J, Dauber A, Shen Y (2015b) De novo mutations in ARID1B associated with both syndromic and non-syndromic short stature. BMC genomics 16:701.

Yue J, Zhang Y, Liang WG, Gou X, Lee P, Liu H, Lyu W, Tang WJ, Chen SY, Yang F, Liang H, Wu X (2016) In vivo epidermal migration requires focal adhesion targeting of ACF7. Nature communications 7:11692.

Zaoui K, Benseddik K, Daou P, Salaun D, Badache A (2010) ErbB2 receptor controls microtubule capture by recruiting ACF7 to the plasma membrane of migrating cells. Proc Natl Acad Sci U S A 107:18517-18522.

Zerucha T, Stuhmer T, Hatch G, Park BK, Long Q, Yu G, Gambarotta A, Schultz JR, Rubenstein JL, Ekker M (2000) A highly conserved enhancer in the Dlx5/Dlx6 intergenic region is the site of cross-regulatory interactions between Dlx genes in the embryonic forebrain. J Neurosci 20:709-721.

Zhou FQ, Snider WD (2005) Cell biology. GSK-3beta and microtubule assembly in axons. Science 308:211-214.

Zhou FQ, Zhou J, Dedhar S, Wu YH, Snider WD (2004) NGF-induced axon growth is mediated by localized inactivation of GSK-3beta and functions of the microtubule plus end binding protein APC. Neuron 42:897-912.

Zhu J, Beattie EC, Yang Y, Wang HJ, Seo JY, Yang LX (2005) Centrosome impairments and consequent cytokinesis defects are possible mechanisms of taxane drugs. Anticancer research 25:1919-1925.

Zigman M, Laumann-Lipp N, Titus T, Postlethwait J, Moens CB (2014) Hoxb1b controls oriented cell division, cell shape and microtubule dynamics in neural tube morphogenesis. Development 141:639-649.